2019

Mathematical Investigation of the Spatial Spread of an Infectious Disease in a Heterogeneous Environment

Arielle Gaudiello
University of Central Florida

MATHEMATICAL INVESTIGATION OF THE SPATIAL SPREAD OF AN
INFECTIOUS DISEASE IN A HETEROGENEOUS ENVIRONMENT

by

ARIELLE GAUDIELLO
M.S. University of Central Florida, 2015
B.S. Stockton University, 2013

A dissertation submitted in partial fulfilment of the requirements
for the degree of Doctor of Philosophy
in the Department of Mathematics
in the College of Sciences
at the University of Central Florida
Orlando, Florida

Summer Term
2019

Major Professor: Zhisheng Shuai

ABSTRACT

Outbreaks of infectious diseases can devastate a population. Researchers thus study the spread of an infection in a habitat to learn methods of control. In mathematical epidemiology, disease transmission is often assumed to adhere to the law of mass action, yet there are numerous other incidence terms existing in the literature. With recent global outbreaks and epidemics, spatial heterogeneity has been at the forefront of these epidemiological models.

We formulate and analyze a model for humans in a homogeneous population with a nonlinear incidence function and demographics of birth and death. We allow for the combination of host immunity after recovery from infection or host susceptibility once the infection has run its course in the individual. We compute the basic reproduction number, $\mathcal{R}_0$, for the system and determine the global stability of the equilibrium states. If $\mathcal{R}_0 \leq 1$, the population tends towards a disease-free state. If $\mathcal{R}_0 > 1$, an endemic equilibrium exists, and the disease is persistent in the population. This work provides the framework needed for a spatially heterogeneous model.

The model is then expanded to include a set of cities (or *patches*), each of which is structured from the homogeneous model. Movement is introduced, allowing travel between the cities at different rates. We assume there always exists a potentially non-direct route between two cities, and the movement need not be symmetric between two patches. Further, each city has its own nonlinear incidence function, demographics, and recovery rates, allowing for realistic interpretations of country-

wide network structures. New global stability results are established for the disease-free equilibrium and endemic equilibrium, the latter utilizing a graph theoretic approach and Lyapunov functions. Asymptotic profiles are determined for both the disease-free equilibrium and basic reproduction number as the diffusion of human individuals is faster than the disease dynamics. A numerical investigation is performed on a star network, emulating a rural-urban society with a center city and surrounding suburbs. Numerical simulations give rise to similar and contrasting behavior for symmetric movement to the proposed asymmetric movement. Conjectures are made for the monotonicty of $\mathcal{R}_0$ in terms of the diffusion of susceptible and infectious individuals. The limiting behavior of the system as the diffusion of susceptibles halts is shown to experience varying behavior based on the location of hot spots and biased movement.

ACKNOWLEDGMENTS

This is dedicated to my family and friends.

TABLE OF CONTENTS

LIST OF FIGURES

xiii

xiv

LIST OF TABLES

CHAPTER 1: INTRODUCTION

Throughout history, outbreaks of infectious diseases can be catastrophic within a civilization. Cholera, measles, SARS, smallpox, and other infections can lead to devastating amounts of deaths. Viral infections, like measles [31] and chicken-pox [1], do grant long-term immunity to the host individual after recovery. However, many bacterial and sexually transmitted infections, such as gonorrhea [11] and chlamydia [30], have the ability to infect an individual numerous times. Even tuberculosis also offers no immunity to the host [38]. With such a diverse scope in the dynamics of each type of infection, strategies for prevention and control have been at the forefront of many scholars' research.

Mathematicians, biologists, physicians, epidemiologists, and other researchers have studied the spread of infectious diseases in a host population. There have been many outstanding papers published shaping the influence of epidemiology, but three papers published by Kermack and McKendrick in the early 20th century greatly impacted the field [43–45]. Kermack and McKendrick created a foundation for modeling the spread of an infectious disease within a population. Within these papers, the susceptible-infected-removed (SIR) compartmental model was first formulated, which has proven to be effective in modeling diseases that provide immunity to the host after recovery.

From these models, scholars have been able to expand their work to include different characteristics that might impact the spread of diseases. We can now incorporate for more diverse dynamics, like networks in a population, age-structured

models, demographics, and much more. Compartments can be added in a model or removed as well. We can remove host immunity and allow infectives to return to the susceptible class immediately after the infection ends. This creates a susceptible-infectious-susceptible (SIS) model. For other models, allowing for a transitioning phase before the individual becomes infectious can be pertinent. An exposure period is introduced, where the host is infected but cannot transmit the disease to the susceptible individuals immediately. This type of model can be classified as susceptible-exposed-infectious-removed (SEIR) or as susceptible-exposed-infectious-susceptible (SEIS) model, depending on the particular disease; e.g. [14, 34]. The addition of vectors can help provide insight to mosquito-borne diseases like Zika [27, 62, 66] and malaria [7, 29, 56] or bacterial infections like cholera [13, 23, 66].

Researchers are commonly concerned with the global stability of the equilibria in these systems. A common threshold value, called the basic reproduction number $\mathcal{R}_0$, is often calculated. Biologically, this threshold parameter represents the number of secondary cases resulting from a single infectious individual introduced into a wholly susceptible population, see [21] and [68]. If $\mathcal{R}_0 \leq 1$, the disease should become extinct, leading researchers to be concerned with global stability of the disease-free equilibrium. If $\mathcal{R}_0 > 1$, the disease should persist and give rise to the existence of an endemic equilibrium. For the homogeneous model, we have common Lyapunov functions and methods used to guarantee global asymptotic stability of this disease-free and endemic equilibrium; e.g. [14, 35, 36, 46, 67, 69].

Since these homogeneous populations have been meticulously studied, the sensible

next step is to investigate the impact on the disease dynamics when neighboring populations interact. Global outbreaks have been prominent throughout history. The SARS epidemic from 2002-2003 spread from China to Singapore, Vietnam, Taiwan, and numerous other countries in the Asia-Pacific region [40]. In 2009, the H1N1 influenza caused a widespread epidemic across the United States and into Mexico [50]. The Ebola virus ravaged several countries in West Africa [16]. The Zika virus gained prominence in the news after cases began appearing in Brazil, Puerto Rico, and other nations [25]. More recently, another Ebola virus outbreak occurred in the North Kivu and Ituri provinces in the Democratic Republic of the Congo [75]. Although these infections may have been dominant in one nation, travel between neighboring populations may lead to a global spread.

Models involving spatial heterogeneity have been considered lately as a result of these global epidemics. If the spatial habitat is assumed to be discrete, a patchy environment emerges, where each region or city is represented by a patch in the environment. The disease dynamics within each patch can be described by the homogeneous epidemiological model mentioned before, while travel between patches couples these homogeneous models together, forming a heterogeneous model. Due to the high dimension and nonlinearity, complex dynamical phenomena can arise in heterogeneous disease models, which also pose significant challenges in their mathematical investigation. For example, Kang and Castillo-Chavez showed different dynamics existed for a two-patch SI model in 2014 [42]. Depending on the strength of dispersal of individuals, source-sink dynamics, stabilization, or synchronization were exhibited within the model. As a result, studying global stability can be a challenging barrier to overcome, since the dynamics can vary widely as a result

3

of the coupling and high dimension.

Many researchers have made great advances into the mathematical investigation of these models though. Wang and Mulone [70] proposed a two patch SIS model in 2002 and proved global stability for the disease-free equilibrium. Local stability results are established for the endemic equilibrium when movement of susceptibles or infectives is inhibited. In 2003, Arino and van den Driessche [9] established an n-patch SIS model. They proved local stability results for a constant population size, and numerical simulations indicated $\mathcal{R}_0$ acts as a threshold between extinction and persistence of the infectious disease. That same year, Arino and van den Driessche [8] provided lecture notes on calculating the basic reproduction number for a multi-city SEIRS model and proving local asymptotic stability of the disease-free equilibrium. Wang and Zhao [71] proposed an SIS model in a patchy environment allowing for a varying population size in 2004. Arino [5] published lecture notes regarding known structures and techniques to study global stability of the disease-free equilibrium and existence of an endemic equilibrium. In 2017, Arino [6] further showed the persistence of a population under certain movement criteria and provided restrictions for local stability in an SLIRS (susceptible-latent-infective-recovered-susceptible) population. Global stability for the disease-free equilibrium is established when the dispersal of individuals occurs at the same rate, while varying dispersal can allow for the spread of the infection even when the disease would not persist in isolated patches.

Techniques to establish global stability of the endemic equilibrium are not as readily known. Currently, there are two main methods to obtaining such stability results.

4

For the patch SIR model, a graph theoretic approach has been used in the construction of a Lyapunov function to prove global stability of the endemic equilibrium, e.g. [53]. In the case of an SIS patch model, theory from monotone dynamical systems can potentially be used if the patch model can be reduced to a monotone dynamical system, e.g. [28, 41, 65]. However, if the system cannot be reduced, global stability results regarding the endemic equilibria are still widely left open.

Since the homogeneous systems can be more readily studied, we can utilize the knowledge regarding the dynamics on each patch to study the dynamics of the coupled system. For instance, studying the asymptotic profile of the system has proven to be beneficial in studying these global dynamics. In 2007, Allen, Bolker, Lou, and Nevai [2] showed the limiting behavior of the population in a patch SIS model, in which patches were classified as high-risk and low-risk for the infection. Movement between patches was assumed symmetric, allowing them to show the infectives tended towards extinction as the movement of the susceptible individuals halted. Further, the susceptible population persisted on the low-risk patches, leading to important implications for the control of an infection. This paper in particular sparked inspiration for the impact of the effect of asymmetric movement on the spatial spread of an infection in a heterogeneous environment. Results regarding asymmetric movement are largely open for the discrete spatially heterogeneous habitat, but researchers in partial differential equation models have made some progress in the field.

If the spatial habitat is assumed to be continuous, a partial differential equation model can be used to describe the spatial spread of the infectious disease. These

5

models can incorporate asymmetric or symmetric movement by using an advection-diffusion model or a convection-diffusion model. For example, Allen, Bolker, Lou, and Nevai [3] produced results similar to the patch model [2] regarding this partial differential equation SIS model. Since then, researchers have been able to show various phenomena within these types of heterogeneous disease models, see for example [20, 59, 61, 74]. Recently, Cui, Lam, and Lou included advection in the SIS partial differential equation model and explored the impact of asymmetric movement (advection) on the disease spread [18]. Other researchers have also incorporated the use of advection into their models, which has helped in determining whether the infection will persist in this heterogeneous environment [17, 19, 47, 58]. These studies on advection models motivate our studies in the patchy environment.

In this thesis, we will propose a general framework of a heterogeneous model in a patchy environment to investigate the spatial spread of an infectious disease. In particular, our model will include both the SIS and SIR models as special cases, where both models cannot be reduced to a monotone dynamical system. The global stability of the endemic equilibrium for both the SIS and SIR models will be established using the graph theoretic approach. With this framework, we are able to explore how biased movement can affect disease transmission and spread in a heterogeneous environment. For example, if an outbreak occurs in a city, people may travel out rapidly to try to avoid the infection. With this skewed movement, will an outbreak spread throughout the country? On the contrary, if the movement between cities stays symmetric, will the dynamics stay the same? Will halting the movement of susceptible individuals allow for extinction of the infection as in [2]? To answer these questions, we will utilize our knowledge and techniques from the ho-

6

mogeneous model to help obtain these results in the spatially heterogeneous model. Specifically, we will investigate how asymmetric movement ultimately effects the spatial spread of the disease theoretically and via simulations. Many varying dynamics will be incorporated in our model to account for the diverse differences between cities. This highlights the difference of symmetric and asymmetric movement on the disease impact.

This document is arranged in the following chapters:

In Chapter 2, we propose a general framework of homogeneous infectious disease models and provide basic results in mathematical epidemiology. Sharp-threshold results are revisited, along with the terminology and background for this foundation model. We also provide the necessary definitions and terminology from matrix theory and graph theory.

In Chapter 3, a spatially heterogeneous model is built based on the homogeneous model in Chapter 2, which also incorporates nonlinear incidence. We allow a varying population size, with each patch varying at a different rate. Each patch will have its own dynamics and directed asymmetric movement is permitted between the patches. Existence and uniqueness of the disease free equilibrium is proven. We determine the threshold value, $\mathcal{R}_0$, for this heterogeneous model. Global stability results for the disease-free equilibrium and varying cases for stability of the endemic equilibrium for both the SIS and SIR models are established.

In Chapter 4, the limiting profile for both the disease free equilibrium and the basic reproduction number are derived when the diffusion of human individuals is faster

than the disease dynamics. An explicit form is calculated for two well-known incidence functions.

In Chapter 5, we employ a star network to simulate the spread of an infectious disease in a metropolitan area. The frequency dependent incidence function is used in this chapter, while mass action incidence is used in Chapter 6. Known results for a population without demographics are revisited via simulations, and we determine the demographic effect in persistence of an infection. The impact of asymmetric movement on disease persistence is investigated when no demographics are present.

In Chapter 6, the monotone/non-monotone property of the basic reproduction number in terms of diffusion coefficients is explored numerically. A new phenomenon of a movement induced hot spot is demonstrated.

In Chapter 7, the results are summarized and ideas for future studies are formulated.

CHAPTER 2: PRELIMINARIES

2.1 Mathematical Epidemiology

In this section, we will provide terminology, concepts, and new results within mathematical epidemiology to be used throughout this thesis.

When creating a *compartmental epidemiological model*, the population is divided into different compartments of individuals that depend on the type of infection we want to study. In this section, we present a general homogeneous model that combines the SIS and SIR compartmental models. By allowing for an arbitrary *incidence function*, which represent the rate of new infections in the population, this model can be used in various future epidemic studies. We begin by investigating this homogeneous model, providing the framework to introduce spatial interaction between neighboring populations in Chapter 3.

2.1.1 A Basic Homogeneous Model

Consider the following homogeneous epidemiological model that includes demographics, i.e. birth and death within the population. We have

$$S' = \Lambda - f(S, I) - \mu^S S + \delta I, \tag{2.1}$$

$$I' = f(S, I) - (\mu^I + \gamma + \delta)I, \tag{2.2}$$

$$R' = \gamma I - \mu^R R, \tag{2.3}$$

where $S = S(t)$, $I = I(t)$, and $R = R(t)$ represent the population density of susceptible, infectious, and removed individuals, respectively, at time t, with non-negative initial conditions $S(0), I(0), R(0)$, and $S(0) + I(0) + R(0) > 0$. Here $'$ is the derivative with respect to time. Table 2.1 provides an outline for the parameter definitions. Each of these parameters Λ, μ^S, μ^I, and β are positive values, while δ and γ are non-negative. Figure 2.1 gives a visualization of the model.
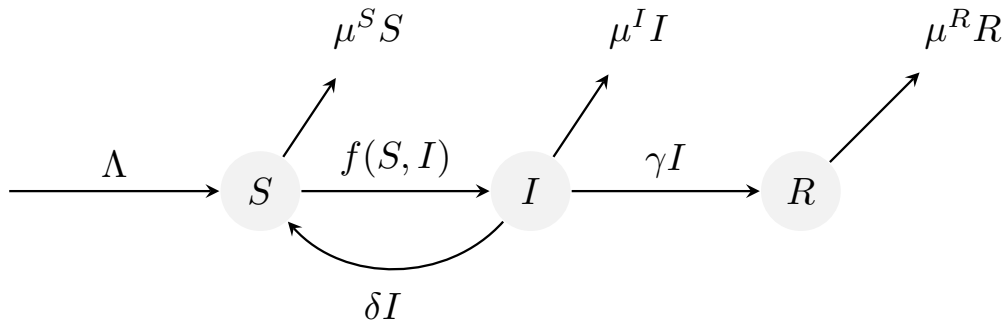
Figure 2.1: Flowchart for the basic model with demographics.

Table 2.1: A table outlining the parameters used in (2.1)-(2.3)

Parameter	Definition	Units
Λ	birth rate of susceptible individuals	people/time
β	transmission coefficient	$(\text{people} \cdot \text{time})^{-1}$
μ^S	death rate of susceptible individuals	time^{-1}
μ^I	death rate of infectious individuals	time^{-1}
μ^R	death rate of removed individuals	time^{-1}
δ, γ	disease recovery rates	time^{-1}

Notice the model (2.1)-(2.3) includes both the SIS and SIR model as special cases. For example, if $\gamma = 0$ and $\delta > 0$, host immunity is lost and R is completely

decoupled from the system, resulting in a Susceptible-Infectious-Susceptible (SIS) model. On the other hand, if $\gamma > 0$ and $\delta = 0$, all individuals recovering from the infection gain immunity, yielding a Susceptible-Infectious-Removed (SIR) model.

The incidence function $f(S, I)$ can take many forms. For instance, if one assumes an average member of the population makes contact sufficient to transmit the infection with $\beta \bar{N}$ others per unit of time, where $\bar{N} = S + I + R$ denotes the total population size, the number of new infections per unit time is $\beta \bar{N} \cdot S/\bar{N}$. This leads to the rate of new infections as $f(S, I) = \beta \bar{N} \cdot S/\bar{N} \cdot I = \beta SI$, commonly known as *mass action incidence*. Another option for the incidence function is $\beta SI/\bar{N}$, called *standard incidence* [14, Chapter 2]. Additionally, there are other nonlinear incidence terms, such as $\beta SI/(S+I)$, $\beta S^q I^p$, and $\beta SI^p/(1+\alpha I^p)$; see [2], [52], [37] respectively.

The following assumptions on $f(S, I)$ are required either biologically or for the need of mathematical rigor:

(i) $f(S, I) \geq 0$ for all $S, I \geq 0$;

(ii) $f \in C([0, \infty) \times [0, \infty))$; i.e. f is continuous for $0 \leq S < \infty$ and $0 \leq I < \infty$;

(iii) $f(S, 0) = f(0, I) = 0$ for all $S, I \geq 0$;

(iv) $\displaystyle\lim_{I \to 0^+} \frac{f(S, I)}{I}$ exists for all $S \geq 0$.

11

Since R does not appear in (2.1) and (2.2), we can study the reduced system

$$S' \;=\; \Lambda - f(S,I) - \mu^S S + \delta I, \tag{2.4}$$

$$I' \;=\; f(S,I) - (\mu^I + \gamma + \delta)I. \tag{2.5}$$

Then, the dynamics of R can be further studied.

2.1.2 Disease-Free and Endemic Equilibria

The system (2.4)-(2.5) admits two types of equilibria: a *disease-free equilibrium* (DFE), denoted $P^0 = (S^0, 0)$ with $S^0 = \dfrac{\Lambda}{\mu^S}$, and a possible *endemic equilibrium* (EE), denoted $P^* = (S^*, I^*)$ where $S^* > 0$ and $I^* > 0$. A solution to the EE must satisfy

$$0 = \Lambda - f(S^*, I^*) - \mu^S S^* + \delta I^*, \tag{2.6}$$

$$0 = f(S^*, I^*) - (\mu^I + \gamma + \delta)I^*. \tag{2.7}$$

The existence of an EE will be further discussed in Section 2.1.6.

2.1.3 Feasible Region

Biologically, a population cannot contain negative individuals, but there are other conditions arriving from our system. Let $\mu^* = \min\{\mu^S, \mu^I + \gamma + \delta\}$ and $N = S + I$, where N represents the total population influencing the disease dynamics. It fol-

12

lows that

$$N' = S + I \leq \Lambda - \mu^* N.$$

Solving the differential inequality, we arrive at $N(t) \leq \Lambda/\mu^* - N(0)e^{-\mu^* t}$, and hence $\limsup_{t\to\infty} N(t) \leq \Lambda/\mu^*$. We call our feasible region Γ and define it as

$$\Gamma = \left\{ (S, I) \in \mathbb{R}_+^2 \,\middle|\, S + I \leq \frac{\Lambda}{\mu^*} \right\}.$$

A region is positively invariant with respect to a system if trajectories that start within the region remain there for all time, see [76] and [33].

Lemma 2.1.1. *Feasible region Γ is a positively invariant set and globally attractive with respect to (2.4)-(2.5).*

Proof. Note that

$$\left.\frac{dS}{dt}\right|_{S=0} = \Lambda + \delta I > 0 \qquad \text{and} \qquad \left.\frac{dI}{dt}\right|_{I=0} = 0,$$

hence S and I are non-negative if $S(0) \geq 0$ and $I(0) \geq 0$. Further, since

$$N \leq \Lambda/\mu^* - N(0)e^{-\mu^* t},$$

we obtain $N \leq \Lambda/\mu^*$ if $N(0) \leq \Lambda/\mu^*$, giving us Γ is a positively invariant set. If $N(0) > \Lambda/\mu^*$, then $\limsup_{t\to\infty} N(t) \leq \Lambda/\mu^*$. Thus, Γ is globally attractive.

$\square$

13

2.1.4 Basic Reproduction Number

To study local stability of our equilibrium points, we typically linearize the system around the equilibrium point and study the eigenvalues of the corresponding Jacobian matrix; e.g. [32, Chapter 4].

For example, consider a system of autonomous ordinary differential equations

$$\dot{\mathbf{x}} = \mathbf{f}(\mathbf{x}),$$

where $\mathbf{x} = (x_1, x_2, \ldots, x_n)^T$ and $\mathbf{f} = (f_1, f_2, \ldots, f_n)^T$. Suppose an equilibrium $\mathbf{x}^*$ exists such that $\mathbf{f}(\mathbf{x}^*) = 0$. The Jacobian matrix

$$J = \begin{bmatrix} \dfrac{\partial f_1}{\partial x_1} & \dfrac{\partial f_1}{\partial x_2} & \cdots & \dfrac{\partial f_1}{\partial x_n} \\ \dfrac{\partial f_2}{\partial x_1} & \dfrac{\partial f_2}{\partial x_2} & \cdots & \dfrac{\partial f_2}{\partial x_n} \\ \vdots & \vdots & \ddots & \vdots \\ \dfrac{\partial f_n}{\partial x_1} & \dfrac{\partial f_n}{\partial x_2} & \cdots & \dfrac{\partial f_n}{\partial x_n} \end{bmatrix}$$

is then evaluated at the equilibrium to obtain the matrix $J(\mathbf{x}^*)$. From Theorem 4.4 of [32], $\mathbf{x}^*$ will be locally stable if all eigenvalues of $J(\mathbf{x}^*)$ have negative real part.

In mathematical epidemiology, a *basic reproduction number*, $\mathcal{R}_0$, is often calculated to determine the stability of the DFE, and hence correspondingly determining the dynamics of the disease. Biologically, the basic reproduction number is the average number of secondary cases produced by a single infectious individual when intro-

duced in a wholly susceptible population; e.g. [4], [21], and [68] and [14, Chapter 6]. In order to compute $\mathcal{R}_0$ for an epidemiological model, the method of the *next-generation matrix* will be used; e.g. [21], and [68].

We will study the infectious compartment and linearize around the disease-free equilibrium. The infectious compartment can be split into two categories:

$$\dot{x}_i = f_i(x) = \mathcal{F}_i(x) - \mathcal{V}_i(x), \;\; i = 1, 2, \ldots, n,$$

where $\mathcal{F}_i(x)$ is the rate of new infectious individuals in compartment i and $\mathcal{V}_i(x)$ is the rate of transfers of infectious individuals out of compartment i. Essentially, these will be infectious individuals recovering, being quarantined, dying, or moving to some other category set-up by the compartmental model.

We linearize this splitting about the disease-free equilibrium, $\mathbf{x_0}$, to obtain

$$\dot{\mathbf{x}} = (F - V)\mathbf{x},$$

where $\mathbf{x} = (x_1, x_2, \ldots, x_n)^T$, $F - V = D\mathbf{f}(P^0)$, and $\mathbf{f} = (f_1, f_2, \ldots, f_n)^T$.

Here F represents the rate of appearance of new infected individuals and V is comprised of the number of infected transferred between patches. From [21], the matrix FV^{-1} is the *next-generation matrix* for the model. Biologically, the entries of FV^{-1} represent the expected number of new infections produced by this single infectious individual introduced into the population.

We can then define $\mathcal{R}_0 = \rho(FV^{-1})$, where ρ represents the spectral radius. Theo-

rem 2 of [68] shows the the disease-free equilibrium is locally asymptotically stable if $\mathcal{R}_0 < 1$ but unstable if $\mathcal{R}_0 > 1$. This is equivalent to showing the eigenvalues of $F - V$ have negative real part.

If the partial derivative of f with respect to I exists, then $\frac{\partial f}{\partial I}(S^0, 0) = \lim_{I \to 0+} \frac{f(S^0, I)}{I}$. The assumptions on f guarantee this Jacobian matrix exists without requiring the differentiability of f. Thus, for system (2.4)-(2.5), we can perform this splitting to find the basic reproduction number. Define the 1×1 new disease matrix

$$F = \left[\lim_{I \to 0+} \frac{f(S^0, I)}{I} \right]$$

and the 1×1 disease transfer matrix

$$V = \left[\mu^I + \gamma + \delta \right].$$

The next-generation matrix is $FV^{-1} = \left[\dfrac{1}{\mu^I + \gamma + \delta} \cdot \lim_{I \to 0+} \dfrac{f(S^0, I)}{I} \right]$ and hence for system (2.4)-(2.5), the basic reproduction number is

$$\mathcal{R}_0 = \frac{1}{\mu^I + \gamma + \delta} \cdot \lim_{I \to 0+} \frac{f(S^0, I)}{I}. \tag{2.8}$$

2.1.5   *Global Stability of Disease-Free Equilibrium*

From Theorem 2 of van den Driessche and Watmough [68], we know the DFE is locally asymptotically stable if $\mathcal{R}_0 < 1$ and locally unstable if $\mathcal{R}_0 > 1$, giving us the following proposition.

16

Proposition 2.1.2. *If $\mathcal{R}_0 < 1$, the DFE of (2.4)-(2.5) is locally stable. If $\mathcal{R}_0 > 1$, the DFE is unstable.*

The following results show the DFE is globally asymptotically stable if $\mathcal{R}_0 \leq 1$.

Theorem 2.1.3. *Assume $\mathcal{R}_0 \leq 1$, and*

$$0 \leq f(S, I) \leq \left(\lim_{I \to 0^+} \frac{f(S^0, I)}{I} \right) I \tag{2.9}$$

with equality if and only if $S = S^0$. Then the DFE is globally asymptotically stable in Γ.

Proof. Using the Lyapunov function $L = I$, we can obtain global asymptotic stability.

Taking the derivative of L along a trajectory in Γ gives us

$$
\begin{aligned}
\dot{L} &= I' \\
&= f(S, I) - (\mu^I + \gamma + \delta)I \\
&\leq \left(\lim_{I \to 0^+} \frac{f(S^0, I)}{I} \right) I - (\mu^I + \gamma + \delta)I \\
&= \frac{1}{\mu^I + \gamma + \delta} \left(\mathcal{R}_0 - 1 \right) I \\
&\leq 0
\end{aligned}
$$

since $\mathcal{R}_0 \leq 1$. Now, $\dot{L} = 0$ implies either $\mathcal{R}_0 = 1$ or $I = 0$. If $\mathcal{R}_0 < 1$, then we must have $I = 0$ and hence $S = S^0$. If $\mathcal{R}_0 = 1$, from our assumption we obtain

17

$S = S^0$. As a result, the largest invariant set in Γ is thus the singleton $\{P^0\}$. By the LaSalle Invariance Principle [49], we obtain P^0 is globally asymptotically stable.

$\square$

Commonly used incidence functions in the literature satisfy condition (2.9). In particular, the following corollary holds for the frequency dependent incidence function.

Corollary 2.1.4. *Let* $f(S, I) = \beta \dfrac{SI}{S+I}$, *then* $\mathcal{R}_0 = \dfrac{\beta}{\mu^I + \gamma + \delta}$. *If* $\mathcal{R}_0 \leq 1$, *the disease-free equilibrium* P^0 *of* (2.4)-(2.5) *is globally asymptotically stable in* Γ.

Proof. Note that

$$\left(\lim_{I \to 0^+} \frac{f(S^0, I)}{I} \right) I = \left(\lim_{I \to 0^+} \frac{S^0}{S^0 + I} \right) I$$
$$= I,$$

and

$$0 \leq \frac{SI}{S+I} \leq I,$$

with equality holding if and only if $I = 0$ and hence $S = S^0$. Thus, the frequency dependent function $f(S, I) = \beta \dfrac{SI}{S+I}$ satisfies condition (2.9), giving us global asymptotic stability.

$\square$

For mass action incidence, condition (2.9) will hold for the SIR model. Since

$$S' = \Lambda - f(S, I) - \mu^S S$$

$$\leq \Lambda - \mu^S S,$$

solving this differential inequality leads to $\limsup_{t\to\infty} S(t) \leq \dfrac{\Lambda}{\mu^S} = S^0$. Thus, the additional condition $S(t) \leq S^0$ can be imposed in the feasible region. As a result, condition (2.9) is satisfied, leading to the following corollary.

Corollary 2.1.5. *Let* $f(S, I) = \beta S I$ *and* $\delta = 0$, *then* $\mathcal{R}_0 = \dfrac{\Lambda \beta}{\mu^S (\mu^I + \gamma)}$. *If* $\mathcal{R}_0 \leq 1$, *the disease-free equilibrium* P^0 *of* (2.4)-(2.5) *is globally asymptotically stable in* Γ.

Proof. Note that

$$\left(\lim_{I \to 0^+} \frac{f(S^0, I)}{I} \right) I = \left(\lim_{I \to 0^+} \beta S^0 \right) I$$

$$= \beta S^0 I,$$

and since

$$0 \leq \beta S I \leq \beta S^0 I$$

with equality holding if and only if $I = 0$ or $S = S^0$. Thus, the mass action incidence function $f(S, I) = \beta S I$ satisfies condition (2.9), giving us global asymptotic stability.

$\square$

19

A similar argument cannot be applied for the SIS model. In Section 2.1.8, the SIS model with mass action incidence will be further discussed.

2.1.6 Existence of Endemic Equilibrium

An explicit expression of the EE exists for certain types of incidence functions. For example, if $f(S, I) = \beta S I$, we obtain $P^* = (S^*, I^*)$ where

$$S^* = \frac{\mu^I + \gamma + \delta}{\beta}, \tag{2.10}$$

$$I^* = \frac{\mu^S}{\mu^I} \left(S^0 - S^* \right) \tag{2.11}$$

$$= \frac{\mu^S(\mu^I + \gamma + \delta)}{\beta \mu^I} \left(\mathcal{R}_0 - 1 \right). \tag{2.12}$$

For the frequency dependent incidence function, $f(S, I) = \beta S I / (S + I)$, the EE is given by

$$S^* = \frac{\Lambda - (\mu^I + \gamma + \delta)}{\mu^S + (\mathcal{R}_0 - 1)\delta}, \tag{2.13}$$

$$I^* = \frac{(\mathcal{R}_0 - 1)(\Lambda - (\mu^I + \gamma + \delta))}{\mu^S + (\mathcal{R}_0 - 1)\delta}. \tag{2.14}$$

Theorem 2.1.6 shows existence of an endemic equilibrium for a general incidence function when $\mathcal{R}_0 > 1$ through the theory of uniform persistence.

Theorem 2.1.6. *If $\mathcal{R}_0 > 1$, then there exists at least one endemic equilibrium $P^* = (S^*, I^*)$ for the system (2.4)-(2.5) in the interior of Γ.*

20

Proof. Let $L = I$. Then,

$$\dot{L} = f(S, I) - (\mu^I + \gamma + \delta)I$$
$$= \left(\frac{f(S, I)}{I} - V\right)I,$$

where V is as defined in Section 2.1.4. Note, $\lim_{(S,I)\to(S^0,0)} \dfrac{f(S, I)}{I} = F$. Taking the limit of $\dot{L}$ as the system approaches the disease-free equilibrium, we obtain

$$\begin{aligned}
\lim_{(S,I)\to(S^0,0)} \dot{L} &= \lim_{(S,I)\to(S^0,0)} \left(\frac{f(S, I)}{I} - V\right)I \\
&= (F - V) \lim_{(S,I)\to(S^0,0)} I \\
&= V\left(FV^{-1} - 1\right) \lim_{(S,I)\to(S^0,0)} I \\
&= V\left(\mathcal{R}_0 - 1\right) \lim_{(S,I)\to(S^0,0)} I.
\end{aligned}$$

Thus, if $\mathcal{R}_0 > 1$, we have $\dot{L} > 0$ for some neighborhood $N_\epsilon(P_0)$ about P_0, implying P_0 is unstable. Trajectories beginning close enough to the DFE will thus leave $N_\epsilon(P_0)$. The system (2.4)-(2.5) is uniformly persistent by [26, Theorem 4.3] utilizing a similar argument as in [51, Proposition 3.3]. Boundedness of solutions and uniform persistence in the interior of Γ thus imply the existence of at least one endemic equilibrium (see Theorem D.3 in [64] or Theorem 2.8.6 in [12]).

$\square$

2.1.7 Global Stability of Endemic Equilibrium

In this section, we will assume $\mathcal{R}_0 > 1$, and hence by Theorem 2.1.6, an endemic equilibrium exists.

Proposition 2.1.7 provides criteria for f to obtain global asymptotic stability for an SIR model.

Proposition 2.1.7. *Let $\mathcal{R}_0 > 1$, $\delta = 0$, and $\gamma > 0$. Assume*

$$(S - S^*)\left(f(S, I^*) - f(S^*, I^*)\right) \geq 0 \tag{2.15}$$

and

$$\left(\frac{f(S, I)}{f(S, I^*)} - 1\right)\left(1 - \frac{f(S, I^*)}{f(S, I)}\frac{I}{I^*}\right) \leq 0 \tag{2.16}$$

with equality if and only if $(S, I) = (S^*, I^*)$. Then the endemic equilibrium $P^* = (S^*, I^*)$ is unique and globally asymptotically stable in the interior of Γ.

Proof. At the endemic equilibrium, we have

$$\Lambda = f(S^*, I^*) + \mu^S S^*$$

$$\mu^I + \gamma = \frac{f(S^*, I^*)}{I^*}.$$

Consider the Lyapunov function

$$V = \int_{S^*}^{S}\left(1 - \frac{f(S^*, I^*)}{f(\xi, I^*)}\right) d\xi + I - I^* - I^* \ln \frac{I}{I^*}.$$

We will utilize $\int_1^x \frac{1-u}{u} du < 0$ when $x > 1$, and $n \sqrt[n]{\prod_{i=1}^n a_i} - \sum_{i=1}^n a_i \leq 0$, with equality if and only if each a_i are equivalent. Taking the derivative of V along a trajectory in Γ gives us

$$
\begin{aligned}
\dot{V} =\ & S' - \frac{f(S^*, I^*)}{f(S, I^*)} S' + I' - \frac{I^*}{I} I' \\
=\ & \Lambda - f(S, I) - \mu^S S - \frac{f(S^*, I^*)}{f(S, I^*)} \left(\Lambda - f(S, I) - \mu^S S \right) \\
& + f(S, I) - (\mu^I + \gamma) I - \frac{I^*}{I} \left(f(S, I) - (\mu^I + \gamma) I \right) \\
=\ & \left(f(S^*, I^*) + \mu^S S^* \right) - \mu^S S \\
& - \frac{f(S^*, I^*)}{f(S, I^*)} \left(\left(f(S^*, I^*) + \mu^S S^* \right) - f(S, I) - \mu^S S \right) \\
& - f(S^*, I^*) \frac{I}{I^*} - \frac{I^*}{I} \left(f(S, I) - f(S^*, I^*) \frac{I}{I^*} \right) \\
=\ & f(S^*, I^*) + \mu^S S^* - \mu^S S - f(S^*, I^*) \frac{f(S^*, I^*)}{f(S, I^*)} \\
& - \mu^S S^* \frac{f(S^*, I^*)}{f(S, I^*)} + f(S, I) \frac{f(S^*, I^*)}{f(S, I^*)} + \mu^S \frac{f(S^*, I^*)}{f(S, I^*)} S \\
& - f(S^*, I^*) \frac{I}{I^*} - f(S, I) \frac{I^*}{I} + f(S^*, I^*) \\
=\ & - \mu^S S \left(- \frac{S^*}{S} + 1 + \frac{f(S^*, I^*)}{f(S, I^*)} \frac{S^*}{S} - \frac{f(S^*, I^*)}{f(S, I^*)} \right) \\
& + f(S^*, I^*) \left(2 - \frac{f(S^*, I^*)}{f(S, I^*)} + \frac{f(S, I)}{f(S, I^*)} - \frac{I}{I^*} - \frac{f(S, I)}{f(S^*, I^*)} \frac{I^*}{I} \right) \\
=\ & - \frac{\mu^S}{f(S, I^*)} (S - S^*) (f(S, I^*) - f(S^*, I^*)) \\
& + f(S^*, I^*) \left(3 - \frac{f(S^*, I^*)}{f(S, I^*)} - \frac{f(S, I)}{f(S^*, I^*)} \frac{I^*}{I} - \frac{f(S, I^*)}{f(S, I)} \frac{I}{I^*} \right) \\
& + f(S^*, I^*) \left(\frac{f(S, I)}{f(S, I^*)} - 1 \right) \left(1 - \frac{f(S, I^*)}{f(S, I)} \frac{I}{I^*} \right) \\
& \leq 0.
\end{aligned}
$$

23

Since $\dot{V} = 0$ implies $S = S^*$ and $I = I^*$, the largest invariant set in Γ is the singleton $\{P^*\}$. By the LaSalle Invariance Principle [49], we obtain P^* is globally asymptotically stable and it is unique.

$\square$

The construction for this Lyapunov function can be found in [63]. If $f(S, I)$ is a monotone increasing function of S and I, and concave down in I, then conditions (2.15) and (2.16) will be satisfied. As a result, we can obtain the following corollaries.

Corollary 2.1.8. *Let $\delta = 0$, $f(S, I) = \beta SI$, and $\mathcal{R}_0 = \dfrac{\Lambda\beta}{\mu^S(\mu^I + \gamma)} > 1$. Then the endemic equilibrium P^* of system* (3.1)-(3.2) *is unique and globally asymptotically stable in the interior of Γ.*

Proof. If $f(S, I) = \beta SI$, then

$$
\begin{aligned}
(S - S^*)\left(f(S, I^*) - f(S^*, I^*)\right) &= (S - S^*)\left(\beta SI^* - \beta S^* I^*\right)\\
&= \beta I^* (S - S^*)^2\\
&> 0
\end{aligned}
$$

and

$$
\begin{aligned}
\left(\frac{f(S, I)}{f(S, I^*)} - 1\right)\left(1 - \frac{f(S, I^*)}{f(S, I)}\frac{I}{I^*}\right) &= \left(\frac{\beta SI}{\beta SI^*} - 1\right)\left(1 - \frac{\beta SI^*}{\beta SI}\frac{I}{I^*}\right)\\
&= \left(\frac{I}{I^*} - 1\right)(1 - 1)\\
&= 0
\end{aligned}
$$

24

with equality holding if and only if $S = S^*$ and $I = I^*$. Thus conditions (2.15) and (2.16) are satisfied.

□

Corollary 2.1.9. *Let $\delta = 0$, $f(S, I) = \beta \dfrac{SI}{S + I}$, and $\mathcal{R}_0 = \dfrac{\beta}{\mu^I + \gamma} > 1$. Then the endemic equilibrium P^* of system* (3.1)-(3.2) *is unique and globally asymptotically stable in the interior of* Γ.

Proof. If $f(S, I) = \beta \dfrac{SI}{S + I}$, then

$$
\begin{aligned}
(S - S^*)\left(f(S, I^*) - f(S^*, I^*)\right) &= (S - S^*)\left(\beta \frac{SI^*}{S + I^*} - \beta \frac{S^* I^*}{S^* + I^*}\right) \\
&= \beta I^*(S - S^*)\left(\frac{S}{S + I^*} - \frac{S^*}{S^* + I^*}\right) \\
&= \beta I^*(S - S^*)\left(\frac{S(S^* + I^*) - S^*(S + I^*)}{(S + I^*)(S^* + I^*)}\right) \\
&= \beta I^*(S - S^*)\left(\frac{SI^* - S^*I}{(S + I^*)(S^* + I^*)}\right) \\
&= \beta \frac{(I^*)^2(S - S^*)^2}{(S + I^*)(S^* + I^*)} \\
&\geq 0
\end{aligned}
$$

and

$$
\begin{aligned}
\left(\frac{f(S, I)}{f(S, I^*)} - 1\right)\left(1 - \frac{f(S, I^*)}{f(S, I)}\frac{I}{I^*}\right) &= \left(\frac{\beta SI}{S + I}\frac{S + I^*}{\beta SI^*} - 1\right)\left(1 - \frac{\beta SI^*}{S + I^*}\frac{S + I}{\beta SI}\frac{I}{I^*}\right) \\
&= \left(\frac{I}{I^*}\frac{S + I^*}{S + I} - 1\right)\left(1 - \frac{S + I}{S + I^*}\right) \\
&= \frac{S(S + I^*)}{I^*(S + I)}(I - I^*)(I^* - I)
\end{aligned}
$$

25

$$= -\frac{S(S + I^*)}{I^*(S + I)} \left(I - I^*\right)^2$$

$$\leq 0$$

with equality holding if and only if $S = S^*$ and $I = I^*$. Thus conditions (2.15) and (2.16) are satisfied.

$\square$

Global asymptotic stability has been shown for both of these functions for an SIR model before, but knowing these conditions are satisfied in the homogeneous case will allow us to use a combination of these functions for a heterogeneous model. Further, we can gain an equivalent condition if $f(S, I)$ is a separable nonlinear function.

Corollary 2.1.10. *Let $\delta = 0$, $f(S, I) = g(S)h(I)$, and*

$$\mathcal{R}_0 = \frac{g(S^0)}{\mu^I + \gamma} \lim_{I \to 0^+} \frac{h(I)}{I} > 1.$$

Then the endemic equilibrium P^* of system (3.1)-(3.2) is globally asymptotically stable in Γ if

$$\left(S - S^*\right)\left(h(S) - h(S^*)\right) \geq 0$$

and

$$\left(g(I) - g(I^*)\right)\left(\frac{g(I)}{I} - \frac{g(I^*)}{I^*}\right) \leq 0$$

26

with equality holding if and only if $S = S^*$ and $I = I^*$.

Not all incidence functions will satisfy conditions (2.15) and (2.16). For example, [55] gives rise to the interesting dynamics for incidence function $f(S, I) = \lambda S^q I^p$, where λ and q are positive parameters and $p > 1$. If $q = 1$ and $p = 2$, then the endemic equilibrium is not unique and cannot be globally asymptotically stable. Other dynamics arise for this incidence function, including the occurrence of Hopf bifurcation.

For the case of SIS type models, i.e. $\delta > 0$ and $\gamma = 0$, we can use similar Lyapunov functions with some coefficient modifications. For mass action incidence, i.e. $f(S, I) = \beta S I$ where β is a transmission coefficient, we can use the following Lyapunov function, modified from [69].

Proposition 2.1.11. *Assume $\delta > 0$, $\gamma = 0$, $f(S, I) = \beta SI$. If*

$$\mathcal{R}_0 = \frac{\Lambda \beta}{\mu^S \left(\mu^I + \delta\right)} > 1,$$

then the endemic equilibrium is unique and globally asymptotically stable in the interior of Γ.

Proof. From (2.4)-(2.5) evaluated at P^* we have

$$\mu^S = \frac{\Lambda}{S^*} - \beta I^* + \frac{\gamma I^*}{S^*}$$
$$\mu^I + \gamma = \beta S^*.$$

27

We will use the fact that $\int_1^x \frac{1-u}{u} du < 0$ when $x > 1$, with equality holding if and only if $x = 1$. Define

$$V = \left(S - S^* - S^* \ln \frac{S}{S^*} \right) + \frac{\beta S^* I^* - \gamma I^*}{\beta S^* I^*} \left(I - I^* - I^* \ln \frac{I}{I^*} \right) \geq 0$$

Note from (2.7) it follows that

$$\beta S^* I^* - \gamma I^* = \mu^I I^* > 0$$

inside of Γ. Differentiating along P^* gives us

$$\begin{aligned}
\dot{V} &= S' - \frac{S^*}{S} S' + \frac{\beta S^* I^* - \delta I^*}{\beta S^* I^*} \left(I' - \frac{I^*}{I} I' \right) \\
&= \left(\Lambda - \beta S I - \mu^S S + \gamma I - \frac{S^*}{S} \left(\Lambda - \beta S I - \mu^S S + \gamma I \right) \right) \\
&\quad + \frac{\beta S^* I^* - \delta I^*}{\beta S^* I^*} \left[\beta S I - \left(\mu^I + \gamma \right) I - \frac{I^*}{I} \left(\beta S I - \left(\mu^I + \gamma \right) I \right) \right] \\
&= \left(\Lambda - \beta S I - \mu^S S + \gamma I - \frac{S^*}{S} \left(\Lambda - \beta S I - \mu^S S + \gamma I \right) \right) \\
&\quad + \frac{\beta S^* I^* - \delta I^*}{\beta S^* I^*} \left[\beta S I - \left(\mu^I + \gamma \right) I - \frac{I^*}{I} \left(\beta S I - \left(\mu^I + \gamma \right) I \right) \right] \\
&= (\Lambda - \beta S I - \left(\frac{\Lambda}{S^*} - \beta I^* + \frac{\gamma I^*}{S^*} \right) S + \gamma I - \Lambda \frac{S^*}{S} + \beta S^* I \\
&\quad + \left(\frac{\Lambda}{S^*} - \beta I^* + \frac{\gamma I^*}{S^*} \right) S^* - \gamma \frac{S^*}{S} I) + \\
&\quad \frac{\beta S^* I^* - \delta I^*}{\beta S^* I^*} [\beta S I - \beta S^* I - \beta S I^* + \beta S^* I^*]
\end{aligned}$$

28

$$= \Lambda \left(2 - \frac{S}{S^*} - \frac{S^*}{S}\right) + \beta S^* I^* \left(-\frac{SI}{S^* I^*} + \frac{S}{S^*} + \frac{I}{I^*} - 1\right)$$

$$+ \gamma I \left(-\frac{SI^*}{S^* I} + 1 + \frac{I^*}{I} - \frac{S^*}{S}\right)$$

$$+ (\beta S^* I^* - \gamma I^*) \left[\frac{SI}{S^* I^*} - \frac{I}{I^*} - \frac{S}{S^*} + 1\right]$$

$$= \Lambda \left(2 - \frac{S}{S^*} - \frac{S^*}{S}\right) + \beta S^* I^* \left(-\frac{SI}{S^* I^*} + \frac{S}{S^*} + \frac{I}{I^*} - 1\right)$$

$$+ \gamma I \left(2 - \frac{S^*}{S} - \frac{S}{S^*} - 1 - \frac{SI^*}{S^* I} + \frac{I^*}{I} + \frac{S}{S^*}\right)$$

$$+ (\beta S^* I^* - \gamma I^*) \left[\frac{SI}{S^* I^*} - \frac{I}{I^*} - \frac{S}{S^*} + 1\right]$$

$$= (\Lambda + \gamma I) \left(2 - \frac{S}{S^*} - \frac{S^*}{S}\right)$$

$$\leq 0$$

hence V is a Lyapunov function for system (2.4)-(2.5). Since $\dot{V} = 0$ implies $\frac{S}{S^*} = 1$, the only invariant set such that $\dot{V} = 0$ is $\{P^*\}$. By the LaSalle Invariance Principle [49], we obtain P^* is globally asymptotically stable and it is unique.

$\square$

Additionally, the Lyapunov function

$$V = \frac{1}{2} [(S - S^*) + (I - I^*)]^2 + \frac{\mu^I + \mu^S}{\beta} \left(I - I^* - I^* \ln\left(\frac{I}{I^*}\right)\right)$$

as in [69] can be used to give global asymptotic stability in Proposition 2.1.11. This combination of logarithmic Lyapunov function with a quadratic function being positive does not rely on the condition $\beta S^* I^* - \gamma I^* > 0$.

Requiring this type of Lyapunov function for global stability to avoid secondary conditions in the SIS causes obstacles to extend the homogeneous model to a heterogeneous model. In Chapter 3, we will overcome some of these barriers by imposing some biologically reasonable assumptions.

2.1.8   Equilibria Levels

In this section, we investigate the difference between the SIS and SIR models at the equilibrium states, specifically for the mass action incidence function. Throughout this section, we will assume $f(S, I) = \beta SI$.

For the SIR model, the additional condition $S(t) \leq S^0$ can be imposed in the feasible region, see Section 2.1.5.

On the contrary, the same may not necessarily be true for the SIS model. The endemic equilibrium is given by $P^* = (S^*, I^*) = \left(\dfrac{\mu^I + \gamma}{\beta}, \dfrac{\mu^S}{\mu^I} \left(S^0 - S^* \right) \right)$. Depending on the values of the compartmental death rates, we can prove a relationship between the two equilibrium states for mass action incidence.

Recall from Section 2.1.1, the total population influencing the disease dynamics is given by $N = S + I$.

Theorem 2.1.12. *Let $P^0 = (S^0, 0)$ and $P^* = (S^*, I^*)$ be the disease-free equilibrium and endemic equilibrium for system (2.4)-(2.5), respectively.*

(i) If $\mu^I = \mu^S$, then $N^* = N^0$.

(ii) If $\mu^I > \mu^S$, then $N^* < N^0$.

(iii) If $\mu^I < \mu^S$, then $N^* > N^0$.

Proof. Consider

$$N^* - N^0 = I^* + S^* - S^0$$
$$= \frac{\mu^S}{\mu^I}\left(S^0 - S^*\right) + S^* - S^0$$
$$= \left(\frac{\mu^S}{\mu^I} - 1\right)\left(S^0 - S^*\right).$$

If $\mu^I = \mu^S$, we have $\left(\dfrac{\mu^S}{\mu^I} - 1\right) = 0$ and hence $N^* = N^0$.

If $\mu^I > \mu^S$, we have $\left(\dfrac{\mu^S}{\mu^I} - 1\right) < 0$ and hence $N^* < N^0$.

If $\mu^I < \mu^S$, we have $\left(\dfrac{\mu^S}{\mu^I} - 1\right) > 0$ and hence $N^* > N^0$.

$\square$

Thus, it is not guaranteed that $S^* + I^* \leq S^0$, unless the additional assumption $\mu^S \leq \mu^I$ is imposed. Biologically, an infection does not typically guarantee host immunity from natural death, so this may be a reasonable assumption for most models. If this condition is imposed, it follows

$$N' = S' + I' = \Lambda - \mu^S S - \mu^I I$$
$$\leq \Lambda - \mu^S N.$$

31

Solving this differential inequality leads to $\limsup_{t\to\infty} N(t) \leq \dfrac{\Lambda}{\mu^S} = S^0$. Thus the additional condition $S(t) + I(t) \leq S^0$ can be imposed in the feasible region, and global asymptotic stability of the DFE for (2.4)-(2.5) with $\delta \geq 0$ and $\gamma \geq 0$ is obtained from Theorem 2.1.3.

In Chapter 3, we can impose a similar biologically reasonable assumption to help obtain global stability of our equilibria.

2.2 Matrix Theory

In this section, we provide an overview of definitions and results from matrix theory to be used in this thesis. Further definitions and properties can be found in [39] and [77].

Throughout this section, let A be an $n \times n$ square matrix with real entries, i.e. $A \in \mathbf{M}_n(\mathbb{R})$.

2.2.1 Basic Definitions

First, we start with our basic definitions.

Let $A \in \mathbf{M}_n(\mathbb{R})$. The *minor* associated to the $(i,j)^{\text{th}}$ entry is the determinant of the submatrix of A formed by deleting the ith row and j^{th} column. If $i = j$, then the minor is called a *principal minor*. The minor associated the $(i,j)^{\text{th}}$ entry is often denoted as $M(i|j)$ or $M_{i,j}$.

The *cofactor* associated to the $(i, j)^{\text{th}}$ entry of A is denoted $C_{i,j}$. A cofactor is simply a signed minor. Explicitly, we have $C_{i,j} = (-1)^{i+j} M_{i,j}$ to define the relationship between cofactors and minors. The *adjoint* of matrix A is also an $n \times n$ matrix, denoted $\text{adj}(A)$; its entries are $(\text{adj}(A))_{ij} = C_{i,j}$.

The adjoint of A, in conjunction with the determinant of A, is used to the find the inverse of A. If the determinant is nonzero, i.e. $\det(A) \neq 0$, then the matrix is invertible and is defined by $A^{-1} = \dfrac{1}{\det(A)} \text{adj}(A)$; otherwise the inverse does not exists [77].

We will utilize cofactors to find the limiting behavior of our disease-free equilibrium and basic reproduction number in Chapter 3.

To introduce our next concept, we begin by defining a *permutation matrix*, P. A *permutation matrix*, P, is a square matrix where each column and row has exactly one entry with element 1 and all remaining entries with 0. A permutation matrix will permute the rows of A by left multiplication, PA; likewise, it will permute the columns of A by right multiplication, AP. From permutation matrices, we obtain an important matrix characterization.

A matrix A is *reducible* if there exists a permutation matrix P such that $P^T AP$ is an upper-block triangular matrix, i.e.

$$
P^T AP = \begin{bmatrix} B & C \\ \mathbf{0} & D \end{bmatrix},
$$

where $B \in \mathbf{M}_k(\mathbb{R})$, $C \in \mathbf{M}_{k,n-k}(\mathbb{R})$, $D \in \mathbf{M}_{n-k}(\mathbb{R})$, and $\mathbf{0}$ is a $k \times (n-k)$ matrix

whose entries are zero. If no such permutation matrix exists, then A is said to be *irreducible*.

We will use the concept of a matrix being irreducible to impose assumptions for our epidemiological model and in turn prove global asymptotic stability results. We will also see a connection between irreducibility and a strongly connected digraph in Section 2.3.

Finally, we introduce some common notation for comparing matrices. Let $A = [a_{ij}]$ and $B = [b_{ij}]$ be matrices such that $A, B \in \mathbf{M}_n(\mathbb{R})$. We say $A \geq B$ if $a_{ij} \geq b_{ij}$ for all $i, j = 1, 2, \ldots, n$. Further, if $a_{ij} > 0$ for all $i, j = 1, 2, \ldots, n$, then $A > 0$ is a *positive* matrix.

2.2.2 M-Matrices

Properties of M-matrices will consistently be used throughout this dissertation, and thus present a formal definition regarding this class of matrices.

Often in epidemiology, matrices of the form

$$
A = \begin{bmatrix}
a_{11} & -a_{12} & -a_{13} & \cdots & -a_{1n} \\
-a_{21} & a_{22} & -a_{23} & \cdots & -a_{2n} \\
-a_{31} & -a_{32} & a_{33} & \cdots & -a_{3n} \\
\vdots & \vdots & \vdots & \ddots & \vdots \\
-a_{n1} & -a_{n2} & -a_{n3} & \cdots & a_{nn}
\end{bmatrix},
$$

where $a_{ij} \geq 0$ for all $i, j \in \{1, 2, \ldots, n\}$, will arise. A matrix A of this form can be classified as an M-*matrix*. More formally, we have the following definition.

If $A = sI - B$, where $B = [b_{ij}]$ with $b_{ij} \geq 0$ for all $i, j \in \{1, 2, \ldots, n\}$ and $s \geq \rho(B)$, then A is said to be a **M**-*matrix*. Further, A is a non-singular M-matrix, if $s > \rho(B)$.

Plemmons provides a survey of forty conditions equivalent to the statement "A is a non-singular M-matrix" in [60, Theorem 1]. The following proposition provides a few such characterizations.

Proposition 2.2.1. *If $A \in \mathbf{M}_n(\mathbb{R})$, then each of the following conditions is equivalent to the statement: A is a nonsingular M-matrix.*

(a) *All principal minors of A are positive.*

(b) *Every real eigenvalue of A is positive.*

(c) *$A + \alpha I$ is nonsingular for each scalar $\alpha \geq 0$.*

(d) *There exists lower and upper triangular matrices L and U, respectively, with positive diagonals, such that $A = LU$.*

(e) *A is inverse-positive. That is A^{-1} exists and $A^{-1} \geq 0$.*

(f) *A is monotone. That is, $Ax \geq 0$ implies $x \geq 0$ for all $x \in \mathbb{R}^n$.*

Equivalent condition (e) will be useful for many of our results in Chapter 3.

2.2.3   Perron-Frobenius Theorem

Finally, we present the Perron-Frobenius Theorem. This theorem is particularly important for the construction of Lyapunov functions in Chapter 3.

Perron-Frobenius Theorem: *Let $A \in \mathbf{M}_n(\mathbb{R})$ be an irreducible nonnegative matrix.*

(i) *The spectral radius $\rho(A)$ of A is an eigenvalue of A, that is, A has a positive eigenvalue r that is greater than or equal to the absolute value of every eigenvalue of A. The number r, which is the same as the spectral radius of A, is sometimes called the Perron eigenvalue of A.*

(ii) *The algebraic multiplicity, and so the geometric multiplicity, of the Perron eigenvalue r equals 1, that is, r is a simple root of the characteristic polynomial of A.*

(iii) *Corresponding to the Perron eigenvalue r there is a positive eigenvector ω: $A\omega = r\omega$, where ω is a positive vector. The vector ω, and each of its positive multiples, is called a Perron vector of A. The matrix A has no other nonnegative eigenvectors (corresponding to any eigenvalue) other than positive multiples of its Perron vector.*

(iv) *If A' is a principal submatrix of A, then*

$$\rho(A') \leq \rho(A)$$

with equality if and only if $A' = A$.

36

(v) If B is a nonnegative matrix with $A \geq B$, then

$$\rho(A) \geq \rho(B)$$

with equality if and only if $B = A$.

A proof can be seen in [10].

2.3   Graph Theory

In this section, we provide an overview of definitions and results from graph theory which will be used in this thesis. Further definitions and results can be found in [15], [22], or [72].

2.3.1   Basic Terminology
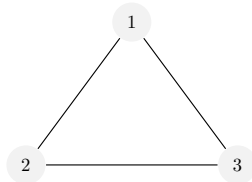
Figure 2.2: Visualization of a graph with 3 nodes.

A *graph* is a pair $G = (V, E)$ of two sets V and E where $E \subseteq [V]^2$. The elements of V are the *vertices*, or *nodes*, and the elements of E are 2-element subsets of V,

called the *edges*. Figure 2.2 gives an example of a simple graph where the vertex set is $V = \{1, 2, 3\}$ and the edge set is $E = \{(1, 2), (1, 3), (2, 3)\}$.

In a graph, the edges are unordered pairs. For example, edge $(1, 2)$ would be equivalent to $(2, 1)$ in Figure 2.2. For this thesis, the direction between nodes have a significant impact in our results. Thus, we need to consider a *directed graph*, or *digraph*. A *directed graph* is a pair $G = (V, E)$, where E is a set of ordered pairs called *directed arcs*. If $e = (x, y) \in E$ and $x, y \in V$, then x is the *initial vertex* of e and y is the *terminal vertex* of e. If $x = y$, then $e = (x, x)$ is a *loop* at vertex x.

(a) A directed graph

(b) Weighted directed graph
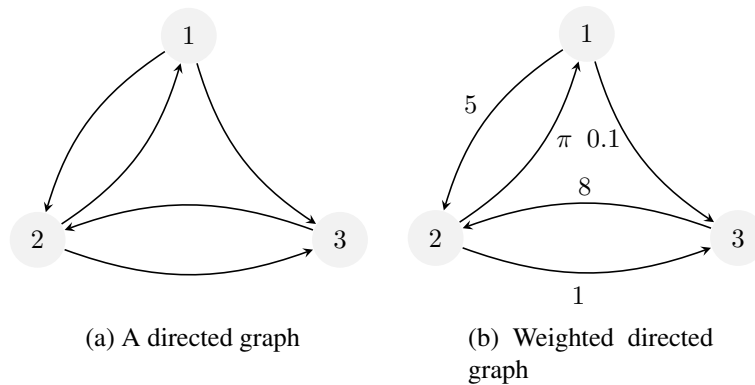
Figure 2.3: Visualizations of two directed graphs with the same arc set. (a) is an unweighted directed graph and (b) is a weighted directed graph.

Figure 2.3 gives a visualization of a directed graph, where $V = \{1, 2, 3\}$ and $E = \{(1, 2), (1, 3), (2, 1), (2, 3), (3, 2)\}$. Additionally, weights can be assigned to each of the directed arcs, as shown in Figure 2.3.

Let $A \in \mathbf{M}_n(\mathbb{R})$ where $A = [a_{ij}]$. We can associate A to a *directed graph* $\mathcal{D}(A)$ with n vertices. For each element $a_{ij} \neq 0$ for $i, j = 1, 2, \ldots, n$, there exists a

38

directed arc from vertex j to vertex i with weight a_{ij}. If $a_{ii} \neq 0$, then a_{ii} forms a loop at vertex i. If $a_{ij} = 0$, then no edge exists between vertex j and vertex i [15]. For instance, Figure 2.3(b) is the directed graph associated to the matrix

$$
A = \begin{bmatrix} 0 & \pi & 0 \\ 5 & 0 & 8 \\ 0.1 & 1 & 0 \end{bmatrix}.
$$

From $\mathcal{D}(A)$, the *Laplacian matrix*, L, is thus formed as follows:

$$
L = \begin{bmatrix} \displaystyle\sum_{j\neq 1}^{n} a_{j1} & -a_{12} & \dots & -a_{1n} \\ -a_{21} & \displaystyle\sum_{j\neq 2}^{n} a_{j2} & \dots & -a_{2n} \\ \vdots & \vdots & \ddots & \vdots \\ -a_{n1} & -a_{n2} & \dots & \displaystyle\sum_{j\neq n}^{n} a_{jn} \end{bmatrix}.
$$

The off-diagonal entries of L are defined as the negative corresponding entries in A, and the diagonal entries of L are chosen such that the column sums of L are zero, hence L is a singular matrix.

A *subgraph*, $G' = (V', E')$, is a directed graph such that $E' \subseteq E$ and $V' \subseteq V$. We say G' is a *spanning subgraph* if $V' = V$. Notationally, we can say $G' \subseteq G$ whenever G' is a subgraph of G. Figure 2.4 gives a simple visual of a subdigraph and spanning subdigraph.
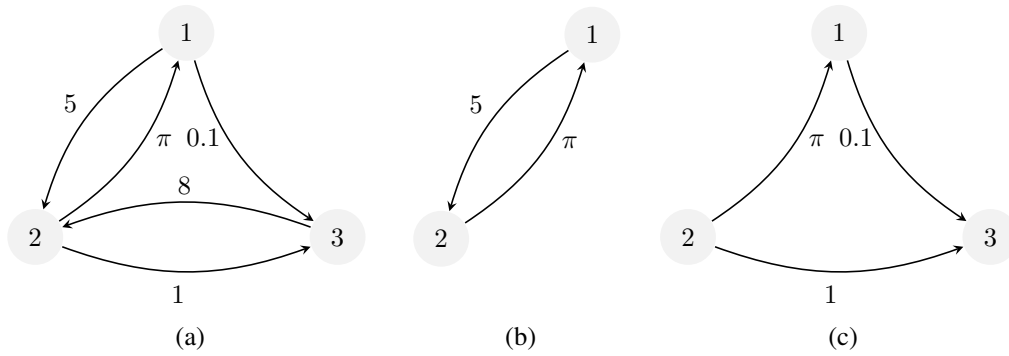
Figure 2.4: Visualization of subgraphs. (a) The directed graph G. (b) A subgraph G' of G. (c) A spanning subgraph G'' of G.

Within each directed graph, there are many structures, subgraphs, and characterizations that can be useful in determining properties about a directed graph or associated matrices.

A *walk* in a directed graph G joining vertices u and v is a sequence, γ, of vertices $u = x_0, x_1, \ldots, x_k = v$ and edges $e_0, e_1, \ldots, e_{k-1}$ such that $e_i = (x_i, x_{i+1})$ is a directed edge from vertex x_i to x_{i+1} for all $i = 0, 1, \ldots, k - 1$. If the vertices $u = x_0, x_1, \ldots, x_k = v$ are distinct, then we say γ is a *path* in G. If $u = v$, then γ is a *cycle* in G. Figure 2.5 gives visualizations for each type of subgraph.

Further, paths lead to a second important characterization of a graph. A directed graph G is *strongly connected* if for each pair of distinct vertices u and v, there exists a path from u to v and a path from v to u.

Since each matrix is associated to a directed graph, a matrix $A \in \mathbf{M}_n(\mathbb{R})$ is *irreducible* provided the associated digraph $D(A)$ is strongly connected. Since A

cannot be permuted to an upper-block triangular matrix, there is no partition of the vertex set into two nonempty sets U and W such that each edge of $D(A)$ has its initial vertex in U and terminal vertex in W.

(a) Graph G (b) Path P (c) Cycle C
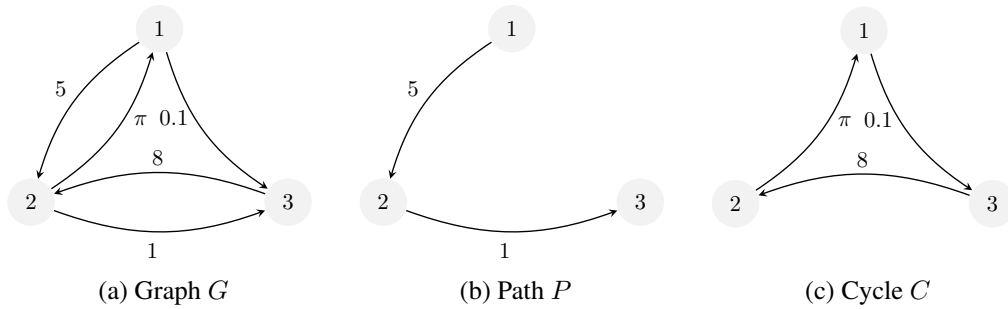
Figure 2.5: Visualization of some special subgraphs. (a) The directed graph G. (b) A path P in G. (c) A cycle C in G.

(a)   (b)   (c)
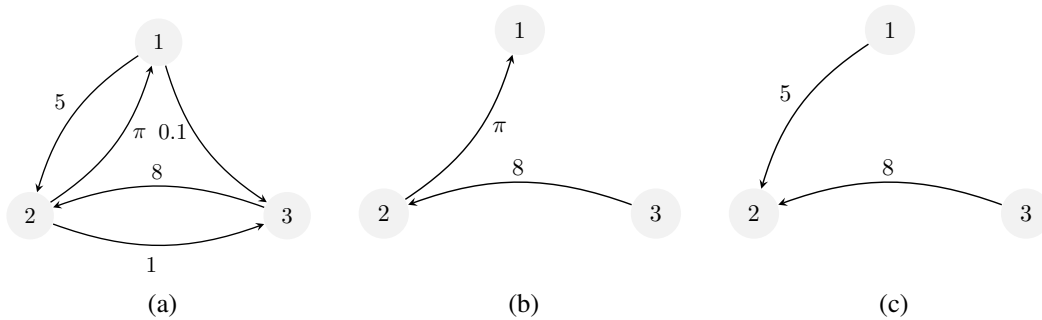
Figure 2.6: Visualizations of spanning rooted-in trees. (a) The directed graph G. (b) A spanning tree rooted at vertex 1 with weight 8π. (c) A spanning tree rooted at vertex 2 with weight 40.

The last particular subgraph is a special spanning subgraph. A *spanning tree rooted-in at vertex k*, denoted $\mathcal{T} = (E', V')$, is a spanning, acyclic, connected subgraph of

41

G such that $V' = V$ and for each vertex $i \neq k$, the out-degree of $i = 1$, while the out-degree of $k = 0$. Further the subgraph is *acyclic*, and hence contains no cycles. The weight of the spanning tree in a directed graph is the product of the weights of the arcs in the spanning tree. Figure 2.6 gives a visualization of two spanning rooted-in trees.

2.3.2   Matrix Tree Theorem

Kirchhoff's Matrix Tree Theorem relates the cofactors of the Laplacian matrix to the spanning trees of an undirected graph [72]. We present the generalized version for directed graphs.

Matrix Tree Theorem for Directed Graphs: *Assume $n \geq 2$. Then*

$$C_{i,i} = \sum_{\mathcal{T} \in \mathbb{T}_i} \prod_{(s,r) \in E(\mathcal{T})} a_{rs}$$

for $i = 1, 2, \ldots, n$, where $\mathbb{T}_i$ is the set of all spanning trees $\mathcal{T}$ of G that are rooted at vertex i and $E(\mathcal{T})$ is the arc set of $\mathcal{T}$.

A proof can be found in [57].

In Figure 2.7, we provide an example to calculate the cofactors of the matrix

$$A = \begin{bmatrix} 0 & \pi & 0 \\ 5 & 0 & 8 \\ 0.1 & 1 & 0 \end{bmatrix}.$$

42

Figure 2.7(a) shows the visualization for the directed graph associated with A. Figure 2.7(b) shows the only spanning rooted-in tree at vertex 1, with weight 8π. Thus, $C_{1,1} = 8\pi$ from the Matrix Tree Theorem for Directed Graphs. In Figure 2.8, we can see there are two spanning rooted-in trees at vertex 2, $\mathcal{T}$ and $\mathcal{T}'$. The weight of $\mathcal{T}$ is 40 and the weight of $\mathcal{T}'$ is 0.8, hence $C_{2,2} = 40.8$.

(a) Graph $G = \mathcal{D}(A)$

(b) Spanning rooted-in tree at vertex 1
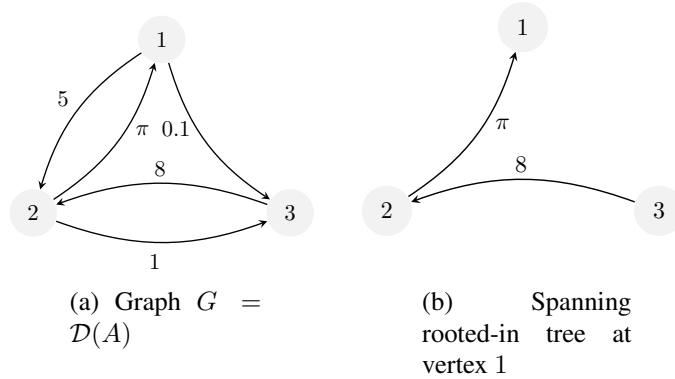
Figure 2.7: (a) The directed graph G. (b) The only spanning rooted tree at vertex 1.

(a) $\mathcal{T}$

(b) $\mathcal{T}'$
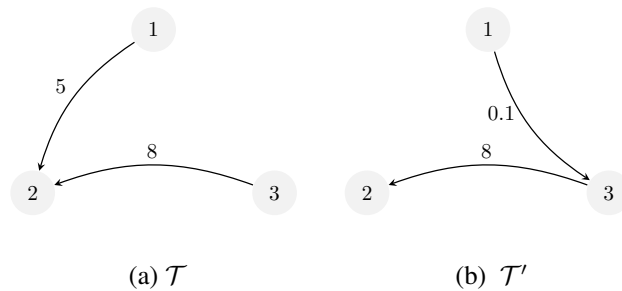
Figure 2.8: (a) One spanning rooted-in tree at vertex 2, denoted $\mathcal{T}$. (b) A second spanning rooted-in tree at vertex 2, denoted $\mathcal{T}'$.

43

As a result of the Matrix Tree Theorem for Directed Graphs, the cofactors of the Laplacian matrix are determined by the structure and arc weights of the corresponding directed graph. Since L is a singular matrix and an associated eigenvector to eigenvalue 0 has components $C_{i,i}$, we will see a connection to the rooted-in trees in Chapter 3.

CHAPTER 3: ANALYTICAL INVESITIGATION OF A HETEROGENEOUS MODEL

In this chapter, an n-patch model is introduced. Each patch can represent a city, country, etc., indexed by the set $\{1, 2, \ldots, n\}$. Within each ith patch, a model with the structure from Section 2.1 is applied. An arbitrary incidence function and separate demographics are considered among each patch. Directed movement is incorporated to account for travel between patches, where the movement can be asymmetric between two locations. Asymmetric movement allows the travel to be skewed towards some patches, since movement into a major city can have a larger rate than the movement out into the surrounding areas. This extends the prior homogeneous model to account for spatial heterogeneity.

3.1 A General Heterogeneous Model

We will focus primarily on the following n-patch model ($n \geq 1$) which includes demographics. Let

$$S_i' = \Lambda_i - f_i(S_i, I_i) - \mu_i^S S_i + \delta_i I_i + d_S \sum_{j=1}^{n} m_{ij} S_j - d_S \sum_{j=1}^{n} m_{ji} S_i, \qquad (3.1)$$

$$I_i' = f_i(S_i, I_i) - (\mu_i^I + \gamma_i + \delta_i) I_i + d_I \sum_{j=1}^{n} m_{ij} I_j - d_I \sum_{j=1}^{n} m_{ji} I_i, \qquad (3.2)$$

$$R_i' = \gamma_i I_i - \mu_i^R R_i + d_R \sum_{j=1}^{n} m_{ij} R_j - d_R \sum_{j=1}^{n} m_{ji} R_i, \qquad (3.3)$$

for $i = 1, 2, \ldots, n$, with nonnegative initial conditions $S_i(0), I_i(0), R_i(0)$, where $S_i = S_i(t)$, $I_i = I_i(t)$, and $R_i = R_i(t)$ represent the population density of susceptible, infectious, and removed individuals, respectively, at time t, and

$$\sum_{i=1}^{n} (S_i(0) + I_i(0)) > 0. \tag{3.4}$$

Here $'$ is the derivative with respect to time. Table 3.1 outlines the parameter definitions. Each of these parameters Λ_i, μ_i^S, μ_i^I, and β_i are positive values, and γ_i and δ_i are non-negative. Figure 3.1 gives a visualization of the model for $n = 2$. The $n \times n$ matrix $M = [m_{ij}]$ describes the directed movement of individuals among the patches. Specifically, each (i, j) entry of the movement matrix represents the directed moving from patch j to patch i, and hence $m_{ij} \geq 0$ for all i and j.

Table 3.1: A table outlining the parameters used in (3.1)-(3.3)

Parameter	Definition	Units
Λ_i	birth rate of susceptible individuals in patch i	people/time
β_i	transmission coefficient in patch i	$(\text{people} \cdot \text{time})^{-1}$
μ_i^S	death rate of susceptible individuals in patch i	time^{-1}
μ_i^I	death rate of infectious individuals in patch i	time^{-1}
μ_i^R	death rate of removed individuals in patch i	time^{-1}
γ_i, δ_i	disease recovery rates in patch i	time^{-1}
m_{ij}	movement rate of individuals from patch j to patch i	time^{-1}
d_S	diffusion coefficient for susceptible individuals	unitless
d_I	diffusion coefficient for infectious individuals	unitless
d_R	diffusion coefficient for removed individuals	unitless
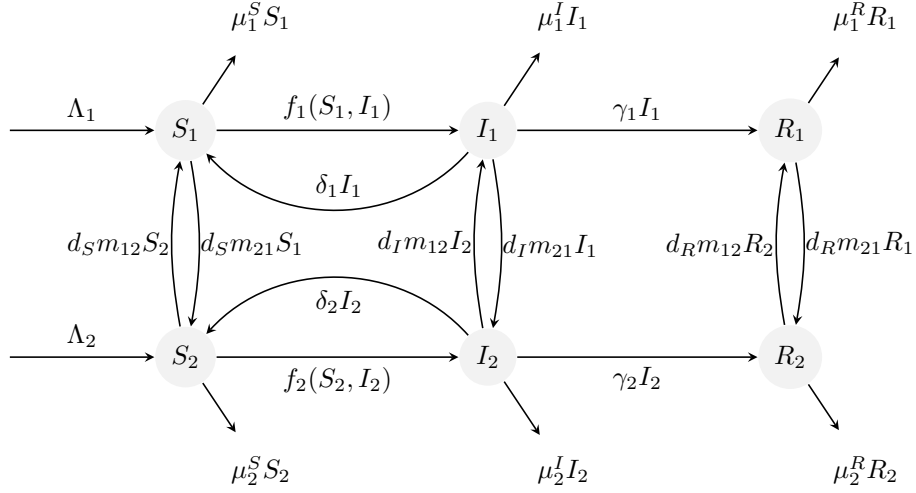
Figure 3.1: Flowchart for 2-patch model with demographics.

In a similar manner as the heterogeneous model, the following assumptions on $f_i(S_i, I_i)$, for $i = 1, 2, \ldots, n$, are required either biologically or mathematically:

(i) $f_i(S_i, I_i) \geq 0$ for all $S_i, I_i \geq 0$;

(ii) $f_i \in C([0, \infty) \times [0, \infty))$;

(iii) $f_i(S_i, 0) = f_i(0, I_i) = 0$ for all $S_i, I_i \geq 0$;

(iv) $\displaystyle\lim_{I_i \to 0^+} \frac{f_i(S_i, I_i)}{I_i}$ exists for all $S_i \geq 0$.

Similar to the homogeneous model, since R_i does not appear in (3.1)-(3.2) we can

study the reduced system

$$S_i' = \Lambda_i - f_i(S_i I_i) - \mu_i^S S_i + \delta_i I_i + d_S \sum_{j=1}^{n} m_{ij} S_j - d_S \sum_{j=1}^{n} m_{ji} S_i, \qquad (3.5)$$

$$I_i' = f_i(S_i I_i) - (\mu_i^I + \gamma_i + \delta_i) I_i + d_I \sum_{j=1}^{n} m_{ij} I_j - d_I \sum_{j=1}^{n} m_{ji} I_i. \qquad (3.6)$$

Then, the dynamics of R_i can be further studied.

3.2   Disease-Free Equilibrium

The system (3.5)-(3.6) admits two types of equilibria. To find the DFE, each $I_i = 0$ for $i = 1, 2, \ldots, n$. Thus, from (3.5)-(3.6), for $i = 1, 2, \ldots, n$ we have

$$\begin{aligned} 0 &= \Lambda_i - f_i(S_i, 0) - \mu_i^S S_i + d_S \sum_{j=1}^{n} m_{ij} S_j - d_S \sum_{j=1}^{n} m_{ji} S_i. \\ &= \Lambda_i - \mu_i^S S_i + d_S \sum_{j=1}^{n} m_{ij} S_j - d_S \sum_{j=1}^{n} m_{ji} S_i. \end{aligned}$$

Hence,

$$\Lambda_i = \left(\mu_i^S + d_S \sum_{j=1}^{n} m_{ji} \right) S_i - d_S \sum_{j=1}^{n} m_{ij} S_j, \quad \text{for } i = 1, 2, \ldots, n. \quad (3.7)$$

Let $\Lambda = (\Lambda_1, \Lambda_2, \ldots, \Lambda_n)^T$, $S = (S_1, S_2, \ldots, S_n)^T$, and define

$$D = \begin{bmatrix} \mu_1^S + d_S \sum_{j \neq 1}^{n} m_{j1} & -d_S m_{12} & \ldots & -d_S m_{1n} \\ -d_S m_{21} & \mu_2^S + d_S \sum_{j \neq 2}^{n} m_{j2} & \ldots & -d_S m_{2n} \\ \vdots & \vdots & \ddots & \vdots \\ -d_S m_{n1} & -d_S m_{n2} & \ldots & \mu_n^S + d_S \sum_{j \neq n}^{n} m_{jn} \end{bmatrix}.$$

We can write the linear system (3.7) as the matrix equation $\Lambda = DS$.

Lemma 3.2.1. *There exists a unique solution to $\Lambda = DS$, and hence the disease free equilibrium is unique.*

Proof. Since D is a nonsingular M-matrix, D^{-1} exists and is non-negative [60], hence $S = D^{-1}\Lambda \geq 0$.

□

Defining $S^0 = (S_1^0, S_2^0, \ldots, S_n^0) = D^{-1}\Lambda$, we then denote the disease-free equilibrium to be $P_0 = (S_1^0, 0, S_2^0, 0, \ldots, S_n^0, 0)$.

3.3   Positively Invariant Sets

In this section, two different positively invariant sets are determined. First, a feasible region is calculated in Section 3.3.1 which is determined by the system (3.5)-(3.6). In this region, global asymptotic stability of the SIR heterogeneous model

with nonlinear incidence is studied. In Section 3.3.2, a second positively invariant set is calculated after two biological assumptions, in which global stability of the SIS heterogeneous model with mass action incidence is studied.

3.3.1 Feasible Region Γ

Let $\overline{\Lambda} = \sum_{i=1}^{n}(\Lambda_i)$, $\mu^* = \min\{\mu_i^S, \mu_i^I + \gamma_i + \delta_i\}$, and $N = \sum_{i=1}^{n}(S_i + I_i)$, where N represents the total population influencing the disease dynamics. It follows that

$$N' = \sum_{i=1}^{n}(S_i' + I_i') \leq \overline{\Lambda} - \mu^* N.$$

Solving the differential inequality, we arrive at $N(t) \leq \overline{\Lambda}/\mu^* - N(0)e^{-\mu^* t}$, and hence $\limsup_{t \to \infty} N(t) \leq \overline{\Lambda}/\mu^*$. We call our feasible region Γ and define it as

$$\Gamma = \left\{ (S_1, I_1, \ldots, S_n, I_n) \in \mathbb{R}_+^{2n} \,\middle|\, \sum_{i=1}^{n}(S_i + I_i) \leq \frac{\overline{\Lambda}}{\mu^*} \right\}.$$

It can be verified Γ is positively invariant in a similar method to Lemma 2.1.1.

Next, we verify there are no other equilibria on the boundary of Γ.

Theorem 3.3.1. *Assume the movement matrix $M = [m_{ij}]$ is irreducible. Then P_0 is the only equilibrium point on the boundary of Γ.*

Proof. Let $I_i = 0$ for some i. From (3.6) we obtain

$$0 = \sum_{j \neq i}^{n} m_{ij} I_j. \tag{3.8}$$

50

Thus, if $I_i = 0$ and $m_{ij} > 0$, then $I_j = 0$ for some j. Using our irreducibility assumption on M, we know that there exists a path from I_i to I_j. Applying (3.8), we see

$$0 = m_{ie_1}I_{e_1} + m_{e_1e_2}I_{e_2} + \cdots + m_{e_{m-1}e_m}I_m + m_{e_mj}I_j,$$

and hence

$$I_{e_1} = 0, I_{e_2} = 0, \ldots, I_m = 0.$$

It thus follows $I_j = 0$ for all j. Thus, when M is irreducible and $I_i = 0$ for some i, we must have $I_i = 0$ for all $i = 1, \ldots, n$. It follows P_0 is the only equilibrium point on the boundary.

$\square$

3.3.2   Region $\widetilde{\Gamma}$

In this section, we assume $\mu_i^S \leq \mu_i^I$ for $i = 1, 2, \ldots, n$, and hence infection does not grant the host individual immunity against natural death. Consider a second region,

$$\widetilde{\Gamma} = \left\{ (S_1, I_1, \ldots, S_n, I_n) \in \mathbb{R}_+^{2n} \,\middle|\, S_i + I_i \leq S_i^0, \sum_{i=1}^{n}(S_i + I_i) \leq \frac{\overline{\Lambda}}{\mu^*} \right\}.$$

We define this second region to obtain a positively invariant set for the system. The following theorem shows this result.

Theorem 3.3.2. *The feasible region $\widetilde{\Gamma}$ is positively invariant set with respect to (3.5)-(3.6) when $d_S = d_I$.*

Proof. Assume $d_S = d_I$ and let $N = (N_1, N_2, \ldots, N_n)$ where $N_i = S_i + I_i$. Since

$$
\begin{aligned}
N_i' &= S_i' + I_i' \\
&\leq \Lambda_i - \mu_S N_i + d_S \sum_{j=1}^n m_{ij} N_j - d_S \sum_{j=1}^n m_{ji} N_i \\
&= \Lambda_i - \left(\left(\mu_S + d_S \sum_{j=1}^n m_{ij} N_i \right) N_i - d_S \sum_{j=1}^n m_{ij} N_j \right) \\
&= \left[DS^0 - DN \right]_i
\end{aligned}
$$

we have $N_i' \leq 0$ if $N_i \leq S_i^0$. By a similar method in the proof of Lemma 2.1.1, we can obtain $\tilde{\Gamma}$ is positively invariant with respect to (3.5)-(3.6).

□

This second region is a smaller region, in which we can study global asymptotic stability for the SIS multipatch model with mass action incidence. It requires two assumptions: $\mu_i^S \leq \mu_i^I$ for each i and $d_S = d_I$. The first assumption is a natural biological assumption, while the second tells us the infection does not inhibit the travel of infectious individuals. For most sexually transmitted infections, this is a biological reasonable assumption, since the infection would not prevent the host individual from traveling.

Corollary 3.3.3. *Assume the movement matrix $M = [m_{ij}]$ is irreducible and that $I_i = 0$ for some $i = 1, \ldots, n$, then $I_j = 0$ for all $j \neq i$. It then follows P_0 is the only equilibrium point on the boundary of $\tilde{\Gamma}$.*

This result follows in the same fashion as Theorem 3.3.1.

3.4 Basic Reproduction Number $\mathcal{R}_0$

Utilizing the next generation method as described in the paper by van den Driessche and Watmough [68], and as outlined in Section 2.1.4, we define the new disease matrix

$$
F = \begin{bmatrix}
\lim\limits_{I_1 \to 0^+} \dfrac{f_1(S_1^0, I_1)}{I_1} & 0 & \cdots & 0 \\
0 & \lim\limits_{I_2 \to 0^+} \dfrac{f_2(S_2^0, I_2)}{I_2} & \cdots & 0 \\
\vdots & \vdots & \ddots & \vdots \\
0 & 0 & \cdots & \lim\limits_{I_n \to 0^+} \dfrac{f_n(S_n^0, I_n)}{I_n}
\end{bmatrix}
$$

and the disease transfer matrix

$$
V = \begin{bmatrix}
(\mu_1^I + \gamma_1 + \delta_1) + d_I \sum\limits_{j \neq 1}^{n} m_{j1} & -d_I m_{12} & \cdots & -d_I m_{1n} \\
-d_I m_{21} & (\mu_2^I + \gamma_2 + \delta_2) + d_I \sum\limits_{j \neq 2}^{n} m_{j2} & \cdots & -d_I m_{2n} \\
\vdots & \vdots & \ddots & \vdots \\
-d_I m_{n1} & -d_I m_{n2} & \cdots & (\mu_n^I + \gamma_n + \delta + n) + d_I \sum\limits_{j \neq n}^{n} m_{jn}
\end{bmatrix}.
$$

The basic reproduction number is the spectral radius of the next-generation matrix, i.e. $\mathcal{R}_0 = \rho(FV^{-1})$.

3.5 Global Stability of Disease-Free Equilibrium

By Theorem 2 from van den Driessche and Watmough [68], the DFE is locally asymptotically stable if $\mathcal{R}_0 < 1$ and unstable if $\mathcal{R}_0 > 1$.

Proposition 3.5.1. *If $\mathcal{R}_0 < 1$, the DFE of* (3.1)-(3.2) *is locally stable. If $\mathcal{R}_0 > 1$, the DFE is unstable.*

The following results show the DFE is globally asymptotically stable if $\mathcal{R}_0 \leq 1$.

Theorem 3.5.2. *Assume $\mathcal{R}_0 \leq 1$, $M = [m_{ij}]$ is irreducible, and*

$$0 \leq f_i(S, I) \leq \left(\lim_{I_i \to 0^+} \frac{f_i(S_i^0, I_i)}{I_i} \right) I_i, \quad \text{for } i = 1, 2, \ldots, n \qquad (3.9)$$

with equality if and only if $S_i = S_i^0$ for $i = 1, 2, \ldots, n$. Then the DFE for system (3.5)-(3.6) is globally asymptotically stable in the interior of Γ.

Proof. Since V is column diagonally dominant, we can obtain that V is a non-singular M-matrix. Thus $V^{-1} \geq 0$. Further, since $[m_{ij}]$ is irreducible, from Theorem 1.3d in Plemmons and Berman [10] we obtain V^{-1} is also irreducible, and hence FV^{-1} is irreducible. Applying the Perron-Frobenius Theorem, there exists a largest, positive eigenvalue $\nu = \rho(V^{-1}F) = \rho(FV^{-1}) = \mathcal{R}_0$ that is a simple root of the associated characteristic polynomial. Further, the left eigenvector, ω, associated to ν has a one-dimensional eigenspace, and $\omega > 0$. Hence

$$\omega V^{-1} F = \omega \mathcal{R}_0$$
$$\frac{1}{\mathcal{R}_0} \omega = \omega F^{-1} V.$$

Define $c_i = \omega_i / \left(\lim_{I_i \to 0^+} \frac{f_i(S_i^0, I_i)}{I_i} \right)$ for $i = 1, 2, \ldots, n$ and $L = \sum_{i=1}^{n} c_i I_i$.
Taking the derivative of L along a trajectory in Γ gives us

$$\dot{L} = \sum_{i=1}^{n} c_i I_i'$$
$$= \sum_{i=1}^{n} c_i \left(f_i(S_i, I_i) - (\mu_i^I + \gamma_i + \delta_i) I_i + d_I \sum_{j=1}^{n} m_{ij} I_j - d_I \sum_{j=1}^{n} m_{ji} I_i \right)$$

$$\leq \sum_{i=1}^{n} c_i \left(\left(\lim_{I_i \to 0^+} \frac{f(S_i^0, I_i)}{I_i} \right) I_i - (\mu_i^I + \gamma_i + \delta_i)I_i + d_I \sum_{j=1}^{n} m_{ij}I_j - d_I \sum_{j=1}^{n} m_{ji}I_i \right)$$

$$= c(F - V)I$$

$$= cF(1 - F^{-1}V)I$$

$$= \omega((1 - F^{-1}V)I$$

$$= \omega \left(1 - \frac{1}{\mathcal{R}_0} \right) I$$

$$\leq 0,$$

since $\mathcal{R}_0 \leq 1$. Now, $\dot{L} = 0$ implies either $\mathcal{R}_0 = 1$ or $I = 0$. If $\mathcal{R}_0 < 1$, then we must have $I_i = 0$ for $i = 1, 2, \ldots, n$ and hence $S_i = S_i^0$. If $\mathcal{R}_0 = 1$, from our assumption we obtain $S_i = S_i^0$. As a result, the largest invariant set in Γ is thus the singleton $\{P^0\}$. By the LaSalle Invariance Principle [49], we obtain P^0 is globally asymptotically stable.

$\square$

Incidence functions as seen in Corollaries 2.1.4 and 2.1.5 will satisfy Theorem 3.5.2 under the same conditions. The benefit of Theorem 3.5.2 allows a combination of different incidence functions to be used. Thus, if it is beneficial to model one patch using frequency dependent incidence but mass action on another, global stability of the DFE can still be obtained for the SIR model. If the additional assumptions $\mu_i^S \leq \mu_i^I$ for $i = 1, 2, \ldots, n$ and $d_S = d_I$ are imposed, then global stability of the DFE is obtained for the combination SIR and SIS model given by (3.5)-(3.6).

3.6   Existence of Endemic Equilibrium

Theorem 3.6.1. *Let* $\displaystyle\lim_{I_i \to 0^+} \frac{f_i(S_i^0, I_i)}{I_i} > 0$ *for* $i = 1, 2, \ldots, n$. *If* $\mathcal{R}_0 > 1$, *then there exists at least one endemic equilibrium* $P^* = (S^*, I^*)$ *for the system* (3.5)-(3.5) *in the interior of* Γ.

Proof. Let ω_i be the components of the left Perron eigenvector, ω, corresponding to eigenvalue $\mathcal{R}_0 = \rho(V^{-1}F) = \rho(FV^{-1})$. Let $c_i = \omega_i / \left(\lim_{I_i \to 0^+} \dfrac{f_i(S_i^0, I_i)}{I_i} \right)$ and $L = \displaystyle\sum_{i=1}^{n} c_i I_i$. Taking the derivative of L along a trajectory in Γ gives us

$$
\begin{aligned}
\dot{L} &= \sum_{i=1}^{n} c_i I_i' \\
&= \sum_{i=1}^{n} c_i \left(f_i(S_i, I_i) - (\mu_i^I + \gamma_i + \delta_i) I_i + d_I \sum_{j=1}^{n} m_{ij} I_j - d_I \sum_{j=1}^{n} m_{ji} I_i \right) \\
&= \sum_{i=1}^{n} c_i \left[\left(\frac{f_i(S_i, I_i)}{I_i} - (\mu_i^I + \gamma_i + \delta_i) - d_I \sum_{j=1}^{n} m_{ji} \right) I_i + d_I \sum_{j=1}^{n} m_{ij} I_j \right] \\
&= c \left(\tilde{F} - V \right) I,
\end{aligned}
$$

where $\tilde{F} = [\tilde{F}_{ij}]$ is the $n \times n$ matrix with $\tilde{F}_{ii} = \dfrac{f_i(S_i, I_i)}{I_i}$ and $\tilde{F}_{ij} = 0$ for $i \neq j$.
Further, $\displaystyle\lim_{(S_i, I_i) \to (S_i^0, 0)} \tilde{F}_{ii} = F_{ii}$. Thus, taking the limit of $\dot{L}$ as the system approaches the disease-free equilibrium, gives us

$$
\begin{aligned}
\lim_{(S,I) \to (S^0, 0)} \dot{L} &= \lim_{(S,I) \to (S^0, 0)} \left(c \left(\tilde{F} - V \right) I \right) \\
&= c(F - V) \lim_{(S,I) \to (S^0, 0)} I
\end{aligned}
$$

56

$$= \omega \left(1 - \frac{1}{\mathcal{R}_0} \right) \lim_{(S,I) \to (S^0, 0)} I$$

$$> 0.$$

Thus, if $\mathcal{R}_0 > 1$, we have $\dot{L} > 0$ for some neighborhood $N_\epsilon(P_0)$ about P_0, implying P_0 is unstable. All trajectories that start close enough to the DFE will leave $N_\epsilon(P_0)$. The system (2.4)-(2.5) is uniformly persistent by [26, Theorem 4.3] using a similar argument as [51, Proposition 3.3]. Uniform persistence and boundedness of solutions in the interior of Γ imply the existence of at least one endemic equilibrium (see Theorem D.3 in [64] or Theorem 2.8.6 in [12]).

$\square$

3.7   Global Stability of Endemic Equilibrium

In this section, the global stability of the EE will be studied. First, stability of the EE for the SIR model with nonlinear incidence is studied. Second, the stability of the EE for the SIS model with mass action incidence is studied in the region $\tilde{\Gamma}$.

3.7.1   Multipatch SIR Model

Theorem 3.7.1. *Let $\mathcal{R}_0 > 1$, $\delta_i = 0$ and $\gamma_i > 0$ for $i = 1, 2, \ldots, n$. Assume M is irreducible, $d_I > 0$, $d_S = 0$, and the following two conditions hold for*

57

$i = 1, 2, \ldots, n$:

$$(S_i - S_i^*)\left(f_i(S_i, I_i^*) - f_i(S_i^*, I_i^*)\right) \geq 0, \tag{3.10}$$

$$\left(\frac{f_i(S_i, I_i)}{f_i(S_i, I_i^*)} - 1\right)\left(1 - \frac{f_i(S_i, I_i^*)}{f_i(S_i, I_i)}\frac{I_i}{I_i^*}\right) \leq 0 \tag{3.11}$$

with equality if and only if $S_i = S_i^*$ and $I_i = I_i^*$ for $i = 1, 2, \ldots, n$. Then the endemic equilibrium P^* is unique and globally asymptotically stable in the interior of Γ.

Proof. For $i = 1, 2, \ldots, n$, evaluating (3.5)-(3.6) at P^* gives us

$$\Lambda_i = f_i(S_i^*, I_i^*) + \mu_i^S S_i^*$$

$$\mu_i^I + \gamma_i = \frac{f_i(S_i^*, I_i^*)}{I_i^*} + d_I \sum_{j=1}^{n} m_{ij}\frac{I_j^*}{I_i^*} - d_I \sum_{j=1}^{n} m_{ij}.$$

We will utilize $\displaystyle\int_1^x \frac{1-u}{u}\,du < 0$ when $x > 1$, and $n\sqrt[n]{\prod_{i=1}^{n} a_i} - \sum_{i=1}^{n} a_i \leq 0$, with equality if and only if each a_i are equivalent. Define

$$V_i = \int_{S_i^*}^{S_i}\left(1 - \frac{f_i(S_i^*, I_i^*)}{f_i(\xi, I_i^*)}\right)d\xi + I_i - I_i^* - I_i^* \ln\frac{I_i}{I_i^*}.$$

Taking the derivative of V_i along a trajectory in Γ gives us

$$\dot{V}_i = S_i' - \frac{f_i(S_i^*, I_i^*)}{f_i(S_i, I_i^*)}S_i' + I_i' - \frac{I_i^*}{I_i}I_i'$$

58

$$
\begin{aligned}
&= \Lambda_i - f_i(S_i, I_i) - \mu_i^S S_i - \frac{f_i(S_i^*, I_i^*)}{f_i(S_i, I_i^*)} \left(\Lambda_i - f_i(S_i, I_i) - \mu_i^S S_i \right) \\
&\quad + f_i(S_i, I_i) - (\mu_i^I + \gamma_i) I_i + d_I \sum_{j=1}^n m_{ij} I_j - d_I \sum_{j=1}^n m_{ji} I_i \\
&\quad - \frac{I_i^*}{I_i} \left(f_i(S_i, I_i) - (\mu_i^I + \gamma_i) I_i + d_I \sum_{j=1}^n m_{ij} I_j - d_I \sum_{j=1}^n m_{ji} I_i \right) \\
&= f_i(S_i^*, I_i^*) + \mu_i^S S_i^* - \mu_i^S S_i - \left(f_i(S_i^*, I_i^*) + \mu_i^S S_i^* \right) \frac{f_i(S_i^*, I_i^*)}{f_i(S_i, I_i^*)} \\
&\quad + \frac{f_i(S_i^*, I_i^*)}{f_i(S_i, I_i^*)} f_i(S_i, I_i) + \mu_i^S \frac{f_i(S_i^*, I_i^*)}{f_i(S_i, I_i^*)} S_i \\
&\quad - \left(\frac{f_i(S_i^*, I_i^*)}{I_i^*} + d_I \sum_{j=1}^n m_{ij} \frac{I_j^*}{I_i^*} - d_I \sum_{j=1}^n m_{ij} \right) I_i + d_I \sum_{j=1}^n m_{ij} I_j - d_I \sum_{j=1}^n m_{ji} I_i \\
&\quad - f_i(S_i, I_i) \frac{I_i^*}{I_i} + \left(\frac{f_i(S_i^*, I_i^*)}{I_i^*} + d_I \sum_{j=1}^n m_{ij} \frac{I_j^*}{I_i^*} - d_I \sum_{j=1}^n m_{ij} \right) I_i^* \\
&\quad - d_I \sum_{j=1}^n m_{ij} I_j \frac{I_i^*}{I_i} + d_I \sum_{j=1}^n m_{ji} I_i^* \\
&= -\mu_i^S S_i \left(-\frac{S_i^*}{S_i} + 1 + \frac{f_i(S_i^*, I_i^*)}{f_i(S_i, I_i^*)} \frac{S_i^*}{S_i} - \frac{f_i(S_i^*, I_i^*)}{f_i(S_i, I_i^*)} \right) \\
&\quad + f_i(S_i^*, I_i^*) \left(2 - \frac{f_i(S_i^*, I_i^*)}{f_i(S_i, I_i^*)} + \frac{f_i(S_i, I_i)}{f_i(S_i, I_i^*)} - \frac{I_i}{I_i^*} - \frac{f_i(S_i, I_i)}{f_i(S_i^*, I_i^*)} \frac{I_i^*}{I_i} \right) \\
&\quad + d_I \sum_{j=1}^n m_{ij} I_j^* \left(1 - \frac{I_j I_i^*}{I_j^* I_i} - \frac{I_i}{I_i^*} + \frac{I_j}{I_j^*} \right) \\
&= -\frac{\mu_i^S}{f_i(S_i, I_i^*)} (S_i - S_i^*)(f_i(S_i, I_i^*) - f_i(S_i^*, I_i^*)) \\
&\quad + f_i(S_i^*, I_i^*) \left(3 - \frac{f_i(S_i^*, I_i^*)}{f_i(S_i, I_i^*)} - \frac{f_i(S_i, I_i)}{f_i(S_i^*, I_i^*)} \frac{I_i^*}{I_i} - \frac{f_i(S_i, I_i^*)}{f_i(S_i, I_i)} \frac{I_i}{I_i^*} \right) \\
&\quad + f_i(S_i^*, I_i^*) \left(\frac{f_i(S_i, I_i)}{f_i(S_i, I_i^*)} - 1 \right) \left(1 - \frac{f_i(S_i, I_i^*)}{f_i(S_i, I_i)} \frac{I_i}{I_i^*} \right) \\
&\quad + d_I \sum_{j=1}^n m_{ij} I_j^* \left(1 - \frac{I_j I_i^*}{I_j^* I_i} - \frac{I_i}{I_i^*} + \frac{I_j}{I_j^*} \right) \\
&\leq d_I \sum_{j=1}^n m_{ij} I_j^* \left(1 - \frac{I_j I_i^*}{I_j^* I_i} - \frac{I_i}{I_i^*} + \frac{I_j}{I_j^*} \right)
\end{aligned}
$$

$$\leq d_I \sum_{j=1}^{n} m_{ij} I_j^* \left(-\ln\left(\frac{I_j I_i^*}{I_j^* I_i}\right) - \frac{I_i}{I_i^*} + \frac{I_j}{I_j^*} \right)$$

$$= d_I \sum_{j=1}^{n} m_{ij} I_j^* \left[\left(\frac{I_j}{I_j^*} - \ln\frac{I_j}{I_j^*}\right) - \left(\frac{I_i}{I_i^*} - \ln\frac{I_i}{I_i^*}\right) \right]$$

$$= d_i \sum_{j=1}^{n} m_{ij} I_j^* \left[H_j(I_j) - H_i(I_i) \right]$$

where

$$H_i(I_i) = \frac{I_i}{I_i^*} - \ln\frac{I_i}{I_i^*}.$$

Let $\mathcal{W}$ be the weight matrix with entries $[w_{ij}] = \left[d_I m_{ij} I_j^*\right]$. Then we define the weighted digraph $\mathcal{D}$ with associated weight matrix $\mathcal{W}$ as the ordered pair $(\mathcal{D}, \mathcal{W})$. Now, since M is irreducible, it follows $\mathcal{W}$ is irreducible. Let $c_i = \sum_{\mathcal{T} \in \mathbb{T}_i} w(\mathcal{T}) > 0$ as defined in Proposition 2.1 of [54]. Thus, by Theorem 2.3 of [54], we obtain

$$\sum_{i,j=1}^{n} c_i d_I m_{ij} I_j^* \left(H_j(I_j) - H_i(I_i) \right) = 0.$$

By defining $V(S_1, I_1, \ldots, S_n, I_n) = \sum_{i=1}^{n} c_i V_i(S_i, I_i)$, with $c_i > 0$ if $(\mathcal{D}, \mathcal{W})$ is irreducible, it follows

$$\dot{V} = \sum_{i=1}^{n} c_i \dot{V}_i(S_i, I_i)$$

$$\leq \sum_{i=1}^{n} c_i \left(\sum_{j=1}^{n} d_I m_{ij} I_j^* \left(H_j(I_j) - H_i(I_i) \right) \right)$$

$$= 0$$

for all $(S_1, I_1, \ldots, S_n, I_n) \in \widetilde{\Gamma}$ and V is a Lyapunov function for system (3.5)- (3.6).

Since $c_i > 0$ for all i, $\dot{V} = 0$ implies both $S_i^* = S_i$ and $\frac{I_i^*}{I_i} = 1$ for $i = 1, 2, \ldots, n$. Thus, the only invariant set such that $\dot{V} = 0$ is $\{P^*\}$. By the LaSalle Invariance Principle [49], we obtain P^* is globally asymptotically stable and it is unique.

$\square$

3.7.2 Multipatch SIS Model

As seen in Section 2.1.7, a different type of Lyapunov function is needed to prove global asymptotic stability of the EE for the homogeneous model. A similar Lyapunov function can be used for the heterogeneous model with mass action incidence.

Throughout this subsection, assume $\gamma_i = 0$ and $f_i(S_i, I_i) = \beta_i S_i I_i$ for $i = 1, 2, \ldots, n$.

Theorem 3.7.2. *Let $\gamma_i = 0$, $\delta_i > 0$ and $f_i(S_i, I_i) = \beta_i S_i I_i$ for $i = 1, 2, \ldots, n$. If $\mathcal{R}_0 > 1$, an endemic equilibrium P^* of the system (3.5)- (3.6) exists. Suppose one of the following assumptions holds:*

(i) *$d_S = 0$ and $M = [m_{ij}]$ is irreducible*

(ii) *$d_I = 0$ and $M = [m_{ij}]$ is irreducible*

(iii) *There exists a $\lambda > 0$ such that*

$$d_S S_j^* = \lambda \frac{\beta_i S_i^* I_i^* - \delta_i I_i^*}{\beta_i S_i^* I_i^*} d_I I_j^*$$

for all $i, j = 1, 2, \ldots, n$

61

Then the endemic equilibrium P^* is globally asymptotically stable and unique in the interior of $\widetilde{\Gamma}$.

Proof. We will show the result holds when Assumption (iii) is satisfied, as the other two results can be proven similarly. From (3.5)- (3.6) evaluated at P^*, we have

$$
\begin{aligned}
\mu_i^S &= \Lambda_i \frac{1}{S_i^*} - \beta_i I_i^* - \delta_i I_i^* \frac{1}{S_i^*} + d_S \sum_{j=1}^{n} m_{ij} S_j^* \frac{1}{S_i^*} - d_S \sum_{j=1}^{n} m_{ji} \\
\mu_i^I + \delta_i &= \beta_i S_i^* + d_I \sum_{j=1}^{n} m_{ij} I_j^* \frac{1}{I_i^*} - d_I \sum_{j=1}^{n} m_{ji}
\end{aligned}
$$

We will use the fact that $\int_1^x \frac{1-u}{u} du < 0$ for $x > 1$. Define

$$
V_i = S_i - S_i^* - S_i^* \ln\left(\frac{S_i}{S_i^*}\right) + \frac{\beta_i S_i^* I_i^* - \delta_i I_i^*}{\beta_i S_i^* I_i^*}\left(I_i - I_i^* - I_i^* \ln\left(\frac{I_i}{I_i^*}\right)\right).
$$

Note that

$$
\beta_i S_i^* I_i^* - \delta_i I_i^* = \Lambda_i - \mu_i^S S_i^* + d_S \sum_{j=1}^{n} m_{ij} S_j^* - d_S \sum_{j=1}^{n} m_{ji} S_i^* > 0
$$

inside $\widetilde{\Gamma}$. Differentiating along P^* gives us

$$
\dot{V}_i = S_i' - \frac{S_i^*}{S_i} S_i' + \frac{\beta_i S_i^* I_i^* - \delta_i I_i^*}{\beta_i S_i^* I_i^*}\left(I_i' - \frac{I_i^*}{I_i} I_i'\right)
$$

62

$$= \Lambda_i - \beta_i S_i I_i - \mu_i^S S_i + \delta_i I_i + d_S \sum_{j=1}^n m_{ij} S_j - d_S \sum_{j=1}^n m_{ji} S_i$$

$$- \frac{S_i^*}{S_i} \left(\Lambda_i - \beta_i S_i I_i - \mu_i^S S_i + \delta_i I_i + d_S \sum_{j=1}^n m_{ij} S_j - d_S \sum_{j=1}^n m_{ji} S_i \right)$$

$$+ \frac{\beta_i S_i^* I_i^* - \delta_i I_i^*}{\beta_i S_i^* I_i^*} \left[\beta_i S_i I_i - (\mu_i^I + \delta_i) I_i + d_I \sum_{j=1}^n m_{ij} I_j - d_I \sum_{j=1}^n m_{ji} I_i \right.$$

$$\left. - \frac{I_i^*}{I_i} \left(\beta_i S_i I_i - (\mu_i^I + \delta_i) I_i + d_I \sum_{j=1}^n m_{ij} I_j - d_I \sum_{j=1}^n m_{ji} I_i \right) \right]$$

$$= \Lambda_i - \beta_i S_i I_i - \mu_i^S S_i + \delta_i I_i + d_S \sum_{j=1}^n m_{ij} S_j - d_S \sum_{j=1}^n m_{ji} S_i$$

$$- \Lambda_i \frac{S_i^*}{S_i} + \beta_i S_i^* I_i + \mu_i^S S_i^* - \delta_i I_i \frac{S_i^*}{S_i} - d_S \sum_{j=1}^n m_{ij} S_j \frac{S_i^*}{S_i} + d_S \sum_{j=1}^n m_{ji} S_i^*$$

$$+ \frac{\beta_i S_i^* I_i^* - \delta_i I_i^*}{\beta_i S_i^* I_i^*} \left[\, \beta_i S_i I_i - (\mu_i^I + \delta_i) I_i + d_I \sum_{j=1}^n m_{ij} I_j - d_I \sum_{j=1}^n m_{ji} I_i \right.$$

$$\left. - \beta_i S_i I_i^* + (\mu_i^I + \delta_i) I_i^* - d_I \sum_{j=1}^n m_{ij} I_j \frac{I_i^*}{I_i} + d_I \sum_{j=1}^n m_{ji} I_i^* \, \right]$$

63

$$= \Lambda_i - \beta_i S_i I_i - \left(\Lambda_i \frac{1}{S_i^*} - \beta_i I_i^* - \delta_i I_i^* \frac{1}{S_i^*} + d_S \sum_{j=1}^{n} m_{ij} S_j^* \frac{1}{S_i^*} - d_S \sum_{j=1}^{n} m_{ji} \right) S_i$$

$$+ \delta_i I_i + d_S \sum_{j=1}^{n} m_{ij} S_j - d_S \sum_{j=1}^{n} m_{ji} S_i - \Lambda_i \frac{S_i^*}{S_i} + \beta_i S_i^* I_i$$

$$+ \left(\Lambda_i \frac{1}{S_i^*} - \beta_i I_i^* - \delta_i I_i^* \frac{1}{S_i^*} + d_S \sum_{j=1}^{n} m_{ij} S_j^* \frac{1}{S_i^*} - d_S \sum_{j=1}^{n} m_{ji} \right) S_i^*$$

$$- \delta_i I_i \frac{S_i^*}{S_i} - d_S \sum_{j=1}^{n} m_{ij} S_j \frac{S_i^*}{S_i} + d_S \sum_{j=1}^{n} m_{ji} S_i^*$$

$$+ \frac{\beta_i S_i^* I_i^* - \delta_i I_i^*}{\beta_i S_i^* I_i^*} \left[\beta_i S_i I_i - \left(\beta_i S_i^* + d_I \sum_{j=1}^{n} m_{ij} I_j^* \frac{1}{I_i^*} - d_I \sum_{j=1}^{n} m_{ji} \right) I_i \right.$$

$$+ d_I \sum_{j=1}^{n} m_{ij} I_j - d_I \sum_{j=1}^{n} m_{ji} I_i - \beta_i S_i I_i^* + \left(\beta_i S_i^* + d_I \sum_{j=1}^{n} m_{ij} I_j^* \frac{1}{I_i^*} - d_I \sum_{j=1}^{n} m_{ji} \right) I_i^*$$

$$\left. - d_I \sum_{j=1}^{n} m_{ij} I_j \frac{I_i^*}{I_i} + d_I \sum_{j=1}^{n} m_{ji} I_i^* \right]$$

$$= \Lambda_i - \beta_i S_i I_i - \Lambda_i \frac{S_i}{S_i^*} + \beta_i S_i I_i^* + \delta_i I_i^* \frac{S_i}{S_i^*} - d_S \sum_{j=1}^{n} m_{ij} S_j^* \frac{S_i}{S_i^*} + d_S \sum_{j=1}^{n} m_{ji} S_i$$

$$+ \delta_i I_i + d_S \sum_{j=1}^{n} m_{ij} S_j - d_S \sum_{j=1}^{n} m_{ji} S_i - \Lambda_i \frac{S_i^*}{S_i} + \beta_i S_i^* I_i + \Lambda_i - \beta_i S_i^* I_i^*$$

$$- \delta_i I_i^* + d_S \sum_{j=1}^{n} m_{ij} S_j^* - d_S \sum_{j=1}^{n} m_{ji} S_i^* - \delta_i I_i \frac{S_i^*}{S_i} - d_S \sum_{j=1}^{n} m_{ij} S_j \frac{S_i^*}{S_i} + d_S \sum_{j=1}^{n} m_{ji} S_i^*$$

$$+ \frac{\beta_i S_i^* I_i^* - \delta_i I_i^*}{\beta_i S_i^* I_i^*} \left[\beta_i S_i I_i - \beta_i S_i^* I_i - d_I \sum_{j=1}^{n} m_{ij} I_j^* \frac{I_i}{I_i^*} + d_I \sum_{j=1}^{n} m_{ji} I_i \right.$$

$$+ d_I \sum_{j=1}^{n} m_{ij} I_j - d_I \sum_{j=1}^{n} m_{ji} I_i - \beta_i S_i I_i^* + \beta_i S_i^* I_i^* + d_I \sum_{j=1}^{n} m_{ij} I_j^*$$

$$\left. - d_I \sum_{j=1}^{n} m_{ji} I_i^* - d_I \sum_{j=1}^{n} m_{ij} I_j \frac{I_i^*}{I_i} + d_I \sum_{j=1}^{n} m_{ji} I_i^* \right]$$

64

$$= \Lambda_i \left(2 - \frac{S_i}{S_i^*} - \frac{S_i^*}{S_i} \right) + \beta_i S_i^* I_i^* \left(-\frac{S_i I_i}{S_i^* I_i^*} + \frac{S_i}{S_i^*} + \frac{I_i}{I_i^*} - 1 \right)$$

$$+ \delta_i I_i \left(-\frac{I_i^* S_i}{I_i S_i^*} + 1 + \frac{I_i^*}{I_i} - \frac{S_i^*}{S_i} \right) + d_S \sum_{j=1}^{n} m_{ij} S_j^* \left(1 - \frac{S_j S_i^*}{S_j^* S_i} - \frac{S_i}{S_i^*} + \frac{S_j}{S_j^*} \right)$$

$$+ \frac{\beta_i S_i^* I_i^* - \delta_i I_i^*}{\beta_i S_i^* I_i^*} \left[\beta_i S_i^* I_i^* \left(\frac{S_i I_i}{S_i^* I_i^*} - \frac{I_i}{I_i^*} - \frac{S_i}{S_i^*} + 1 \right) \right.$$

$$\left. + d_I \sum_{j=1}^{n} m_{ij} I_j^* \left(1 - \frac{I_j I_i^*}{I_j^* I_i} - \frac{I_i}{I_i^*} + \frac{I_j}{I_j^*} \right) \right]$$

$$= \Lambda_i \left(2 - \frac{S_i}{S_i^*} - \frac{S_i^*}{S_i} \right) + \beta_i S_i^* I_i^* \left(-\frac{S_i I_i}{S_i^* I_i^*} + \frac{S_i}{S_i^*} + \frac{I_i}{I_i^*} - 1 \right)$$

$$+ \delta_i I_i \left(2 - \frac{S_i^*}{S_i} - \frac{S_i}{S_i^*} - 1 + \frac{S_i}{S_i^*} - \frac{I_i^* S_i}{I_i S_i^*} + \frac{I_i^*}{I_i} \right)$$

$$+ d_S \sum_{j=1}^{n} m_{ij} S_j^* \left(1 - \frac{S_j S_i^*}{S_j^* S_i} - \frac{S_i}{S_i^*} + \frac{S_j}{S_j^*} \right)$$

$$+ \frac{\beta_i S_i^* I_i^* - \delta_i I_i^*}{\beta_i S_i^* I_i^*} \beta_i S_i^* I_i^* \left(\frac{S_i I_i}{S_i^* I_i^*} - \frac{I_i}{I_i^*} - \frac{S_i}{S_i^*} + 1 \right)$$

$$+ \frac{\beta_i S_i^* I_i^* - \delta_i I_i^*}{\beta_i S_i^* I_i^*} d_I \sum_{j=1}^{n} m_{ij} I_j^* \left(1 - \frac{I_j I_i^*}{I_j^* I_i} - \frac{I_i}{I_i^*} + \frac{I_j}{I_j^*} \right)$$

$$= (\Lambda_i + \delta_i I_i) \left(2 - \frac{S_i}{I_i^*} - \frac{S_i^*}{S_i} \right) + \beta_i S_i^* I_i^* \left(-\frac{S_i I_i}{S_i^* I_i^*} + \frac{S_i}{I_i^*} + \frac{I_i}{I_i^*} - 1 \right)$$

$$+ \delta_i I_i \left(-1 + \frac{S_i}{I_i^*} - \frac{I_i^* S_i}{I_i I_i^*} + \frac{I_i^*}{I_i} \right) + d_S \sum_{j=1}^{n} m_{ij} S_j^* \left(1 - \frac{S_j S_i^*}{S_j^* S_i} - \frac{S_i}{S_i^*} + \frac{S_j}{S_j^*} \right)$$

$$+ (\beta_i S_i^* I_i^* - \delta_i I_i) \left(\frac{S_i I_i}{S_i^* I_i^*} - \frac{I_i}{I_i^*} - \frac{S_i}{S_i^*} + 1 \right)$$

$$+ \frac{\beta_i S_i^* I_i^* - \delta_i I_i^*}{\beta_i S_i^* I_i^*} d_I \sum_{j=1}^{n} m_{ij} I_j^* \left(1 - \frac{I_j I_i^*}{I_j^* I_i} - \frac{I_i}{I_i^*} + \frac{I_j}{I_j^*} \right)$$

$$= (\Lambda_i + \delta_i I_i) \left(2 - \frac{S_i}{I_i^*} - \frac{S_i^*}{S_i} \right) + \beta_i S_i^* I_i^* \left(- \frac{S_i I_i}{S_i^* I_i^*} + \frac{S_i}{I_i^*} + \frac{I_i}{I_i^*} - 1 \right)$$

$$- \delta_i I_i^* \left(\frac{I_i}{I_i^*} - \frac{S_i I_i}{S_i^* I_i^*} + \frac{S_i}{S_i^*} - 1 \right) + d_S \sum_{j=1}^{n} m_{ij} S_j^* \left(1 - \frac{S_j S_i^*}{S_j^* S_i} - \frac{S_i}{S_i^*} + \frac{S_j}{S_j^*} \right)$$

$$+ (\beta_i S_i^* I_i^* - \delta_i I_i) \left(\frac{S_i I_i}{S_i^* I_i^*} - \frac{I_i}{I_i^*} - \frac{S_i}{S_i^*} + 1 \right)$$

$$+ \frac{\beta_i S_i^* I_i^* - \delta_i I_i^*}{\beta_i S_i^* I_i^*} d_I \sum_{j=1}^{n} m_{ij} I_j^* \left(1 - \frac{I_j I_i^*}{I_j^* I_i} - \frac{I_i}{I_i^*} + \frac{I_j}{I_j^*} \right)$$

$$= (\Lambda_i + \delta_i I_i) \left(2 - \frac{S_i}{I_i^*} - \frac{S_i^*}{S_i} \right) + d_S \sum_{j=1}^{n} m_{ij} S_j^* \left(1 - \frac{S_j S_i^*}{S_j^* S_i} - \frac{S_i}{S_i^*} + \frac{S_j}{S_j^*} \right)$$

$$+ \frac{\beta_i S_i^* I_i^* - \delta_i I_i^*}{\beta_i S_i^* I_i^*} d_I \sum_{j=1}^{n} m_{ij} I_j^* \left(1 - \frac{I_j I_i^*}{I_j^* I_i} - \frac{I_i}{I_i^*} + \frac{I_j}{I_j^*} \right)$$

$$\leq d_S \sum_{j=1}^{n} m_{ij} S_j^* \left(1 - \frac{S_j S_i^*}{S_j^* S_i} - \frac{S_i}{S_i^*} + \frac{S_j}{S_j^*} \right)$$

$$+ \frac{\beta_i S_i^* I_i^* - \delta_i I_i^*}{\beta_i S_i^* I_i^*} d_I \sum_{j=1}^{n} m_{ij} I_j^* \left(1 - \frac{I_j I_i^*}{I_j^* I_i} - \frac{I_i}{I_i^*} + \frac{I_j}{I_j^*} \right)$$

$$\leq \sum_{j=1}^{n} S_j^* \left(- \ln \left(\frac{S_j S_i^*}{S_j^* S_i} \right) - \frac{S_i}{S_i^*} + \frac{S_j}{S_j^*} \right)$$

$$+ \frac{\beta_i S_i^* I_i^* - \delta_i I_i^*}{\beta_i S_i^* I_i^*} d_I \sum_{j=1}^{n} m_{ij} I_j^* \left(- \ln \left(\frac{I_j I_i^*}{I_j^* I_i} \right) - \frac{I_i}{I_i^*} + \frac{I_j}{I_j^*} \right)$$

$$= d_S \sum_{j=1}^{n} m_{ij} S_j^* \left[\left(\frac{S_j}{S_j^*} - \ln \frac{S_j}{S_j^*} \right) - \left(\frac{S_i}{S_i^*} - \ln \frac{S_i}{S_i^*} \right) \right]$$

$$+ \frac{\beta_i S_i^* I_i^* - \delta_i I_i^*}{\beta_i S_i^* I_i^*} d_I \sum_{j=1}^{n} m_{ij} I_j^* \left[\left(\frac{I_j}{I_j^*} - \ln \frac{I_j}{I_j^*} \right) - \left(\frac{I_i}{I_i^*} - \ln \frac{I_i}{I_i^*} \right) \right]$$

$$= \frac{\beta_i S_i^* I_i^* - \delta_i I_i^*}{\beta_i S_i^* I_i^*} d_I \sum_{j=1}^{n} m_{ij} I_j^* \left[\left(\lambda \frac{S_j}{S_j^*} - \lambda \ln \frac{S_j}{S_j^*} + \frac{I_j}{I_j^*} - \ln \frac{I_j}{I_j^*} \right) \right.$$

$$- \left. \left(\lambda \frac{S_i}{S_i^*} - \lambda \ln \frac{S_i}{S_i^*} + \frac{I_i}{I_i^*} - \ln \frac{I_i}{I_i^*} \right) \right]$$

$$= \frac{\beta_i S_i^* I_i^* - \delta_i I_i^*}{\beta_i S_i^* I_i^*} d_I \sum_{j=1}^{n} m_{ij} I_j^* \left[H_j(S_j, I_j) - H_i(S_i, I_i) \right]$$

where

$$H_i(S_i, I_i) = \lambda \frac{S_i}{S_i^*} - \lambda \ln \frac{S_i}{S_i^*} + \frac{I_i}{I_i^*} - \ln \frac{I_i}{I_i^*}.$$

Let $\mathcal{W}$ be the weight matrix with entries $[w_{ij}] = \left[\frac{\beta_i S_i^* I_i^* - \delta_i I_i^*}{\beta_i S_i^* I_i^*} d_I m_{ij} I_j^* \right]$. Then we define the weighted digraph $\mathcal{D}$ with associated weight matrix $\mathcal{W}$ as the ordered pair $(\mathcal{D}, \mathcal{W})$. Now, since B is irreducible and $(\beta_i S_i^* I_i^* - \delta_i I_i^*) > 0$, it follows $\mathcal{W}$ is irreducible. Let $c_i = \sum_{\mathcal{T} \in \mathbb{T}} w(\mathcal{T}) > 0$ as defined in Proposition 2.1 of [54]. Thus, by Theorem 2.3 of [54], we obtain

$$\sum_{i,j=1}^{n} c_i \frac{\beta_i S_i^* I_i^* - \delta_i I_i^*}{\beta_i S_i^* I_i^*} d_I m_{ij} I_j^* \left(H_j(S_j, I_j) - H_i(S_i, I_i) \right) = 0.$$

By defining $V(S_1, I_1, \ldots, S_n, I_n) = \sum_{i=1}^{n} c_i V_i(S_i, I_i)$, with $c_i > 0$ if $(\mathcal{D}, \mathcal{W})$ is irreducible, it follows

$$\begin{aligned}
\dot{V} &= \sum_{i=1}^{n} c_i \dot{V}_i(S_i, I_i) \\
&\leq \sum_{i=1}^{n} c_i \left(\sum_{j=1}^{n} \frac{\beta_i S_i^* I_i^* - \delta_i I_i^*}{\beta_i S_i^* I_i^*} d_I m_{ij} I_j^* \left(H_j(I_j) - H_i(I_i) \right) \right) \\
&= 0
\end{aligned}$$

for all $(S_1, I_1, \ldots, S_n, I_n) \in \widetilde{\Gamma}$ and V is a Lyapunov function for system (3.5)-(3.6). Since $c_i > 0$ for all i, $\dot{V} = 0$ implies both $\frac{S_i^*}{S_i} = 1$ and $\frac{I_i^*}{I_i} = 1$. Thus, the only invariant set such that $\dot{V} = 0$ is $\{P^*\}$. By the LaSalle Invariance Principle [49], we obtain P^* is globally asymptotically stable and it is unique.

$\square$

CHAPTER 4: ASYMPTOTIC PROFILES

In this chapter, we present the limiting behavior of the disease-free equilibrium and the basic reproduction number as the movement of the susceptibles and infectives increases.

4.1 Laurent Series Expansion of the Laplacian Matrix

Recall, the singular Laplacian matrix, L, associated with $\mathcal{D}(M)$ is

$$
L = \begin{bmatrix}
\displaystyle\sum_{j\neq 1}^{n} m_{j1} & -m_{12} & \dots & -m_{1n} \\[2ex]
-m_{21} & \displaystyle\sum_{j\neq 2}^{n} m_{j2} & \dots & -m_{2n} \\[2ex]
\vdots & \vdots & \ddots & \vdots \\[2ex]
-m_{n1} & -m_{n2} & \dots & \displaystyle\sum_{j\neq n}^{n} m_{jn}
\end{bmatrix}.
$$

Let $C_{k,k}$ be the cofactor of the kth diagonal element of L. Let $\mathbb{T}_k$ be the set of all spanning trees, $\mathcal{T}$, of $\mathcal{D}(M)$ that are rooted in at vertex k. Let $E(\mathcal{T})$ be the arc set of $\mathcal{T}$. By the Matrix Tree Theorem for Directed Graphs [57], we have

$$
C_{k,k} = \sum_{\mathcal{T}\in\mathbb{T}_k} \prod_{(s,r)\in E(\mathcal{T})} m_{rs}.
$$

The following lemma shows the existence and convergence of the Laurent series

for a small perturbation to L.

Lemma 4.1.1. *There exists a convergent Laurent series for $(L + \varepsilon B)^{-1}$ in a punctured neighborhood of 0, where $0 < \varepsilon \ll 1$ and $B = [b_{ij}]$ is a diagonal matrix with $b_{ii} > 0$ for $i = 1, 2, \ldots, n$. The Laurent series has a simple pole.*

A proof can be seen in [24]. Further, the Laurent series for $(L + \varepsilon B)^{-1}$ is given by

$$(L + \varepsilon B)^{-1} = \frac{1}{\varepsilon} X_{-1} + X_0 + \varepsilon X_1 + \ldots, \tag{4.1}$$

where

$$X_{-1} = \frac{1}{\sum_j \theta_j \mu_j^S} \begin{bmatrix} \theta_1 & \theta_1 & \ldots & \theta_1 \\ \theta_2 & \theta_2 & \ldots & \theta_2 \\ \vdots & \vdots & \ddots & \vdots \\ \theta_n & \theta_n & \ldots & \theta_n \end{bmatrix}$$

and $\theta_k = \dfrac{C_{k,k}}{\sum_j C_{j,j}}$. The matrix X_0 is the generalized inverse of L. Langenhop [48] showed the higher order terms can be written in terms of the generalized inverse as follows:

$$X_k = (-X_0 B)^K X_0, \quad \text{for } k \geq 1.$$

Thus, for a small perturbation ε, we can obtain

$$(L + \varepsilon B)^{-1} \approx \frac{1}{\varepsilon} X_{-1}. \tag{4.2}$$

The expansion of $(L + \varepsilon B)^{-1}$ is used in the following two sections to find the

limiting behavior of the DFE and $\mathcal{R}_0$ for fast movement of individuals.

4.2   Disease-Free Equilibrium

To solve for the DFE, the matrix

$$D = diag(\mu_i^S) + d_S \begin{bmatrix} \sum_{j\neq 1}^{n} m_{j1} & -m_{12} & \cdots & -m_{1n} \\ -m_{21} & \sum_{j\neq 2}^{n} m_{j2} & \cdots & -m_{2n} \\ \vdots & \vdots & \ddots & \vdots \\ -m_{n1} & -m_{n2} & \cdots & \sum_{j\neq n}^{n} m_{jn} \end{bmatrix}$$

$$= diag(\mu_i^S) + d_S L$$

must be inverted, where L is the Laplacian matrix corresponding to $\mathcal{D}(M)$. Thus, we can find the limiting behavior of the DFE in terms of the spanning rooted-in trees of $\mathcal{D}(M)$.

Since

$$D^{-1} = \left(diag(\mu_i^S) + d_S L \right)^{-1} = \frac{1}{d_S} \left(L + \frac{1}{d_S} diag \left(\mu_i^S \right) \right)^{-1},$$

for fast movement $\frac{1}{d_S}$ is a small perturbation of L. From (4.2), we have

$$D^{-1} = \frac{1}{d_S} \left(d_S X_{-1} + X_0 + \frac{1}{d_S} X_1 + \ldots \right).$$

Thus,

$$S_0 = D^{-1} \Lambda \approx X_{-1} \Lambda.$$

For fast movement we have

$$S_i^0 \approx \frac{\theta_i \sum_j \Lambda_j}{\sum_j \theta_j \mu_j^S} \tag{4.3}$$

for $i = 1, \ldots, n$. For patches with high movement in, we can thus presume there will be more susceptible individuals at the disease-free equilibrium.

We can verify the validity of this approximation using MATLAB, specifically for the mass action incidence function. We use MATLAB to produce a random $n \times 1$ birth rate vector Λ, with entries between 1000 people/year and 50,000 people/year. Similarly, we create random $n \times 1$ birth rate vector μ^S, with an average life expectancy between 50 and 100 years for each individual patch. In Figures 4.1-4.3, we compare the true disease-free equilibrium versus the approximated disease-free equilibrium for three different diffusion coefficients, for a 20-patch population.

Observe in Figure 4.3, the approximated solution is within 5 people for a larger diffusion coefficient ($d_S = 10,000$), but nearly there is a difference of nearly 50,000 people for small diffusion coefficients ($d_S = 1$), see Figure 4.1. Thus, we can see as the diffusion of susceptibles increase, we can use our approximation to obtain a realistic value for the number of susceptibles at each patch in the disease-free equilibrium.
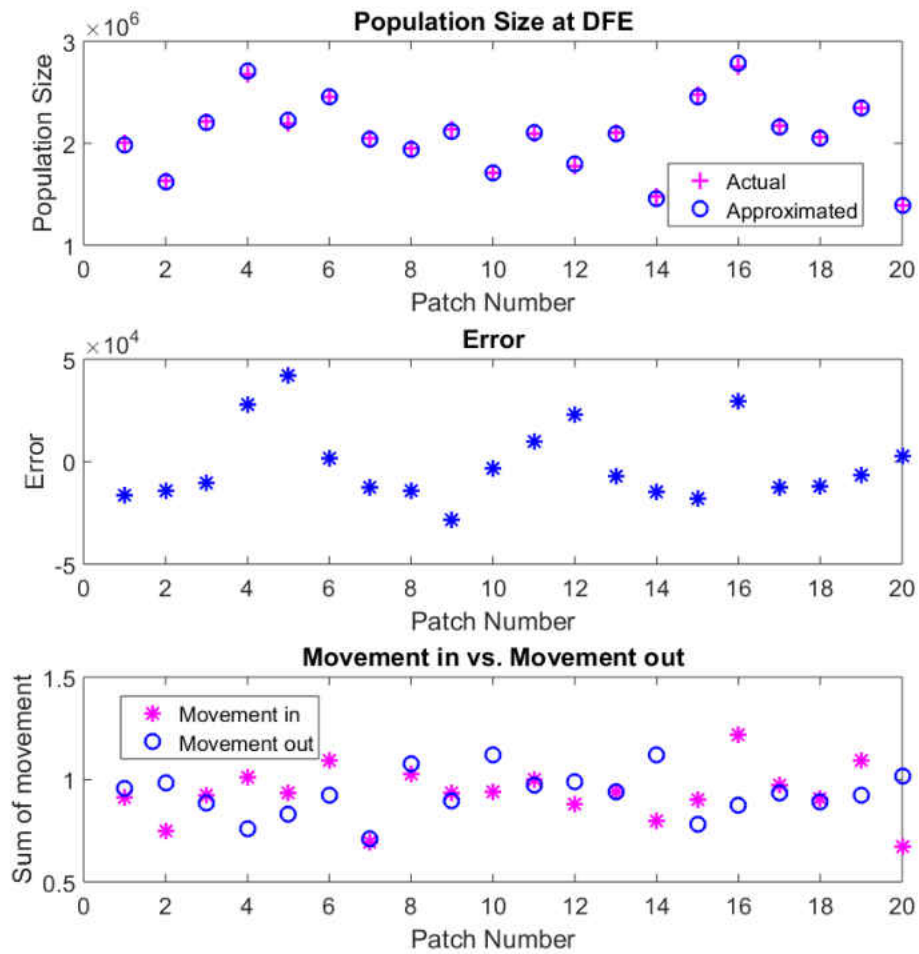
71

Figure 4.1: Here we let $n = 20$ and $d_S = 1$ to represent slow movement of susceptible individuals. The top figure plots the actual DFE vs. the approximated DFE, the middle represents the error (in people), and the bottom figure is the sum of the movement rates in each patch vs. the sum of the movement rates out of the patch.
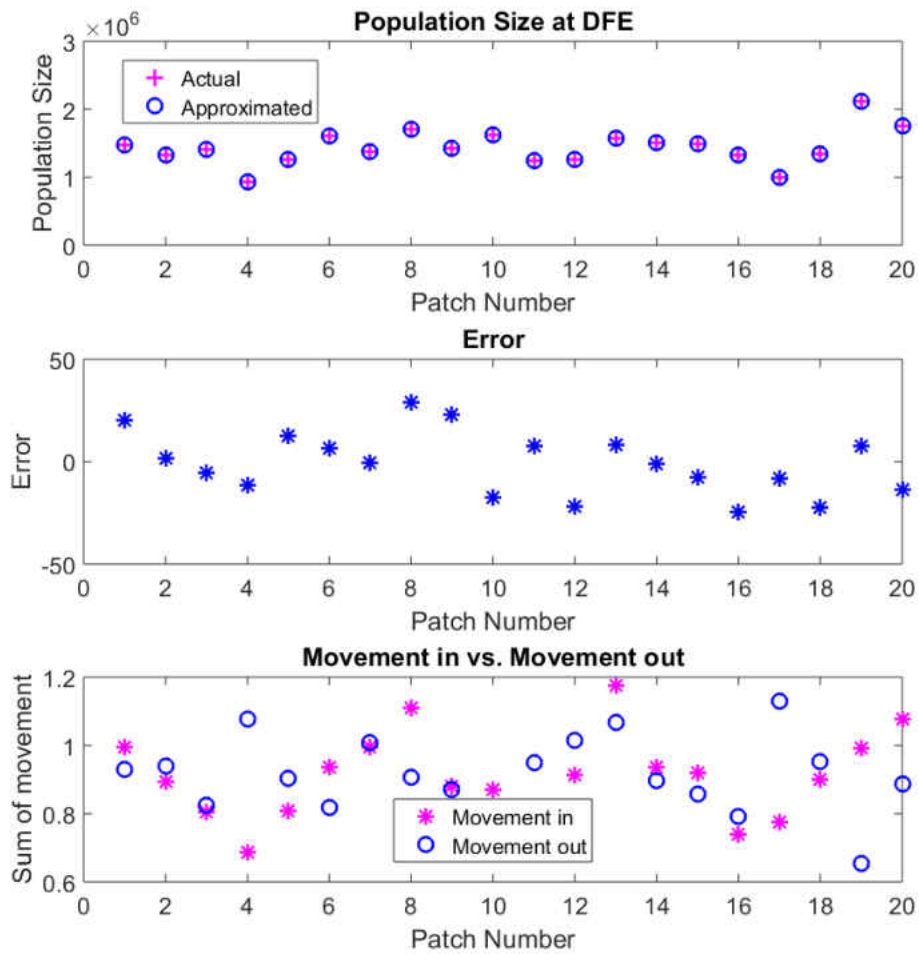
Figure 4.2: Here we let $n = 20$, and vary the diffusion coefficient. We let $d_S = 1000$ to represent intermediate movement of susceptible individuals. The top figure plots the actual DFE vs. the approximated DFE, the middle represents the error (in people), and the bottom figure is the sum of the movement rates in each patch vs. the sum of the movement rates out of the patch.
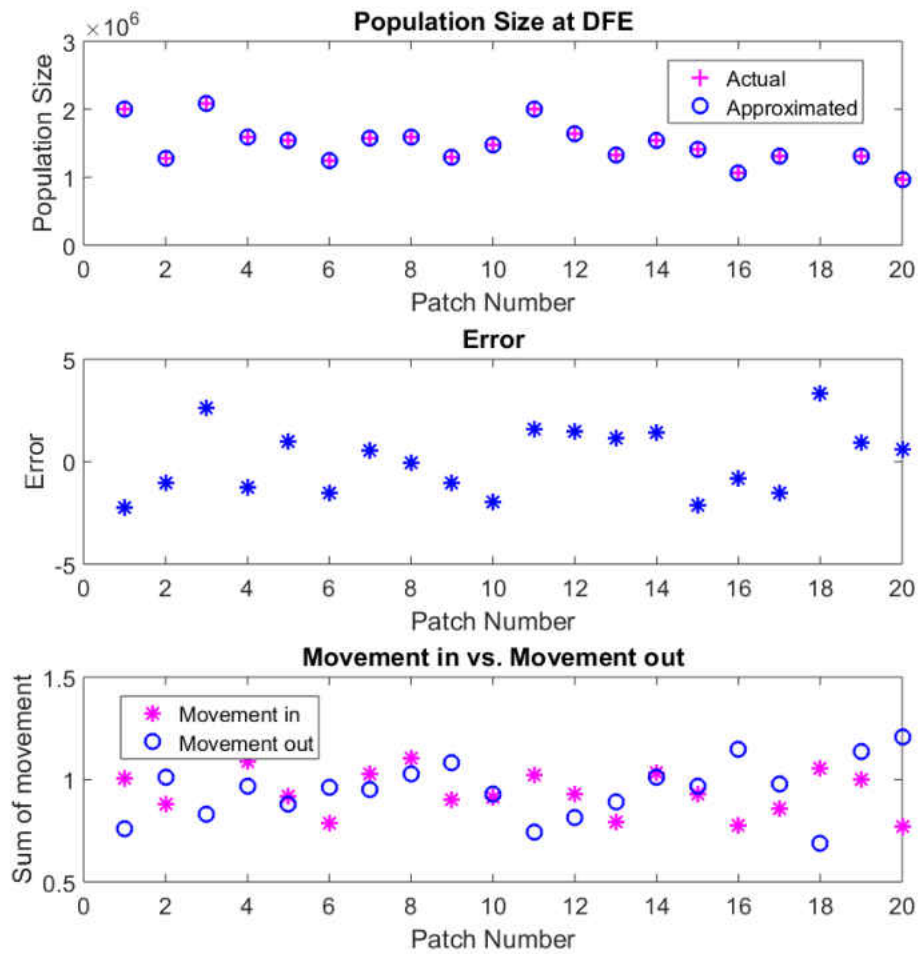
Figure 4.3: Here we let $n = 20$, and vary the diffusion coefficient. We let $d_S = 10,000$ to represent fast movement of susceptible individuals. The top figure plots the actual DFE vs. the approximated DFE, the middle represents the error (in people), and the bottom figure is the sum of the movement rates in each patch vs. the sum of the movement rates out of the patch.

4.3 Basic Reproduction Number

As in Section 4.2, we can find the limiting behavior of the basic reproduction number, since V can be written in terms of the singular Laplacian matrix, L, as follows:

$$V \; = \; diag\left(\mu_i^I + \gamma_i + \delta_i\right) + d_I L$$

Hence to find $\mathcal{R}_0$ through the next-generation matrix approach [68], we must calculate V^{-1}. As a result,

$$V^{-1} = \left(diag(\mu_i^I + \gamma_i + \delta_i) + d_I L\right)^{-1} = \frac{1}{d_I}\left(L + \frac{1}{d_I}diag\left(\mu_i^I + \gamma_i + \delta_i\right)\right)^{-1},$$

so for fast movement, $\frac{1}{d_I}$ is a small perturbation of the singular matrix L. Using the Laurent series expansion for V^{-1}, we have

$$V^{-1} = \frac{1}{d_I}\left(d_I X_{-1} + X_0 + \frac{1}{d_I}X_1 + \dots\right).$$

From [24], we obtain

$$X_{-1} = \frac{1}{\sum_j \theta_j\left(\mu_j^I + \gamma_j + \delta_j\right)} \begin{bmatrix} \theta_1 & \theta_1 & \dots & \theta_1 \\ \theta_2 & \theta_2 & \dots & \theta_2 \\ \vdots & \vdots & \ddots & \vdots \\ \theta_n & \theta_n & \dots & \theta_n \end{bmatrix}$$

where θ_j is as defined in Section 4.2.

Thus, $V^{-1} \approx X_{-1}$. To find $\mathcal{R}_0$, we first find an approximation to FV^{-1}. We have

$$FV^{-1} \approx FX_{-1}$$

$$= \frac{1}{\sum_j \theta_j \left(\mu_j^I + \gamma_j + \delta_j\right)} \begin{bmatrix} \lim_{I_1 \to 0^+} \dfrac{f_1(S_1^0, I_1)}{I_1}\theta_1 & \lim_{I_1 \to 0^+} \dfrac{f_1(S_1^0, I_1)}{I_1}\theta_1 & \cdots & \lim_{I_1 \to 0^+} \dfrac{f_1(S_1^0, I_1)}{I_1}\theta_1 \\ \lim_{I_2 \to 0^+} \dfrac{f_2(S_2^0, I_2)}{I_2}\theta_2 & \lim_{I_2 \to 0^+} \dfrac{f_2(S_2^0, I_2)}{I_2}\theta_2 & \cdots & \lim_{I_2 \to 0^+} \dfrac{f_2(S_2^0, I_2)}{I_2}\theta_2 \\ \vdots & \vdots & \ddots & \vdots \\ \lim_{I_n \to 0^+} \dfrac{f_n(S_n^0, I_n)}{I_n}\theta_n & \lim_{I_n \to 0^+} \dfrac{f_n(S_n^0, I_n)}{I_n}\theta_n & \cdots & \lim_{I_n \to 0^+} \dfrac{f_n(S_n^0, I_n)}{I_n}\theta_n \end{bmatrix}$$

$$= \widetilde{FV}^{-1}.$$

Since $\widetilde{FV}^{-1}$ is a rank one matrix, it follows $\rho\left(\widetilde{FV}^{-1}\right) = \operatorname{tr}\left(\widetilde{FV}^{-1}\right)$, where ρ is the spectral radius. Utilizing this, and our approximation for S_j^0 in Section 4.2, we obtain

$$\mathcal{R}_0 = \rho\left(FV^{-1}\right)$$

$$\approx \rho\left(\widetilde{FV}^{-1}\right)$$

$$= \frac{1}{\sum_{j=1}^n \theta_j \left(\mu_j^I + \gamma_j + \delta_j\right)} \sum_{j=1}^n \left(\lim_{I_j \to 0^+} \frac{f_j(S_j^0, I_j)}{I_j}\theta_j\right)$$

$$\approx \frac{1}{\sum_{j=1}^n \theta_j \left(\mu_j^I + \gamma_j + \delta_j\right)} \sum_{j=1}^n \left(\lim_{I_j \to 0^+} \frac{f_j\left(\frac{\theta_j \sum_k \Lambda_k}{\sum_k \theta_k \mu_k^S}, I_j\right)}{I_j}\theta_j\right)$$

Thus the limiting behavior of the basic reproduction number is

$$\mathcal{R}_0 \approx \frac{1}{\sum_{j=1}^{n} \theta_j \left(\mu_j^I + \gamma_j + \delta_j\right)} \sum_{j=1}^{n} \left(\lim_{I_j \to 0^+} \frac{f_j \left(\frac{\theta_j \sum_k \Lambda_k}{\sum_k \theta_k \mu_k^S}, I_j \right)}{I_j} \theta_j \right). \qquad (4.4)$$

For mass action incidence, i.e. $f_i(S_i, I_i) = \beta_i S_i I_i$ for $i = 1, 2, \ldots, n$, it follows

$$\lim_{I_j \to 0^+} \frac{f_j(S_j^0, I_j)}{I_j} = \lim_{I_j \to 0^+} \beta_j S_j^0 = \beta_j S_j^0.$$

Thus, the limiting behavior of $\mathcal{R}_0$ is

$$\mathcal{R}_0 \approx \frac{\left(\sum_{j=1}^{n} \beta_j \theta_j^2\right) \sum_{j=1}^{n} \Lambda_j}{\left(\sum_{j=1}^{n} \theta_j \left(\mu_j^I + \gamma_j + \delta_j\right)\right) \left(\sum_{j=1}^{n} \theta_j \mu_j^S\right)}. \qquad (4.5)$$

For the frequency dependent incidence function $f_i(S_i, I_i) = \beta_i \dfrac{S_i I_i}{S_i + I_i}$, it follows

$$\lim_{I_j \to 0^+} \frac{f_j(S_j^0, I_j)}{I_j} = \lim_{I_j \to 0^+} \frac{\beta_j S_j^0}{S_j^0 + I_j} = \beta_j.$$

The limiting behavior of $\mathcal{R}_0$ becomes

$$\mathcal{R}_0 \approx \frac{\sum_{j=1}^{n} \beta_j \theta_j}{\sum_{j=1}^{n} \theta_j \left(\mu_j^I + \gamma_j + \delta_j\right)}. \qquad (4.6)$$

CHAPTER 5: THE CORRELATION OF A HOT SPOT LOCATION TO THE PERSISTENCE OF INFECTION

In this chapter, numerical simulations will be applied to investigate the impact of biased movement in contrast to symmetric movement for the model with frequency dependent incidence. The simulations will be built with the following goals in mind:

  (i) Revist the results from [2] on multipatch SIS model with symmetric movement and the exclusion of demographics.

 (ii) Demonstrate how the location of the disease hot spot impacts persistence of the infection with asymmetric movement.

(iii) See how demographics of birth and death alter the limiting behavior in [2].

(iv) Explore the limiting behavior when diffusion of the susceptible individuals is halted for the SIR and SIS models.

5.1   Rural-Urban Star Network Structure

We begin by examining a star network, as depicted in Figure 5.1. In most metropolitan areas, there is often a major city where the majority of people congregate for work or social activities, but surrounding the cities are many smaller suburbs where interaction between the population is higher. The star network represents this com-

munity structure, where the major city is located in the hub (node 1), and the surrounding suburbs are the leafs (nodes 2-5).
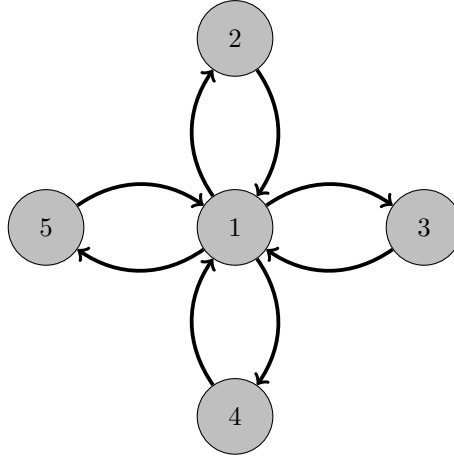

Figure 5.1: Visualization of the star network with one hub and four leafs.

5.2 Set-up of Numerical Experiments

Consider the system (3.5)-(3.6) with $n = 5$ and movement matrix, $M = [m_{ij}]$, corresponding to the star network as in Figure 5.1. We have

$$
M = \begin{bmatrix}
0 & m_{12} & m_{13} & m_{14} & m_{15} \\
m_{21} & 0 & 0 & 0 & 0 \\
m_{31} & 0 & 0 & 0 & 0 \\
m_{41} & 0 & 0 & 0 & 0 \\
m_{51} & 0 & 0 & 0 & 0
\end{bmatrix}.
$$

In this Chapter, we assume frequency dependent incidence

$$f_i(S_i, I_i) = \frac{\beta_i S_i I_i}{S_i + I_i},$$ (5.1)

for $i = 1, 2, 3, 4, 5$, while mass action incidence will be studied in Chapter 6.

Table 5.1: A list of fixed parameter values throughout the simulations.

Parameter	Value
Λ_i	$300 \text{ people} \cdot \text{year}^{-1}$
μ_i^S	$\frac{1}{80} \text{ year}^{-1}$
μ_i^I	$\frac{1}{80} \text{ year}^{-1}$
γ_i	$\frac{1}{2} \text{ year}^{-1}$
δ_i	0 year^{-1}
β_i	varies
m_{ij}	varies
d_S	varies
d_I	varies

Parameters that will be commonly used in our simulations are listed in Table 5.1. Fixed parameters are chosen to closely mirror current population demographics in the Orlando region experiencing a sexually transmitted infection outbreak. We keep the current parameters equivalent among patches to be able to clearly see the impact of biased movement. Each patch initially has 8000 susceptible and 2 infectious individuals.

In (5.1), we fix $\beta_2 = 0.9$ and $\beta_i = 0.225$ for $i = 1, 3, 4, 5$. With these values, the

patch reproduction numbers can be computed as the following:

$$\mathcal{R}_0^{[1]} \approx .4390 \quad \mathcal{R}_0^{[2]} \approx 1.7561 \quad \mathcal{R}_0^{[3]} \approx .4390 \quad \mathcal{R}_0^{[4]} \approx .4390 \quad \mathcal{R}_0^{[5]} \approx .4390.$$

Note that Patch 2 is the disease hot spot.

Three kinds of parameters will be varied in our simulations: some movement rates m_{ij}, the diffusion coefficients d_S and d_I, and a possible new hot spot location. Specifically, varying some movement rate from one patch to another patch (only one direction) will create an asymmetric network, on which the disease impact will be investigated.

5.3 Symmetric Movement

In this section, we revisit the well-known results for symmetric movement without demographics and further explore the disease dynamics with demographics.

5.3.1 Monotone Property of $\mathcal{R}_0$

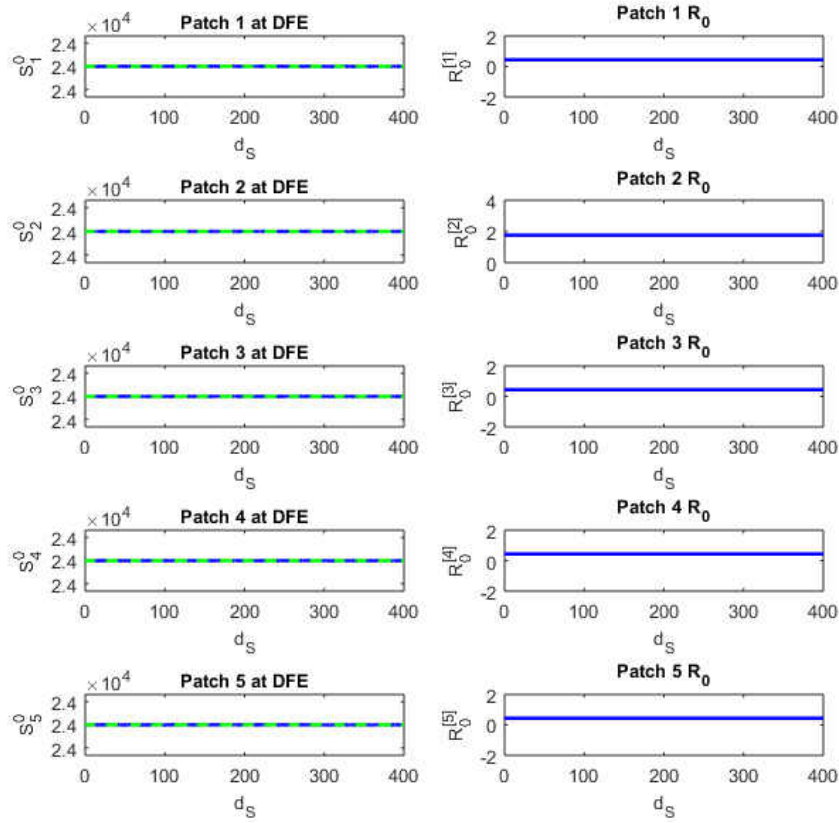By (3.7), the disease-free equilibrium for both the SIS and SIR models is the solution to the matrix equation $\Lambda = DS^0$, where $D = diag(\mu_i^S) + d_S L$. Thus, d_S is the only diffusion coefficient that will play a role in the patch sizes at the disease-free equilibrium, and hence a role in the patch reproduction numbers. Further, the number of susceptibles at the DFE in each patch for the frequency dependent function will vary in the same manner for the mass action incidence function, since the same

81

matrix equation must be solved. However, the DFE does not play a role in the patch reproduction numbers for the frequency dependent incidence function. The patch reproduction number for Patch i is

$$\mathcal{R}_0^{[i]} = \frac{\beta_i}{\mu_i^I + \gamma_i + \delta_i}.$$

Thus, each $\mathcal{R}_0^{[i]}$ is independent of d_S. Further, the patch reproduction numbers for the SIS and SIR models are equivalent if the same value is chosen for the recovery rate in the two infections. Thus, we will run the results using the SIS model, but an analogous conclusion can be made for the SIR model.

Figure 5.2(b) shows this independence in the patch reproduction numbers. Further, the number of individuals in each patch at the disease-free equilibrium is unaltered by the movement of susceptible individuals; see Figure 5.2(b). Since the birth rate, death rate, and recovery rate parameters are chosen to be equivalent for each patch, there are an equal number of susceptibles in each patch at the DFE.

Figure 5.2: Effect of varying the diffusion of susceptibles on the disease-free equilibrium and patch basic reproduction numbers for frequency dependent incidence in the SIS model. (a) The total number of susceptibles at the DFE vary as d_S increases from 0 to 400. The dashed green line represents the approximated DFE from Section 4.2. (b) The corresponding effects on each $\mathcal{R}_0^{[i]}$ as d_S varies.

From [73], it is known $\mathcal{R}_0$ is a monotone decreasing function of d_I when there are no demographics. However, even with demographics, we can see $\mathcal{R}_0$ appears to be

83

monotonically decreasing with respect to d_I; see Figure 5.3.

Since $M = [m_{ij}]$ is symmetric for this experiment, we can obtain $\theta_j = \frac{1}{5}$ for $j = 1, 2, 3, 4, 5$. It follows from (4.6) and Table 5.1 that as $d_I \to \infty$,

$$\mathcal{R}_0 \longrightarrow \frac{1}{5} \sum_{j=1}^{5} \mathcal{R}_0^{[j]} \approx 0.70242, \tag{5.2}$$
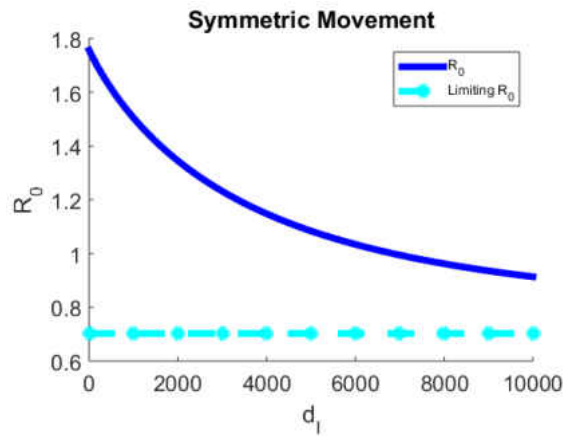
which is the horizontal dashed line in Figure 5.3.

Figure 5.3: The effect on $\mathcal{R}_0$ as d_I increases from 0 to 10,000.

5.3.2 *Profile of Endemic Equilibrium: Demographic Effect*

For system (3.5)-(3.6) with no demographics, Allen, Lou, Bolker, and Nevai [2] were able to show the limiting behavior of the system as $d_S \to 0$. In particular, when $\mathcal{R}_0 > 1$, the solution of the system tends to a disease-free state as $d_S \to 0$, i.e. $(S, I) \to (S^*, 0)$. In Figure 5.4, we replicate these results by setting the demo-

84

graphics of $\Lambda_i = \mu_i^S = \mu_i^I = 0$ for all i and $d_I = 4,000$ fixed. Although $\mathcal{R}_0$ is unchanged and always above 1 as $d_S \to 0$, we can see the infection is eradicated from the population; see (b) and (d) of Figure 5.4. It follows from Figure 5.4(c) that as $d_S \to 0$, the susceptibles in the disease hot spot, Patch 2, approach 0.

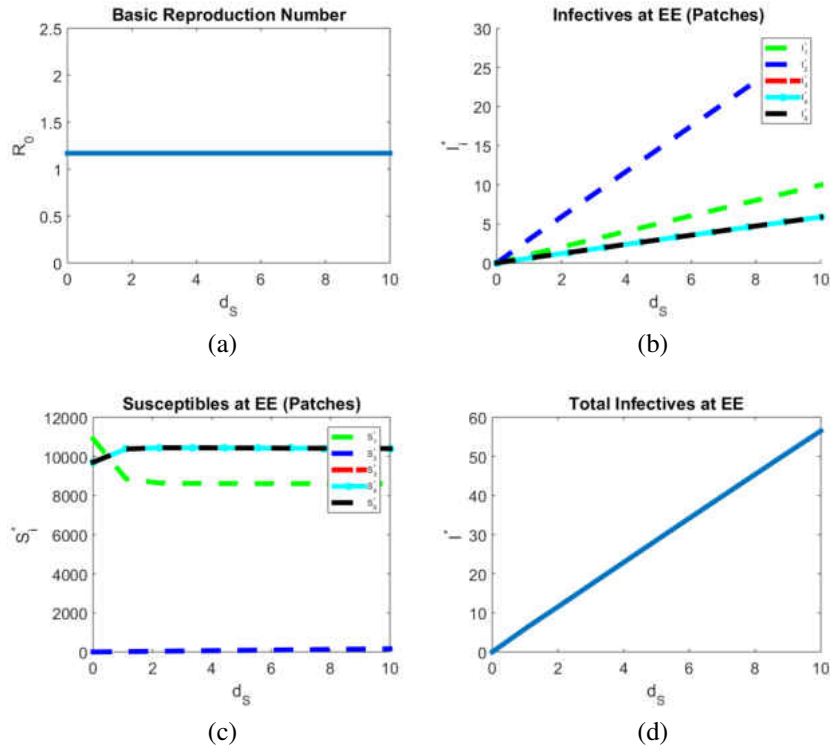### Symmetric Movement with No Demographics
Hot Spot In Leaf 2

Figure 5.4: $d_I = 4,000$ is fixed. (a) The basic reproduction number as d_S tends to 0. (b)-(c) The total number of infectives and susceptibles on each patch, respectively. (d) The total number of infectives in the population.

If we only choose a hot spot located in the hub, similar results hold; see Figure 5.5. Here, the disease dies out as $d_S \to 0$, yet $\mathcal{R}_0 > 1$. Further, we can see the

susceptibles in the hub go extinct, and the population is distributed equally among the remaining leaves.

Symmetric Movement with No Demographics
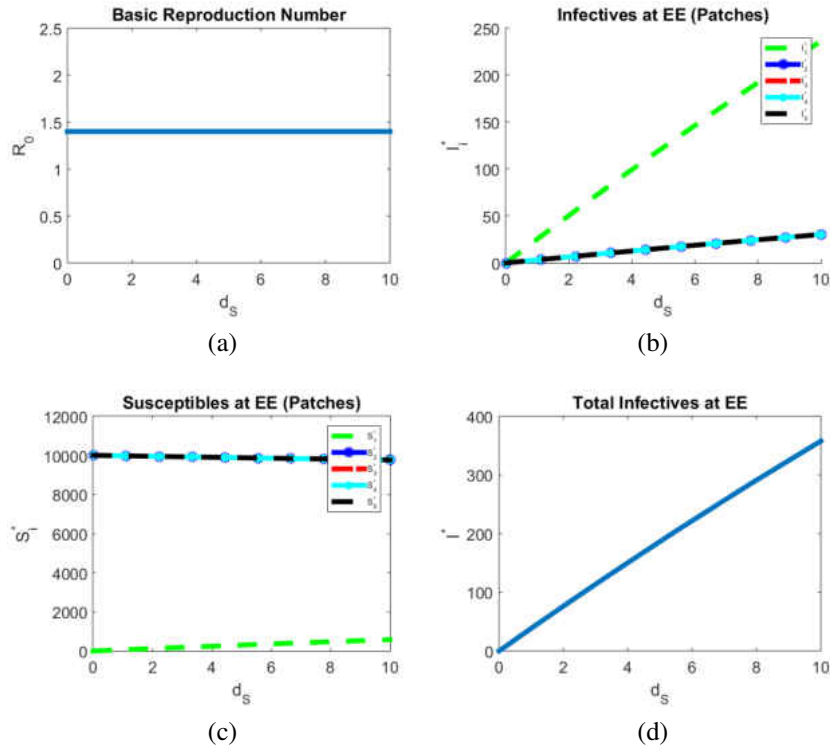**Hot Spot In Hub**

(a)

(b)

(c)

(d)

Figure 5.5: $d_I = 4,000$ is fixed. (a) The basic reproduction number as d_S tends to 0. (b)-(c) The total number of infectives and susceptibles on each patch, respectively. (d) The total number of infectives in the population.

86

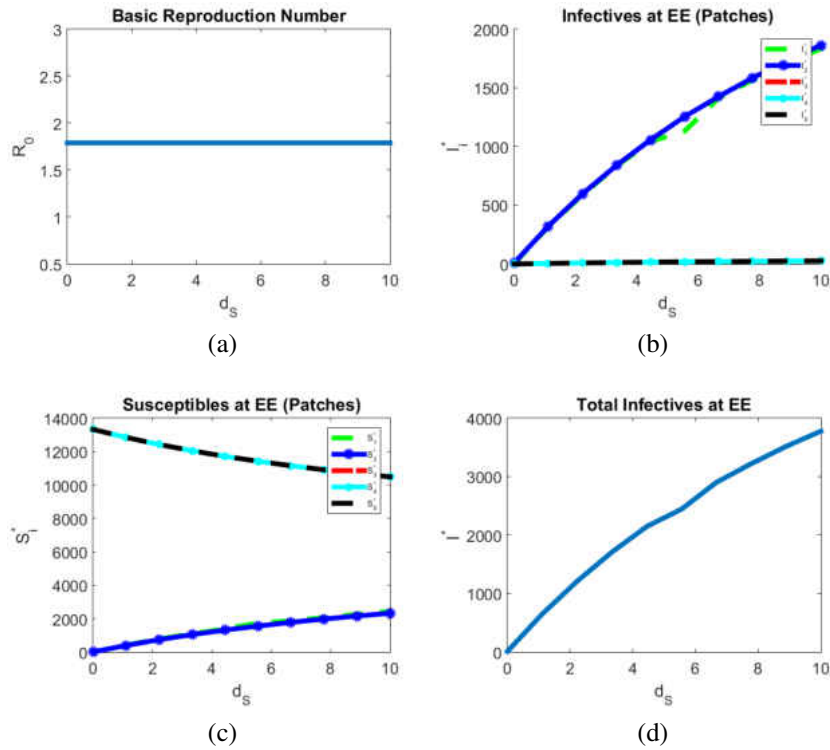**Symmetric Movement with No Demographics**
Hot Spots In Hub and Leaf 2

Figure 5.6: $d_I = 4,000$ is fixed. (a) The basic reproduction number as d_S tends to 0. (b)-(c) The total number of infectives and susceptibles on each patch, respectively. (d) The total number of infectives in the population.

Next, we would like to further explore the situation with multiple hot spots. If we allow a hot spot in the Hub and another hot spot in Leaf 2, then the infection also dies out and the susceptibles in the Hub and Patch 2 both tend to zero as $d_S \to 0$; see Figure 5.6. We will show later asymmetric movement would alter this.

Symmetric Movement with Demographics
Hot Spot In Leaf 2

(a)   (b)
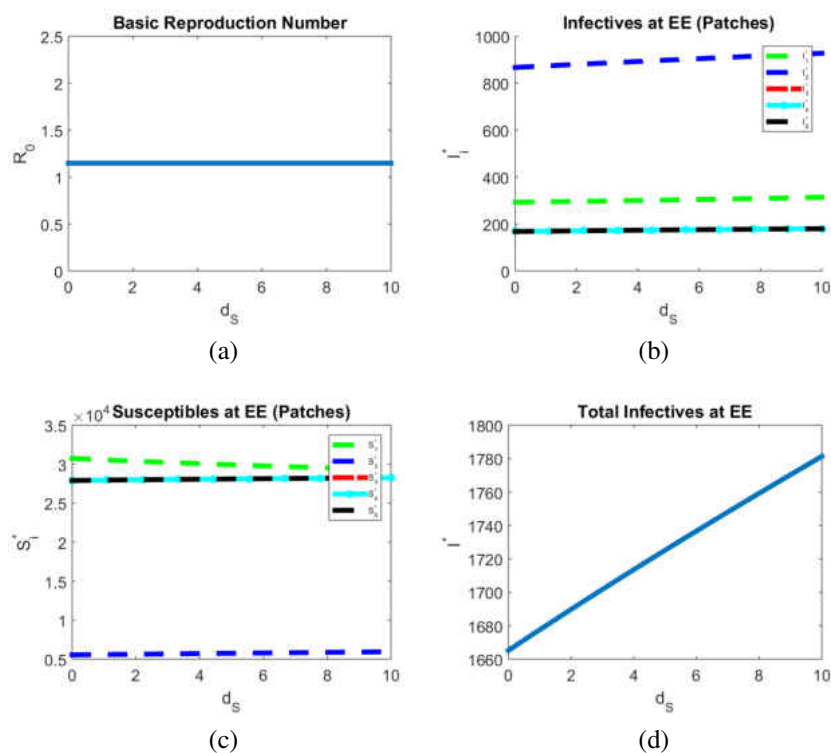
(c)   (d)

Figure 5.7: $d_I = 4,000$ is fixed. (a) The basic reproduction number as d_S tends to 0. (b)-(c) The total number of infectives and susceptibles on each patch, respectively. (d) The total number of infectives in the population..

Now, we show that the introduction of demographics in our simulation would persist the infection. The simulation shows that when $\mathcal{R}_0 > 1$, halting the movement of the susceptibles does not cause extinction of the disease; see Figure 5.7. With demographics, similar results hold for the situation with one hot spot located in the Hub, or two hot spots located in the Hub and Patch 2. We omit these figures.

5.4 Asymmetric Movement

In this section, we see how asymmetric movement impacts the known results for the symmetric movement, and if it causes different behavior.

5.4.1 Monotone Property of $\mathcal{R}_0$

To contrast the known results from Section 5.3, we introduced biased movement between two patches. The non-zero movement rate, m_{ij}, will be chosen as either normal value 0.0001 or larger value 0.001. In particular, the larger value is corresponding to the large arc in the network; see, for example, in Figure 5.8. We will vary the location of the large arc to represent all possible situations. Namely, the large arc will be placed from Patch 2 to Patch 1, Patch 1 to Patch 2, Patch 3 to Patch 1, and Patch 1 to Patch 3, respectively, as (a), (b), (c), and (d) in Figure 5.8.

Since $\mathcal{R}_0$ is independent of the DFE for the system with frequency dependent incidence, varying d_S has no effect on the overall basic reproduction number. Instead, we will solely vary d_I and see the effect on $\mathcal{R}_0$. When considering a single diffusion coefficient, $d = d_S = d_I$, will be completely determined from the value of d_I.

As shown in Figure 5.8, $\mathcal{R}_0$ is a monotone decreasing function of d_I. However, the location of the large arc relative to the disease hot spot is essential in determining the persistence of the disease. Figure 5.8(b) shows disease persistence regardless of the d_I value, while all three other cases, Figure 5.8(a), (c), and (d), can lead to disease extinction with large diffusion coefficient d_I.
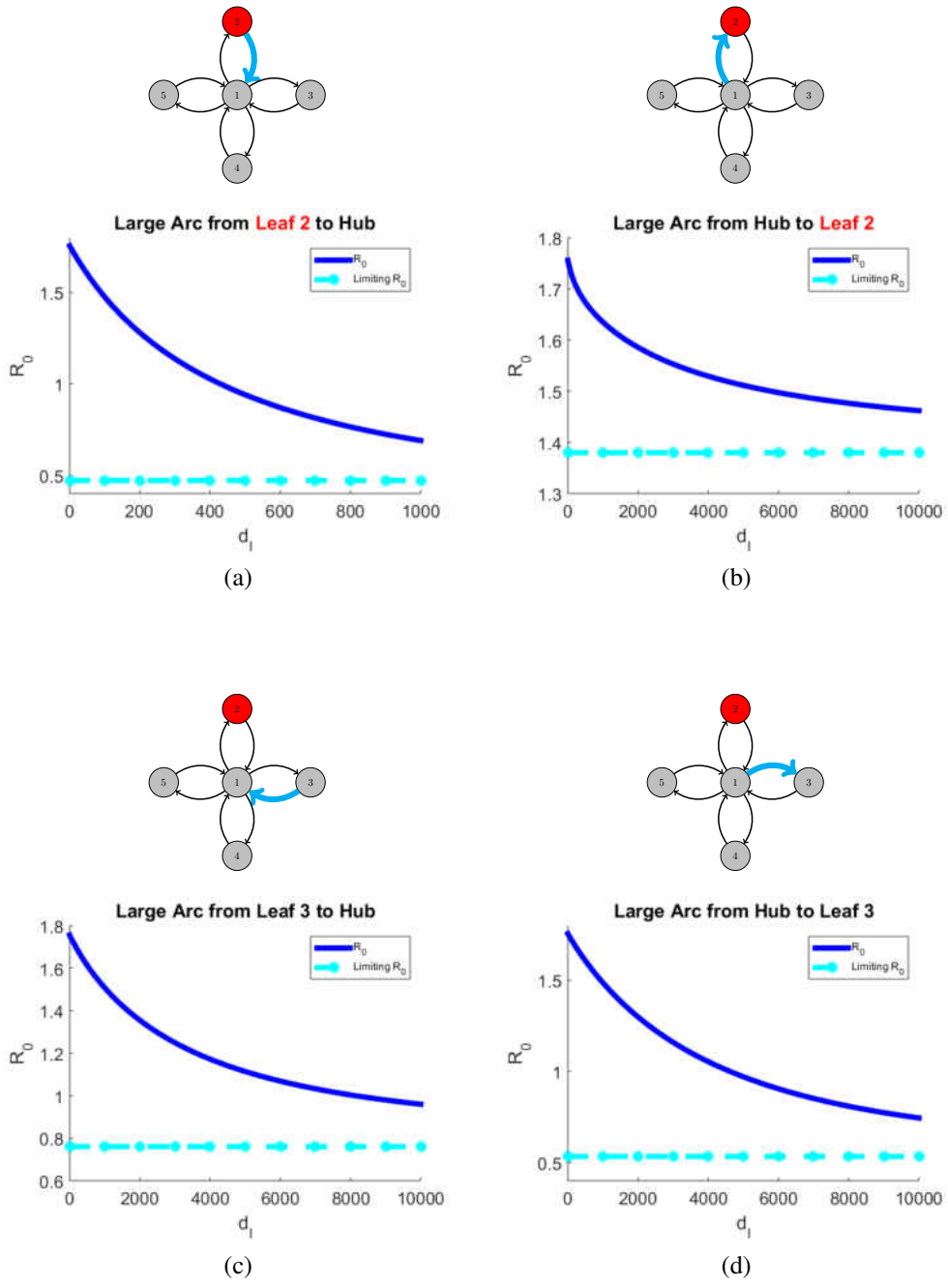
Figure 5.8: The effect on $\mathcal{R}_0$ as d_I increases for large arc locations.

The above phenomena can be explained using the approximation formula (6.1), $\mathcal{R}_0 \to \sum_{j=1}^{5} \theta_j \mathcal{R}_0^{[i]}$ as $d_I \to \infty$. Because of the structure of the star network, each node only has one rooted-in tree. As a result, the cofactors of the Laplacian matrix can be determined as follows:

$$C_{1,1} = m_{12} \, m_{13} \, m_{14} \, m_{15}$$

$$C_{2,2} = m_{21} \, m_{13} \, m_{14} \, m_{15}$$

$$C_{3,3} = m_{31} \, m_{12} \, m_{14} \, m_{15}$$

$$C_{4,4} = m_{41} \, m_{12} \, m_{13} \, m_{15}$$

$$C_{5,5} = m_{51} \, m_{12} \, m_{13} \, m_{14}$$

Then each $\theta_j = C_{j,j} / \sum_k C_{k,k}$ can be calculated. Table 5.2 outlines these values for each large arc location.

Table 5.2: Calculation of θ_j's and limiting $\mathcal{R}_0$ for Figure 5.8.

Large Arc Location	θ_1	θ_2	θ_3	θ_4	θ_5	Limiting $\mathcal{R}_0$
(a) Leaf 2 to Hub	0.2439	0.0244	0.2439	0.2439	0.2439	0.4829
(b) Hub to Leaf 2	0.0714	0.7143	0.0714	0.0714	0.0714	1.4143
(c) Leaf 3 to Hub	0.2439	0.2439	0.0244	0.2439	0.2439	0.7793
(d) Hub to Leaf 3	0.0714	0.0714	0.7143	0.0714	0.0714	0.5464

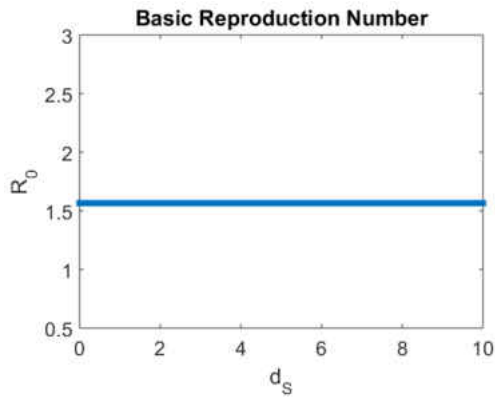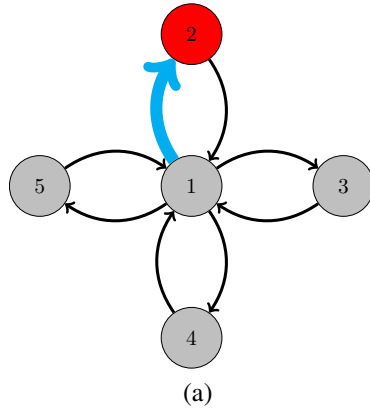### 5.4.2   *Profile of Endemic Equilibrium: the Effect of Biased Movement*

In this section, we investigate the impact of asymmetric movement on the limiting behavior as $d_S \to 0$. In order to compare with the results from [2] and Section 5.3.2,

we set $\Lambda_i = \mu_i^S = \mu_i^I = 0$ for all i and $d_I = 4,000$ fixed; namely, there are no demographics for the population and the total number of individuals is fixed.
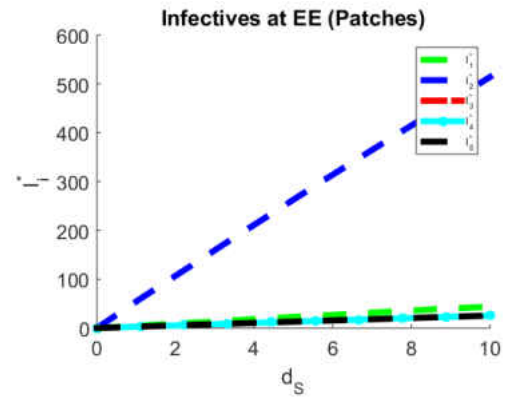
Figure 5.9 shows the results when the movement is biased towards the hot spot. In Figure 5.9(b), we can see the basic reproduction number does not change as $d_S \to 0$, and it is above the threshold value of 1. However, Figure 5.9(c) shows the number of infectives still tends to zero on each patch as $d_S \to 0$. In Figure 5.9(d), we can see the susceptibles do die out in the hot spot, mirroring the results for symmetric movement. Analogous results hold when altering the location of the large arc or switching the location of the hot spot to the hub.

However, the presence of two multiple hot spots and asymmetric movement might alter this limiting behavior. For example, in Figure 5.10, there are two hot spots in the star network: one in the main hub and one in a surrounding leaf. We allow the biased movement from the main hub to the hot spot leaf. Although $\mathcal{R}_0 > 1$ and there are no demographics in the population, Figure 5.10(b) shows persistence of the infectives for very small diffusion of susceptibles.
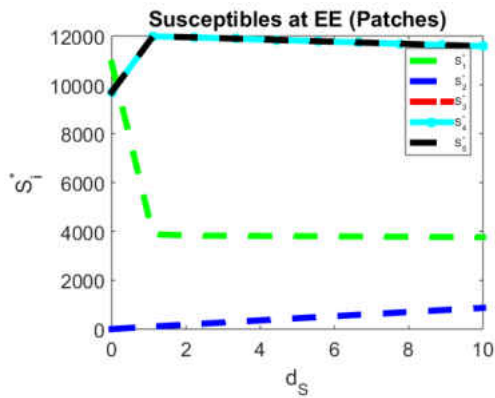
For symmetric movement, the disease does not persist as $d_S \to 0$, see Figure 5.6. Note that the persistence of the infectious population is solely in Patch 2. Both the infectives and susceptibles die out in the main hub, essentially leaving Patch 2 isolated from the remainder of the population. The infectives die out on the remaining leafs, leaving the susceptible population unaltered there.
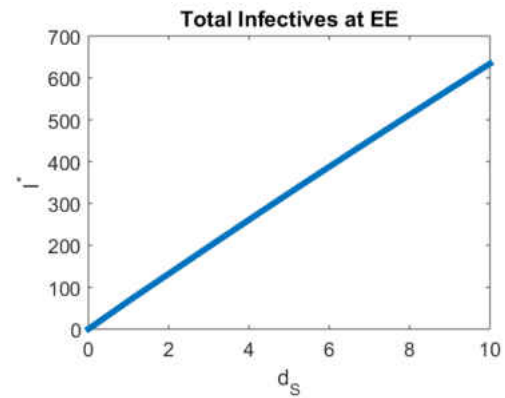
Figure 5.9: (a) Movement network with a large arc from the Hub to Patch 2. (b) The basic reproduction number is independent of d_S. (c)-(d) The total number of infectives and susceptibles on each patch, respectively. (e) The total number of infectives in the population.

93

Figure 5.10: (a) Movement network. (b) The basic reproduction number as d_S tends to 0. (c) The total number of infectives on each patch. (d) The total number of susceptibles per patch. (e) The total number of infectives in the population.
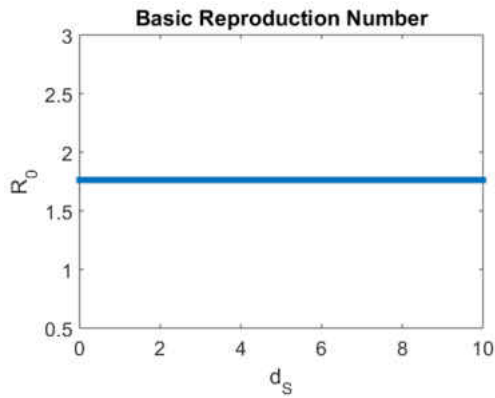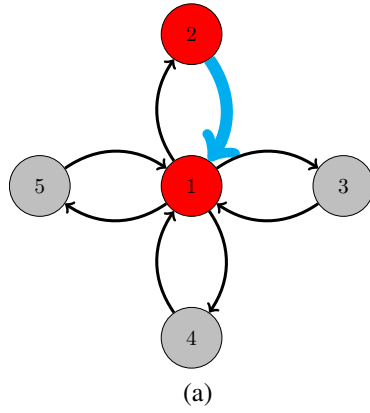
Figure 5.11: (a) Movement network. (b) The basic reproduction number as d_S tends to 0. (c)-(d) The total number of infectives and susceptibles per patch, respectively. (e) The total number of infectives in the population.
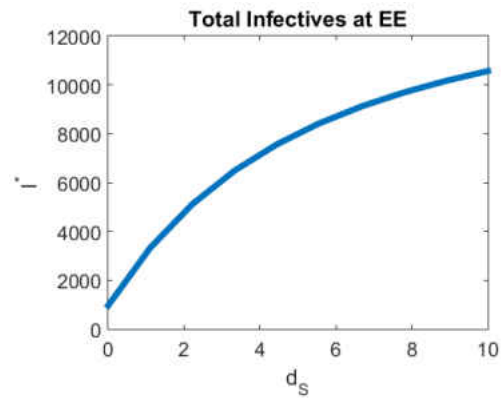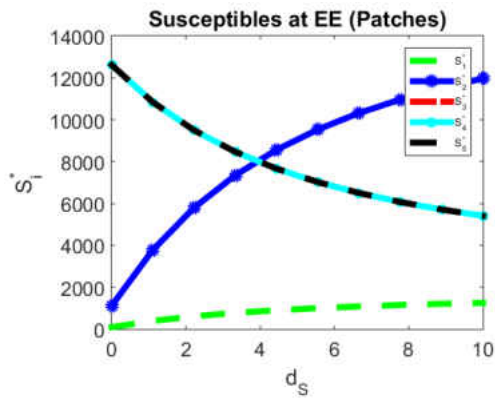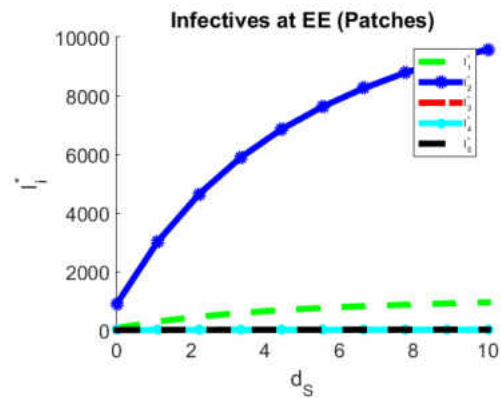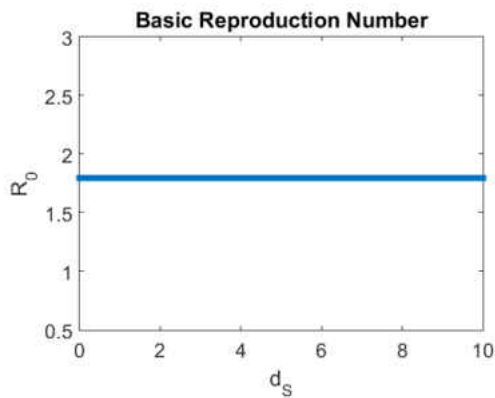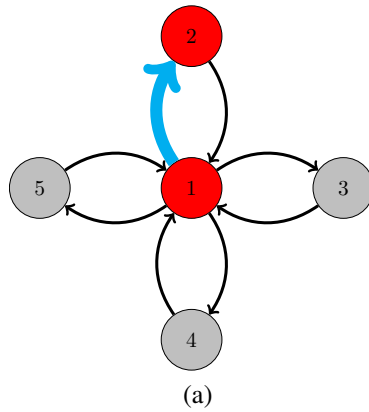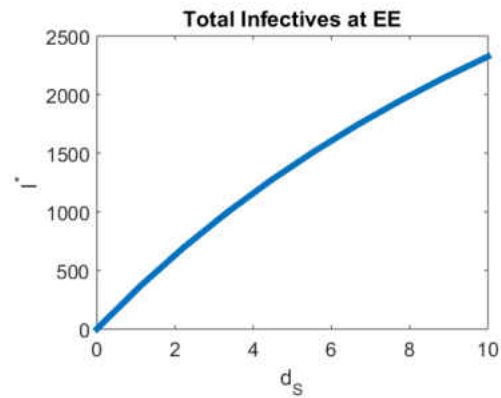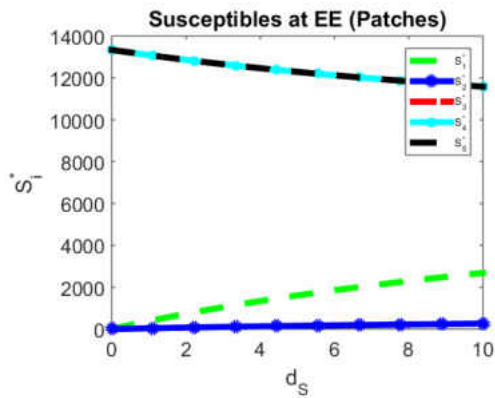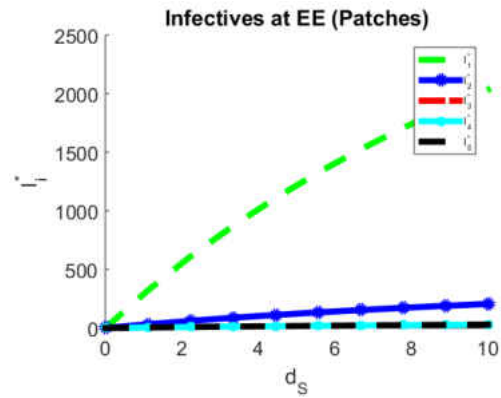
This sole location for the biased movement gives persistence of the infection when multiple hot spots exist. Figure 5.11 shows when the large arc is placed from Patch 2 to the hub, the infection will not persist as $d_S \to 0$. The susceptibles in both the hub and Patch 2 tend to 0. When the location of the large arc is varied from the hub to Patch 3 or Patch 3 to the hub, analogous behavior is exhibited. Thus, under this situation, the biased movement from the center city towards a hot spot causes persistence of the infection.

5.5   Distinction Between SIS and SIR Models

Finally, we contrast the behavior between the SIS and SIR models without demographics in the limiting case as $d_S \to 0$. We will focus on the situation when multiple hot spots exist in the network.

Figure 5.12 shows the results for the SIR model when hot spots are located in the hub and Patch 2 with symmetric movement. The infectious population does not persist on any of the patches, but the infection still passes through some individuals, since $R_i^* > 0$ for each i. However, unlike the SIS model, the susceptibles are able to persist in one of the hot spots. Further, as d_S increases, the susceptible population dies out and most individuals move to the recovered class.

Finally, we see if similar behavior is present for this skewed movement case with a hot spot in the leaf and a hub. In Figure 5.13, the disease does not persist in the population as $d_S \to 0$, but the susceptibles population in the Patch 2 still tend to zero; however, the hub has a larger amount of susceptibles than the symmetric case,

causing few individuals to become infected in this hot spot. Similar results hold when the biased movement is from the hub to Patch 3 and Patch 3 to the hub, thus we omit their figures.

Symmetric Movement with No Demographics SIR Model
Hot Spot In Hub and Leaf 2

(a)

(b)

(c)

(d)
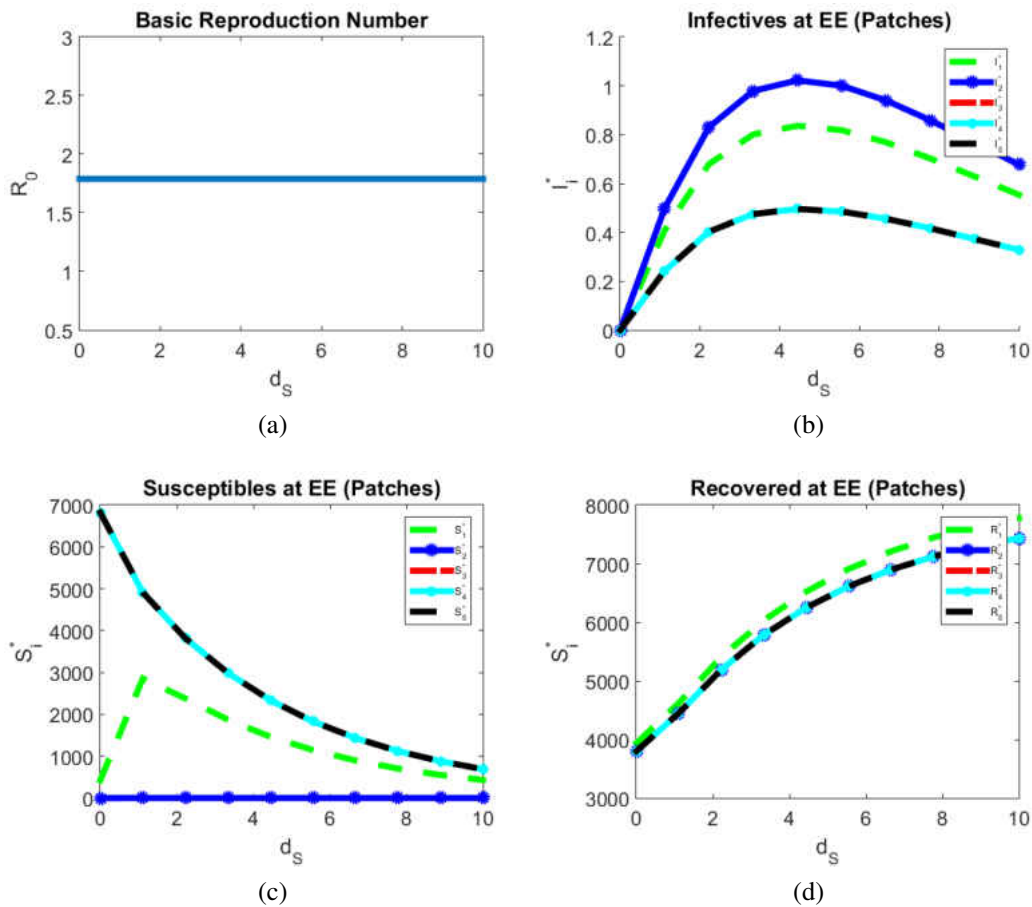
Figure 5.12: Here $d_I = d_R = 4,000$ is fixed. (a) The basic reproduction number as d_S tends to 0. (b)-(c) The total number of infectives and susceptibles on each patch, respectively. (d) The total number of infectives in the population.

97

Asymmetric Movement with No Demographics SIR Model
Hot Spot In Hub and Leaf 2

(a)

(b)

(c)

(d)

(e)
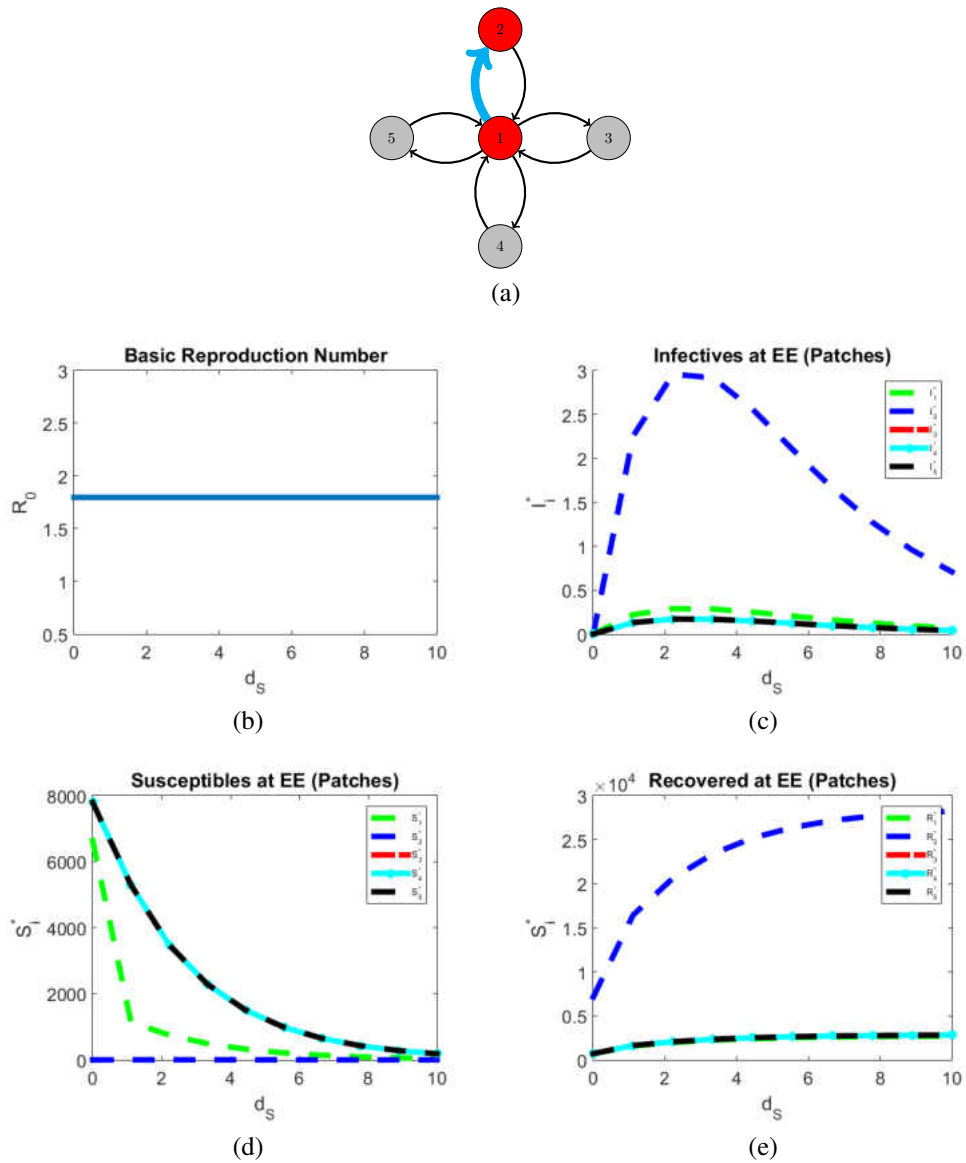
Figure 5.13: Limiting behavior for a population without demographics as $d_S \to 0$ for frequency dependent incidence with symmetric movement when a hot spot exists in a rural area and center city (SIR model). Here $d_I = d_R = 4,000$ is fixed. (a) Movement network. (b) The basic reproduction number as d_S tends to 0. (c)-(d) The total number of infectives and susceptibles on each patch, respectively.

Table 5.3: Summary of behavior of each I_i^* as $d_S \to 0$ for each i on the SIS and SIR models.

	SIS Model	SIR Model
Symmetric Movement (No Demographics)	$I_i^* \to 0$	$I_i^* \to 0$
Symmetric Movement (Demographics)	$I_i^* \not\to 0$	$I_i^* \to 0$
Asymmetric Movement (No Demographics)	I_i^* might not approach 0	$I_i^* \to 0$
Asymmetric Movement (Demographics)	$I_i^* \not\to 0$	$I_i^* \to 0$

Table 5.3 summarizes the comparison between the SIS and SIR models utilizing frequency dependent incidence with and without demographics.

5.6   Summary of Results

Clearly both demographics and asymmetric movement can cause interesting behavior in the persistence of an infection. For symmetric movement, stopping the movement of susceptible individuals causes extinction in the population when using the frequency dependent incidence function without demographics [2], regardless of the location and number of hot spots in the structure.

If demographics are introduced, this phenomenon does not hold anymore. The influx of individuals fuels the infection and allows for persistence even in the absence of movement for susceptible individuals. This influx can also represent a multitude of realistic representations including birth, tourism, and immigration. These dynamics coupled with movement can then help the persistence of the infection.

More interestingly, the dynamics as $d_S \to 0$ for asymmetric movement can vary

according to number of hot spots and location of the biased movement without demographics. Without the presence of new influx of individuals, the infection can also persist in the population as the movement of the susceptibles tends to zero. This behavior varies for our different experiments, but when two hot spots exists and the biased movement is between the two, the infection persists. Consequently, more detailed information is required to determine the limiting behavior of the system.

Further, there is varying behavior for SIS and SIR models utilizing frequency dependent incidence with and without demographics. For the SIR model, the infectives tend to 0 on each patch as $d_S \to 0$, but $S_i^* \not\to 0$ necessarily for each hot spot. For the SIS model, the introduction of demographics allowed for persistence of the infection even as $d_S \to 0$, but does not have the same effect in the SIR model.

CHAPTER 6: CONTRAST IN BEHAVIOR FOR THE BASIC REPRODUCTION NUMBER AND ENDEMIC LEVELS

In this chapter, we create numerical experiments mirroring the set-up from Chapter 5, but utilizing the mass action incidence function. The main goals are outlined below:

  (i) Show biased movement alters the patch reproduction numbers, possibly inducing new disease hot spots.

 (ii) Demonstrate numerically monotone/non-monotone properties of $\mathcal{R}_0$ in terms of d_I, d_S, or a single diffusion coefficient $d = d_S = d_I$.

(iii) Investigate the correlation between the endemic level and diffusion coefficient.

We will continue to use the Star Network as outlined in Section 5.1. Throughout this Chapter, Leaf 2 will be a hot spot where the disease will persist, while all other patches are considered favorable for extinction of the disease when movement vanishes.

Further, we focus solely on the SIS model, since analogous results will hold for the DFE, patch reproduction numbers, and $\mathcal{R}_0$ for the SIR model.

6.1 Parameter Settings

We choose fixed parameters similar to those in Chapter 5; see Table 6.1. We let $\beta_2 = 0.0000375$ and $\beta_i = 0.0000093$ for $i = 1, 3, 4, 5$. In the absence of movement, each patch reproduction number can be computed as follows:

$$\mathcal{R}_0^{[1]} \approx .4348 \quad \mathcal{R}_0^{[2]} \approx 1.7532 \quad \mathcal{R}_0^{[3]} \approx .4348 \quad \mathcal{R}_0^{[4]} \approx .4348 \quad \mathcal{R}_0^{[5]} \approx .4348,$$

where $\mathcal{R}_0^{[i]} = \dfrac{\beta_i S_i^{(0)}}{\mu_i^I + \delta_i} = \dfrac{\Lambda_i \beta_i}{\mu_i^S (\mu_i^I + \delta_i)}$.

Two kinds of parameters will be varied in our experiments: some movement rates, and the diffusion coefficients d_I and d_S. Further, we will allow for a single diffusion coefficient, $d = d_S = d_I$, adopting the behavior for a sexually transmitted infection.

When introducing biased movement, we vary the rates in a similar manner to Section 5.4, skewing movement between two patches. The non-zero movement rate, m_{ij}, will be chosen as either normal value 0.0001 or larger value 0.001.

Table 6.1: A list of fixed parameter values throughout the simulations.

Parameter	Value
Λ_i	$300 \text{ people} \cdot \text{year}^{-1}$
$\mu_i^S = \mu_i^I$	$\frac{1}{80} \text{ year}^{-1}$
δ_i	$\frac{1}{2} \text{ year}^{-1}$
γ_i	0 year^{-1}
$\beta_i, m_{ij}, d_S, d_I$	vary

6.2   Symmetric Movement

For the system with mass action incidence, the DFE is dependent on d_S, which in turn determines the patch reproduction numbers. In this section, we carry out simulations to show the impact of asymmetric movement on $\mathcal{R}_0$ and the EE. We will see how these quantities are affected by the location of the large arc in correlation to the hot spot.

(a)   (b)
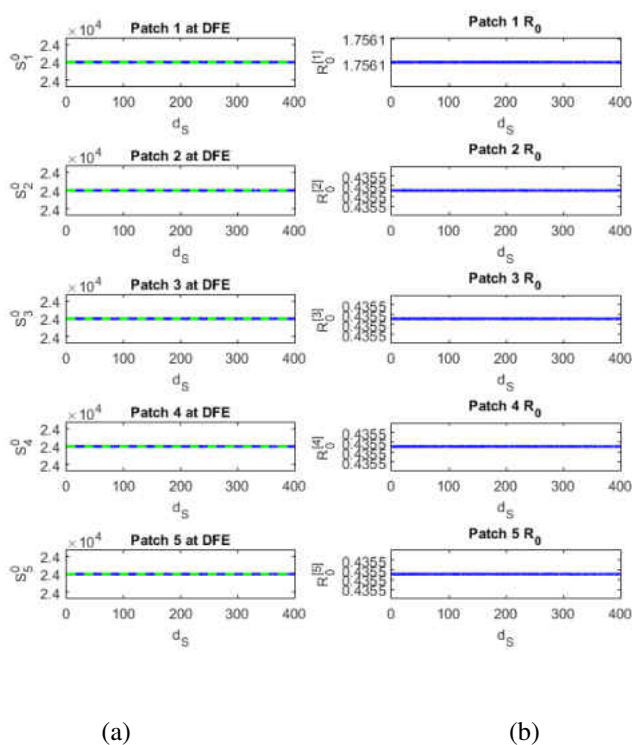
Figure 6.1: (a) The total number of susceptibles at the DFE vary as d_S increases from 0 to 400. The dashed green line represents the approximated DFE from Section 4.2. (b) The corresponding effects on $\mathcal{R}_0^{[i]}$ as d_S varies.

In Figure 6.1, we can see the symmetric movement does not alter the DFE and patch reproduction numbers regardless of the value of d_S, and thus the basic reproduction number $\mathcal{R}_0$ is independent of d_S, see Figure 6.2(b). However, in the next section, this will be altered under asymmetric movement.
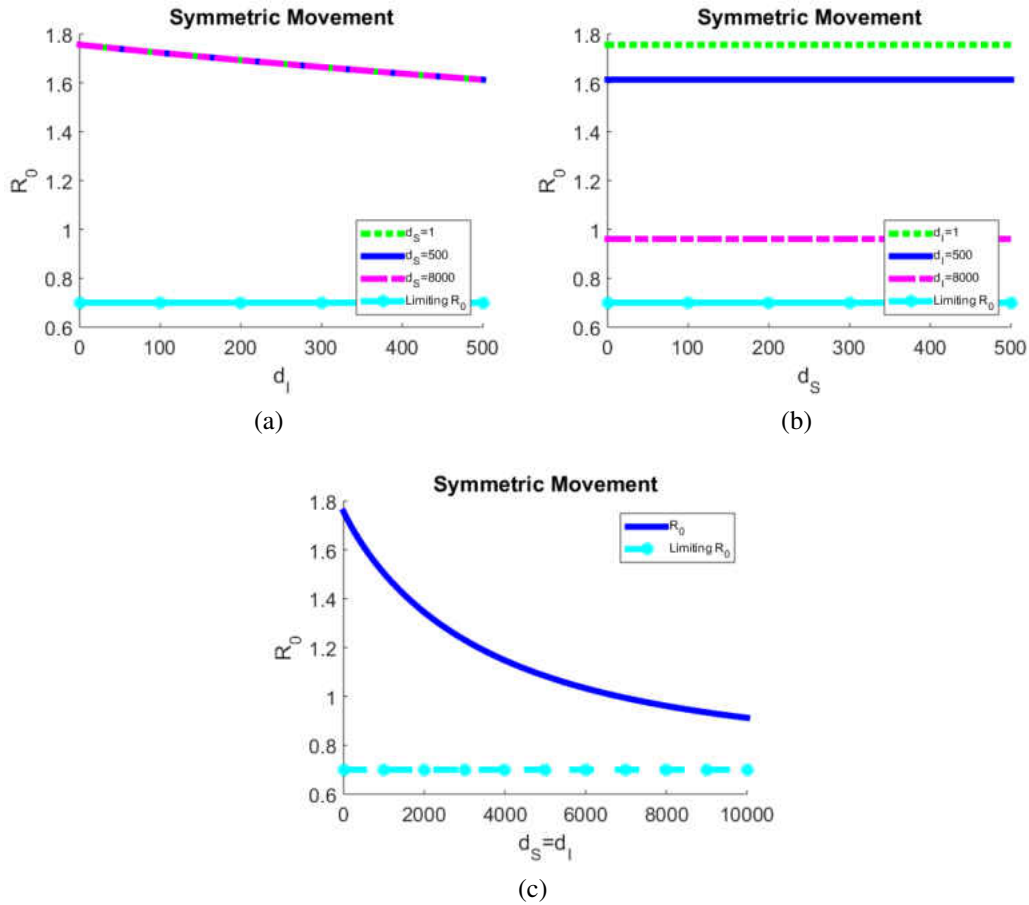
Figure 6.2: (a) The effect on $\mathcal{R}_0$ as d_I varies for fixed values of d_S. (b) The effect on $\mathcal{R}_0$ as d_S varies for fixed values of d_I. (c) The effect on $\mathcal{R}_0$ as a single diffusion coefficient $d = d_S = d_I$ varies.

In contrast to the independence of d_S, $\mathcal{R}_0$ is a monotone decreasing function of

104

d_I; see Figure 6.2(a). Similarly, for a single diffusion coefficient, $d = d_S = d_I$, $\mathcal{R}_0$ is also a monotone decreasing function; see Figure 6.2(c). Using (4.5), we can calculate the limiting value of $\mathcal{R}_0$ as follows:

$$\mathcal{R}_0 \longrightarrow \frac{1}{5} \sum_{j=1}^{5} \mathcal{R}_0^{[j]} \approx 0.69848, \tag{6.1}$$

since $\theta_j = \frac{1}{5}$ for all j. This limiting value is represented as the dashed line in Figure 6.2(c).

Finally, we consider how d_I alters the endemic equilibrium; see Figure 6.3. As $d_I \to \infty$, the number of infectives on each patch tends to 0, while the susceptibles increase monotonically. This results in the concentration of infectives tending to zero; see Figure 6.3(c). The monotonic decrease of $\mathcal{R}_0$ and I^* leads to extinction of the infection when $d_I \gg 1$; however, we will see contrasting behavior with biased movement in combination with varying of d_S.

Figure 6.3: (a) The effect on the total number of infectives and suscepti-
bles in each patch, respectively, as d_I increases. (c) The concentration of
infectives per patch. (d) The total number of infectives. (e) The plot of
the total number of infectives, $I^*(t)$, as d_I varies. (f) The effect on $\mathcal{R}_0$.

106

6.3   Asymmetric Movement Induced Hot Spot

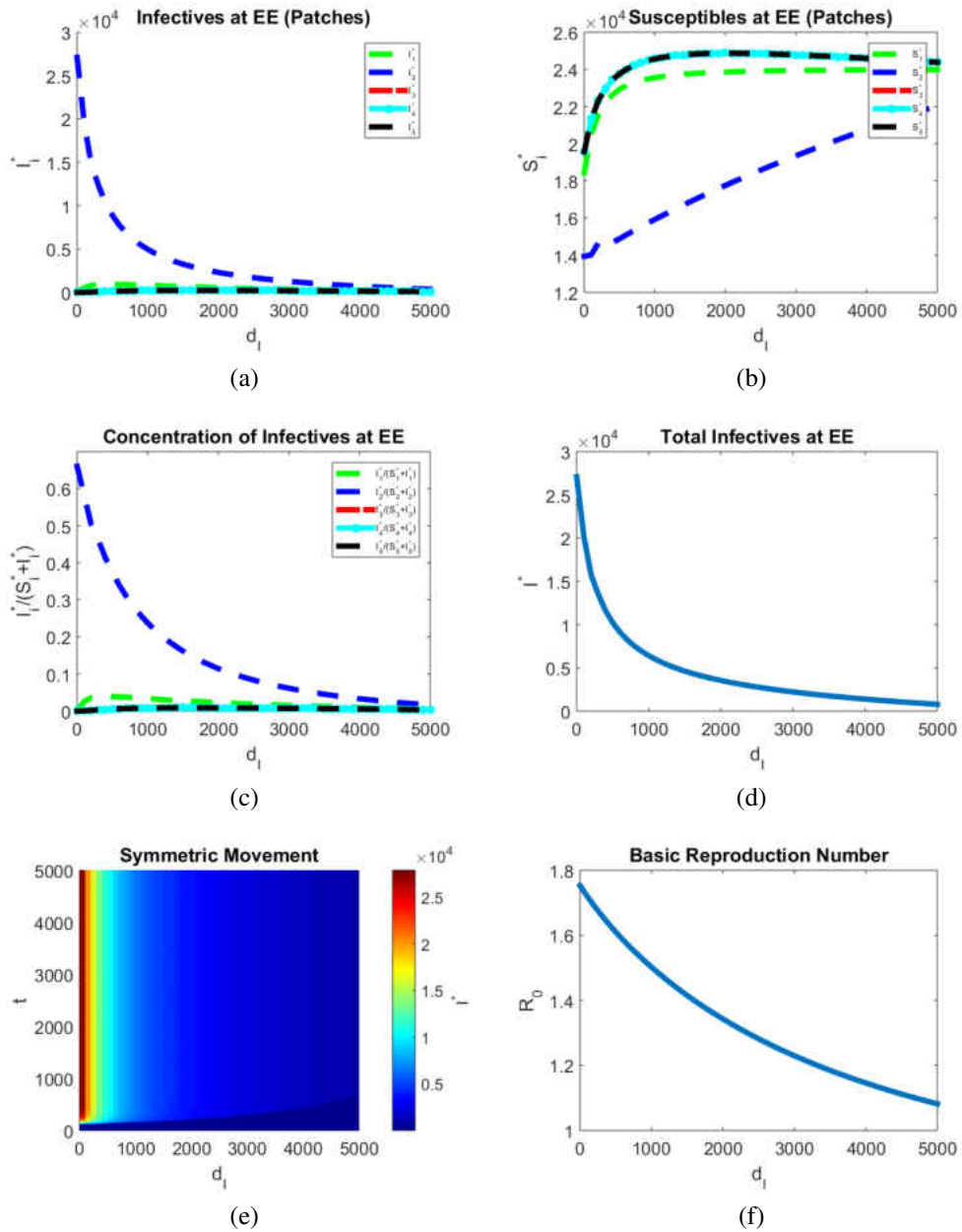In the previous section, we have shown that the DFE, patch reproduction numbers, and the basic reproduction number are independent of the diffusion coefficient d_S. In contrast, all these values would depend on d_S under asymmetric movement, which will be demonstrated numerically in this section.

In Figure 6.4, the large arc is from the hot spot to the main hub. Naturally, the hot spot has a quick decrease in the number of susceptibles at the disease-free equilibrium, which in turn causes the patch reproduction number to rapidly decline below the threshold value 1.

As the individuals move to the hub, there is an initial increase in the size of the population at the disease-free equilibrium; however, as the diffusion of the susceptibles further increases, the population disperses evenly into the remaining leaves. Even though all the remaining patches have a monotonic increase in the number of susceptibles at the disease-free equilibrium, their patch reproduction numbers all remain below 1. The resulting $\mathcal{R}_0$ could be a monotone decreasing function of d_S as shown in Figure 6.4(b) with $d_I = 0$; however, for different d_I values, $\mathcal{R}_0$ might not be a monotone function. This feature will be further explored in the next section. For all cases, $\mathcal{R}_0$ will fall below the threshold value 1 for large diffusion coefficient d_S. Biologically, the disease might tend to die out, if there exists large biased movement out of the hot spot.

107

(a)   (b)

(c)   (d)

Figure 6.4: (a) Location of the large arc in relation to the hot spot. (b) Effect on $\mathcal{R}_0$ as d_S varies and $d_I = 0$. (c) The total number of susceptibles at the DFE vary as d_S increases from 0 to 400. The dashed green line represents the approximated DFE from Section 4.2. (d) The corresponding effects on each $\mathcal{R}_0^{[i]}$ as d_S varies.

108

Considering the reverse case, see Figure 6.5, we allow the large arc to be placed from the hub into the hot spot. Clearly, this would be problematic to skew individuals towards the outbreak; this drastically increases the patch reproduction number of the hot spot, since the number of susceptibles is monotonically increasing for the disease-free equilibrium in Patch 2.

On the other hand, the remaining patches decline steadily in the number of susceptible individuals at the disease-free equilibrium. The flow is consistent between the surrounding leaves and the main hub, so as they move towards the center, these individuals are skewed to travel to the hot spot from the biased movement. Thus, Patch 1, 3, 4, and 5 all have declining patch reproduction numbers. Since Patch 2's behavior is very dominating, the diffusion of the infectious individuals in combination with the diffusion of the susceptibles may result in interesting dynamics due to contrasting behavior. Overall, the biased movement of susceptibles into the hot spot causes a drastic increase in $\mathcal{R}_0$; see Figure 6.5(b).

In Figure 6.6, we let the biased movement occur from Patch 3 to the hub. As d_S grows, each $S_i^{(0)}$ tends towards the weighted average, and each patch reproduction number mimics the same behavior as the disease-free equilibrium. Although Patch 3 has a decline in the number of individuals at the disease-free equilibrium and its patch reproduction number, the other remaining patches all see an increase in these two quantities, in a similar manner to Figure 6.4. Patch 2 always remains a hot spot, while the other patches stay below the threshold value of 1. In contrast to Figure 6.4, Patch 2 does not have a drastic increase in its reproduction number as a result of the skewed movement.
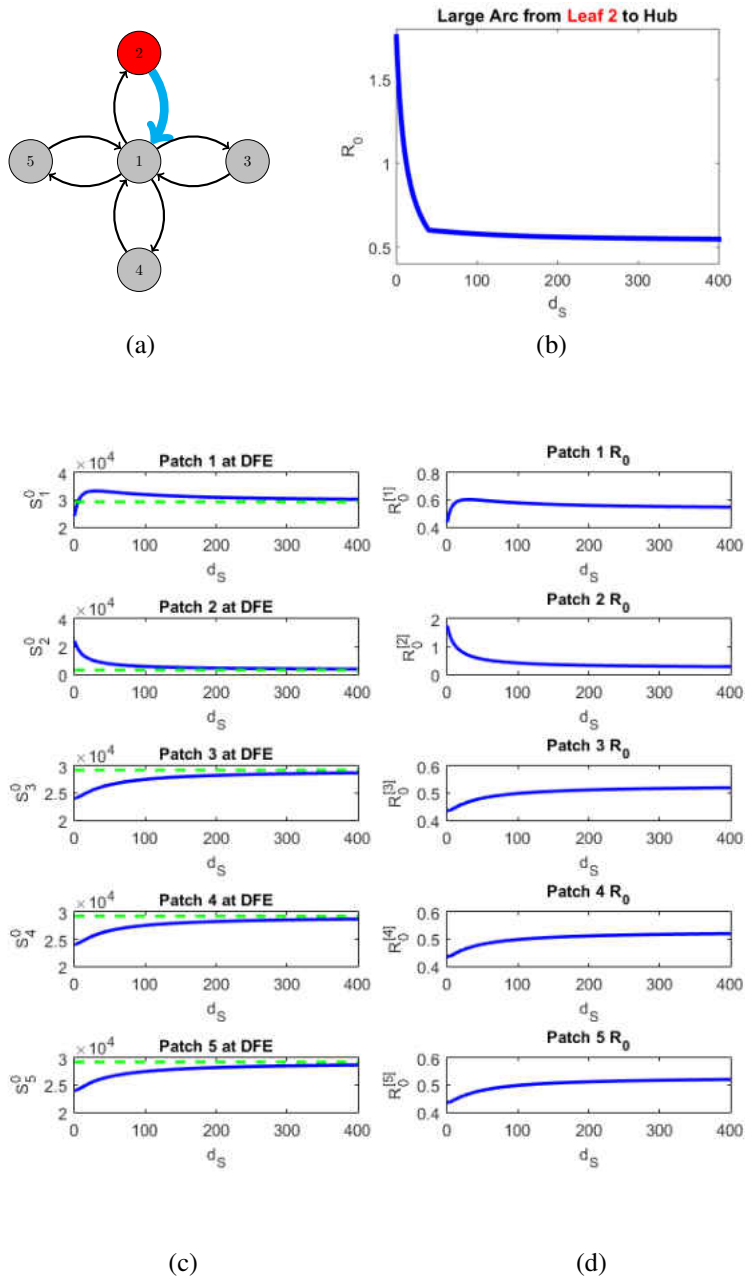
109

Figure 6.5: (a) Location of the large arc in relation to the hot spot. (b) Effect on $\mathcal{R}_0$ as d_S varies and $d_I = 0$. (c) The total number of susceptibles at the DFE vary as d_S increases from 0 to 400. The dashed green line represents the approximated DFE from Section 4.2. (d) The corresponding effects on each $\mathcal{R}_0^{[i]}$ as d_S varies.

110

(a)   (b)

(c)   (d)
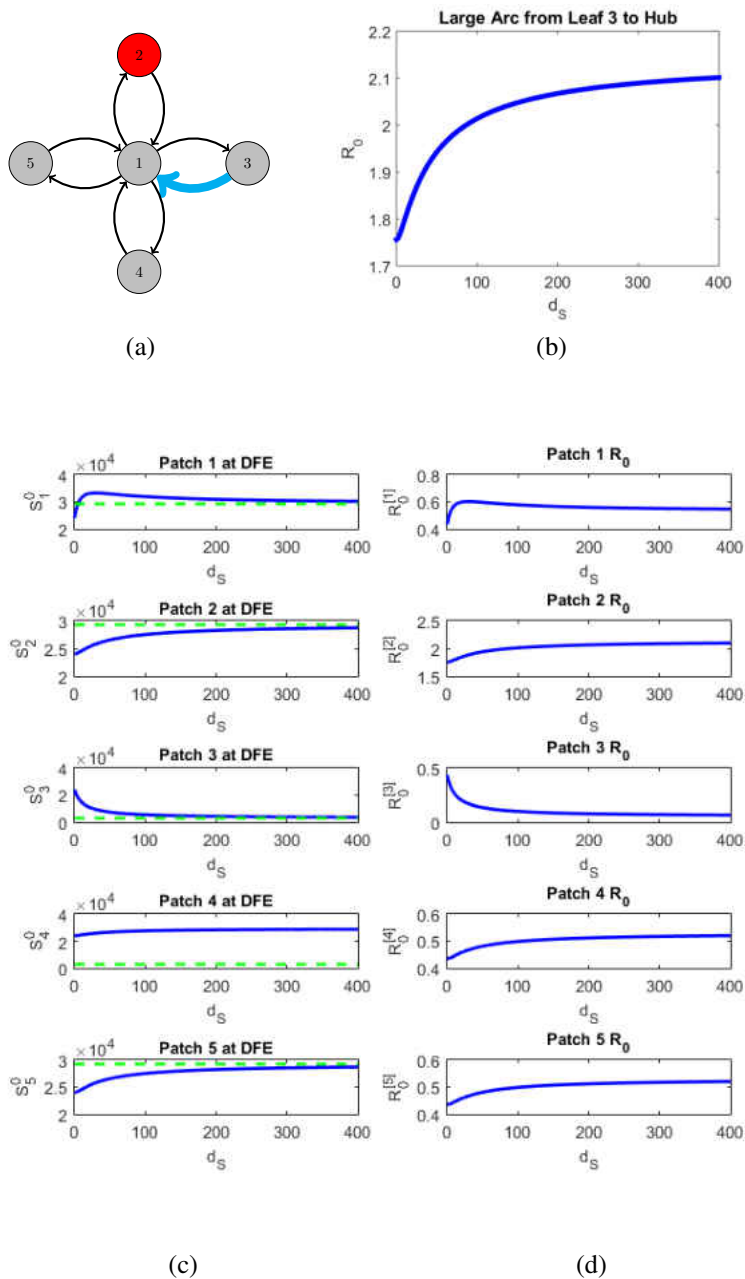
Figure 6.6: (a) Location of the large arc in relation to the hot spot. (b) Effect on $\mathcal{R}_0$ as d_S varies and $d_I = 0$. (c) The total number of susceptibles at the DFE vary as d_S increases from 0 to 400. The dashed green line represents the approximated DFE from Section 4.2. (d) The corresponding effects on each $\mathcal{R}_0^{[i]}$ as d_S varies.

111

Thus, the dynamics between the different diffusion coefficients may vary drastically. Further, we see the same non-monotonicity in the number of susceptibles at the disease-free equilibrium in Patch 1, and the corresponding non-monotonicity in $\mathcal{R}_0^{[1]}$. Overall, Figure 6.6(b) shows this causes a steady increase in $\mathcal{R}_0$ when $d_I = 0$; however, the basic reproduction number does not increase to the same extent as in Figure 6.5(b), but still causes persistence of the infection.

In Figure 6.7, the largest movement is placed from the hub to Patch 3. Each S_i^0 and $\mathcal{R}_0^{[i]}$ are monotonic functions of d_S, with only Patch 3 having monotone increasing functions. Each patch reproduction number graph mimics the same behavior as the graph in the size of the patch at the disease-free equilibrium and the disease-free equilibrium tends towards the weighted average as the diffusion of susceptibles increases.

Notice, as d_S increases, Patch 3 becomes a secondary hot spot. When $d_S \approx 100$, we have $\mathcal{R}_0^{[3]} > 1$ and $\mathcal{R}_0^{[2]} > 1$, causing an asymmetric movement induced hot spot. Because of these contrasting behaviors, we can see non-monotonicty of $\mathcal{R}_0$ as a function of d_S in Figure 6.7(b) when $d_I = 0$. Some diffusion of susceptibles is beneficial to the population, since the patch reproduction number in the hot spot is decreasing. However, when d_S is large enough, the creation of the secondary hot spot causes an increase in $\mathcal{R}_0$.

Due to the symmetry of the parameters chosen, similar graphs as in Figures 6.6 and 6.7 are obtained when the large arc is varied between Patch 4 and the hub and Patch 5 and the hub. We thus omit their figures. With the behavior known in each patch, we turn our attention to the basic reproduction number, $\mathcal{R}_0$.
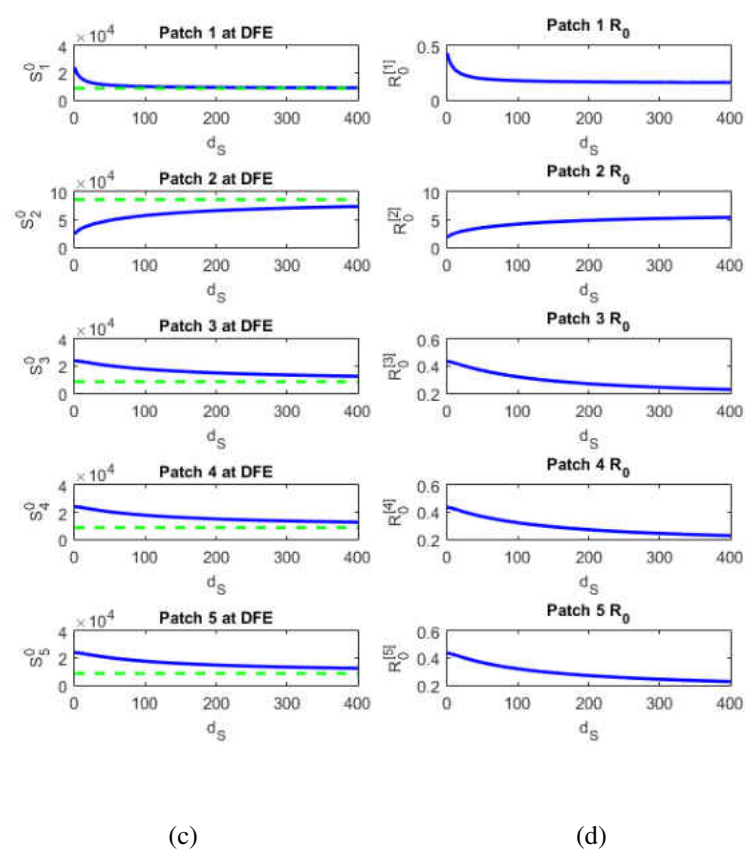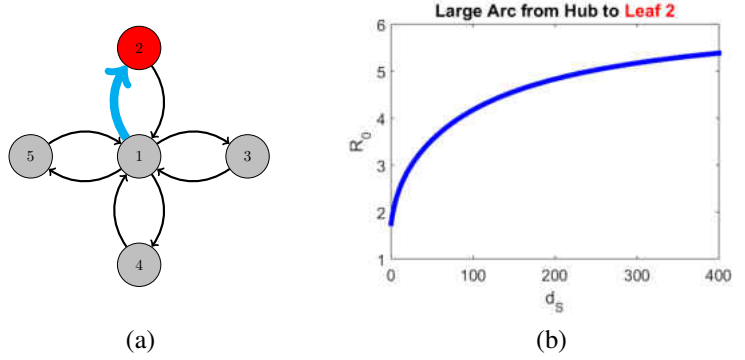
Figure 6.7: (a) Location of the large arc in relation to the hot spot. (b) Effect on $\mathcal{R}_0$ as d_S varies and $d_I = 0$. (c) The total number of susceptibles at the DFE vary as d_S increases from 0 to 400. The dashed green line represents the approximated DFE from Section 4.2. (d) The corresponding effects on each $\mathcal{R}_0^{[i]}$ as d_S varies.
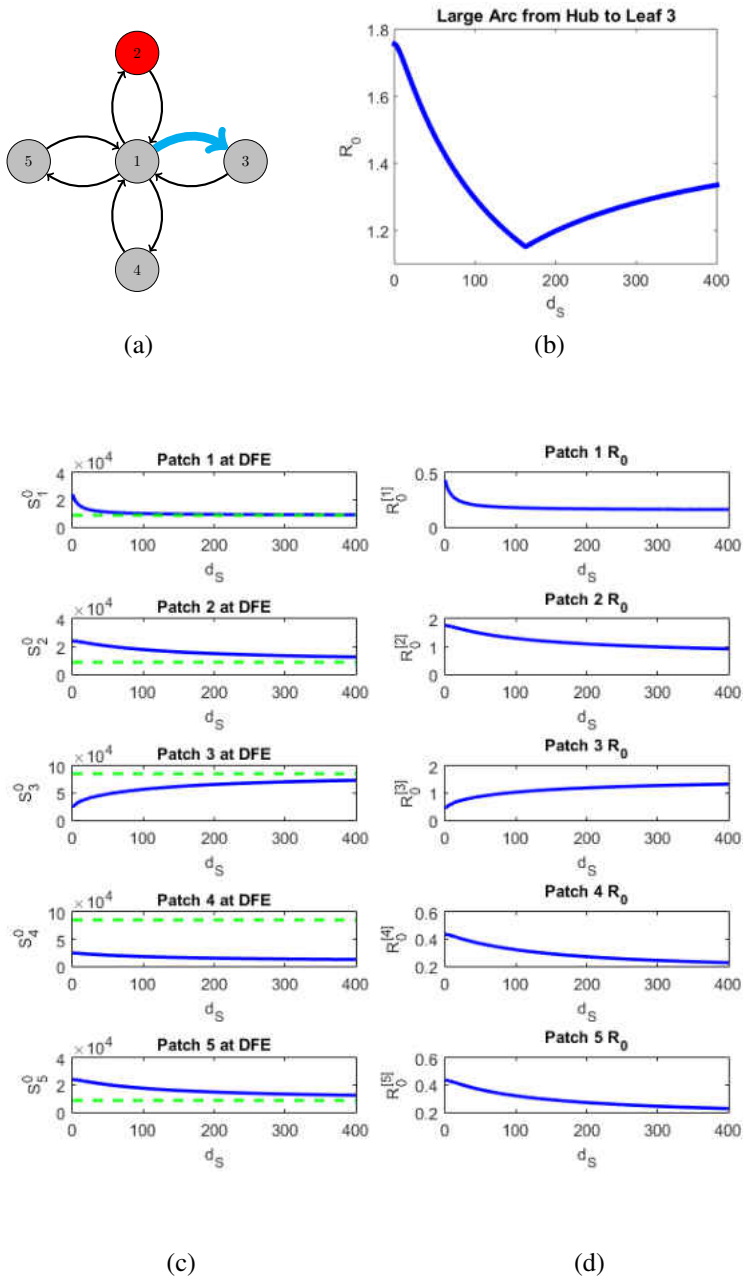
113

6.4 Non-monotone Property of $\mathcal{R}_0$

In the previous section, we have seen the occurrence of non-monotonicity of $\mathcal{R}_0$ when asymmetric movement induces a new hot spot. In this section, we further explore the non-monotone property of $\mathcal{R}_0$. Specifically, we will explore the overall effect of $\mathcal{R}_0$ as the diffusion coefficients are varied. While varying the location of the large arc, we will run three experiments. First, the diffusion of the infectives, d_I, is varied while the diffusion of the susceptibles, d_S, is fixed. Second, d_S varies while d_I is constant. Finally, a single diffusion coefficient $d = d_S = d_I$ is varied to represent infections that will not inhibit movement of infectives, e.g. representing diffusion for a sexually transmitted infection model.

In Figure 6.8(a), we can see R_0 is monotonic with respect to d_I. On the other hand, Figure 6.8(b) shows the behavior of $\mathcal{R}_0$ as a function of d_S varies for fixed d_I. When d_I is small, we can see $\mathcal{R}_0$ is a monotonic decreasing function of d_I. However, for $d_I \gg 1$, the behavior switches and $\mathcal{R}_0$ is a monotone increasing function of d_S.

When considering a single diffusion coefficient, Figure 6.8(c), we see $\mathcal{R}_0$ is a monotone decreasing function of d. Although we have contrasting behavior for $\mathcal{R}_0$ as a function of d_S and d_I, the overall dynamic of $\mathcal{R}_0$ as a function of d is valid. In both instances, $\mathcal{R}_0$ is well below the threshold value of 1. The disease would not persist even for fast movement of susceptibles. Realistically, the individuals are begin pulled from the hot spot at a very fast rate and spreading evenly throughout the remaining patches. As a result, the patch reproduction number of the hot spot is drastically decreased, see Figure 6.4, so the disease cannot persist in the population.
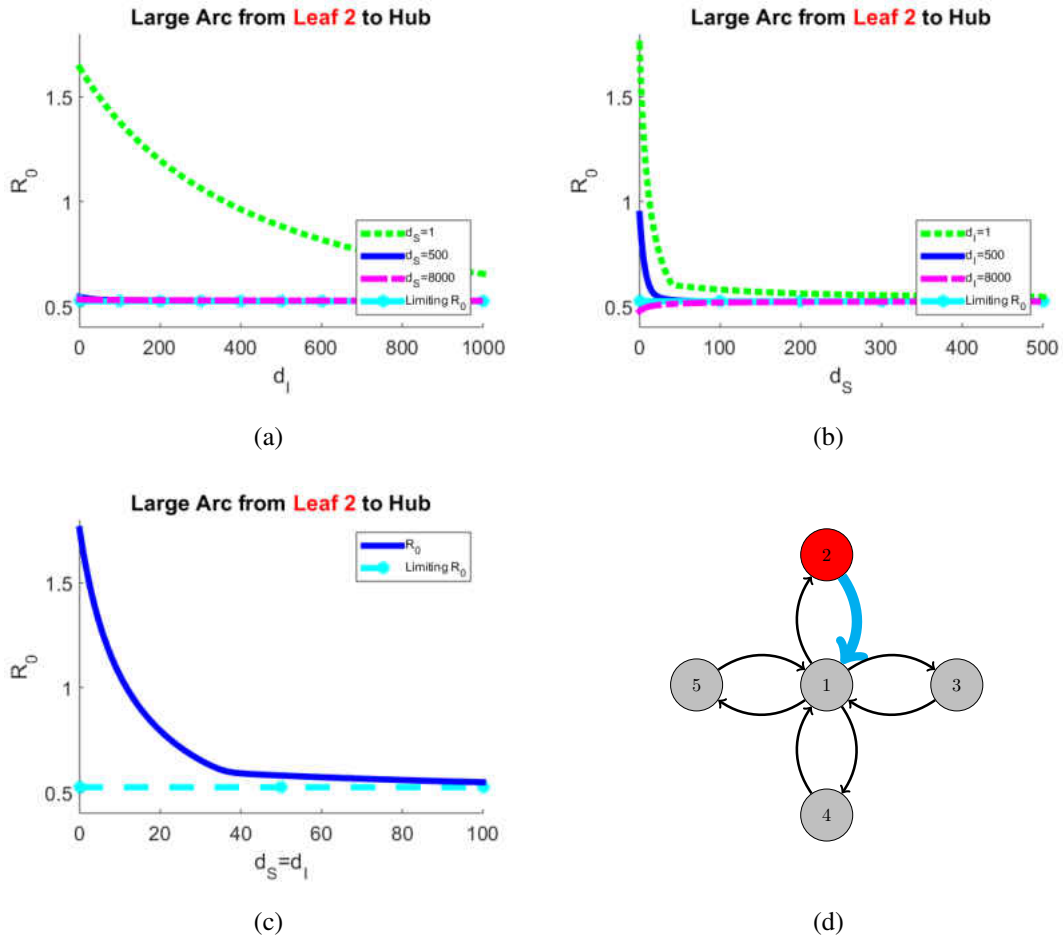
Figure 6.8: (a)-(b) The effect on $\mathcal{R}_0$ as d_I and d_S vary, respectively. (c) The effect on $\mathcal{R}_0$ as a single diffusion coefficient $d = d_S = d_I$ varies. (d) Movement network.

Even with the most movement into the hub, it still follows $\mathcal{R}_0$ is monotone decreasing with respect to d_I, see Figure 6.9(a). It was proven in 2009, the principle eigenvalue is a monotone decreasing function of d_I for a system without demographics and frequency dependent incidence [2].

115
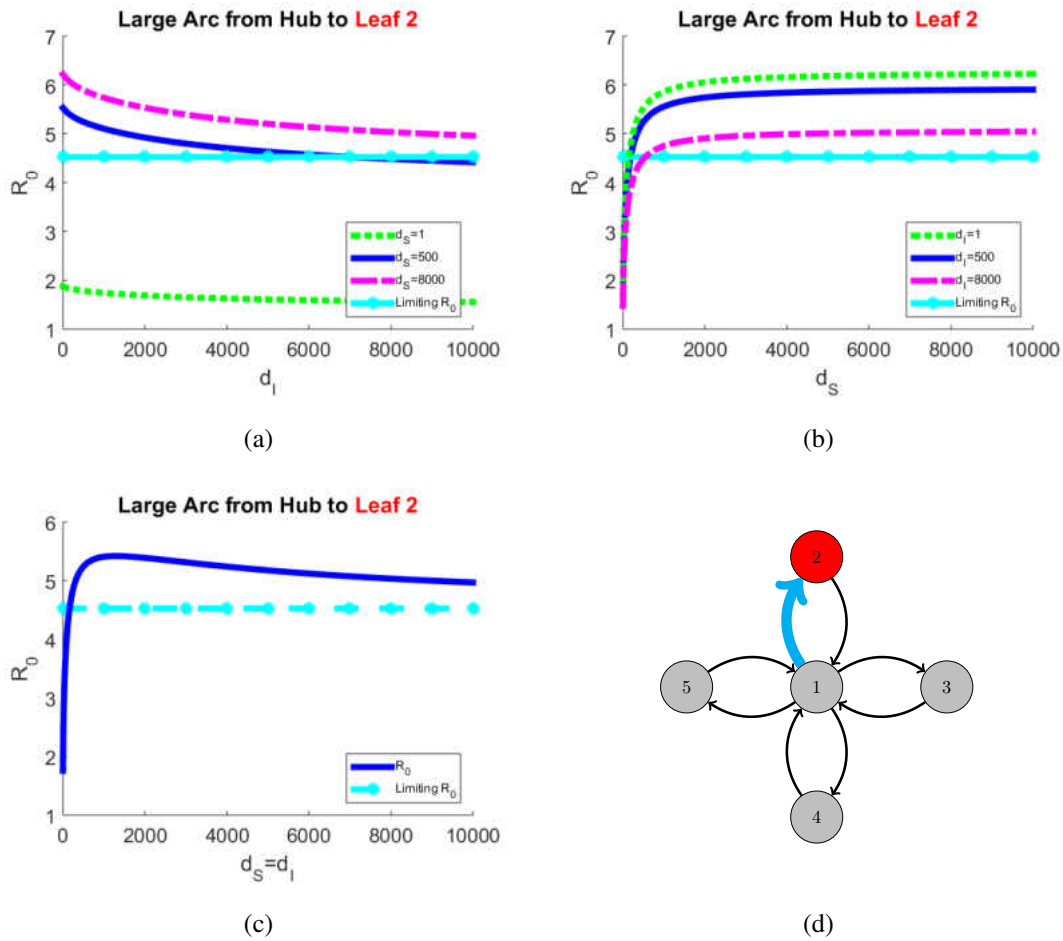
Figure 6.9: (a)-(b) The effect on $\mathcal{R}_0$ as d_I and d_S vary, respectively. (c) The effect on $\mathcal{R}_0$ as a single diffusion coefficient $d = d_S = d_I$ varies. (d) Movement network.

More recently, in a personal conversation with Y. Wu, he discovered a proof to show $\mathcal{R}_0$ is a monotone decreasing function of d_I for the same system [73]. We conjecture this holds true for the asymmetric case as well, but more work must be proven for the principle eigenvalue of the system first.

Recall, from Figure 6.5, the patch reproduction number in the hot spot drastically increases as d_S becomes larger. Thus, increasing the diffusion of the susceptibles demonstrates $\mathcal{R}_0$ as a monotone increasing function of d_S, see Figure 6.9(b). However, as d_I is increased and fixed, the overall basic reproduction number decreases. Thus, even with fast diffusion of susceptibles, increasing the diffusion of the infectives lowers $\mathcal{R}_0$ and likely the size of the outbreak.

Unlike the prior case, this contrasting behavior between d_S and d_I causes non-monotonicity of $\mathcal{R}_0$ as a function of a single diffusion coefficient, d. There is an initial incline in $\mathcal{R}_0$, but after reaching a maximum $\mathcal{R}_0$ decreases slowly towards the limiting $\mathcal{R}_0$ from (4.5). Although there was some contrasting behavior in Figure 6.8, both cases kept $\mathcal{R}_0 < 1$. Here, $\mathcal{R}_0 > 1$ in each instance, which causes the interesting dynamics of this single diffusion coefficient.

Now, due to the symmetry of our parameter selection, we only need to consider the two cases where the large arc is placed from the hub to one of the remaining leafs and from the leaf to the hub. We will select Patch 3 to run these experiments with. First, if we allow travel from one of the good patches into the main hub, regardless of the d_S choice, we can still obtain $\mathcal{R}_0$ is monotone decreasing with respect to d_I, see Figure 6.10(a).

On the other hand, we can see $\mathcal{R}_0$ is monotone increasing with respect to d_S in Figure 6.10(b) in a similar manner to 6.8(b). Thus, when varying both diffusion coefficients simultaneously, we obtain non-monotonicty of $\mathcal{R}_0$ as a function of d. Initially, travel into the main hub creates problems, but eventually when the travel is fast, the reproduction number decreases. From Figure 6.6, the patch reproduction

117

number increases on Patch 1, 2, 4, and 5. Although only Patch 2 has $\mathcal{R}_0^{[i]} > 1$, by pushing susceptibles towards the center, they are dispersing into the hot spot and staying there long enough to become infected. As the diffusion increases, it likely helps reduce the time individuals stay in the hot spot and thus reduces the spread of the infection.

(a)

(b)

(c)

(d)
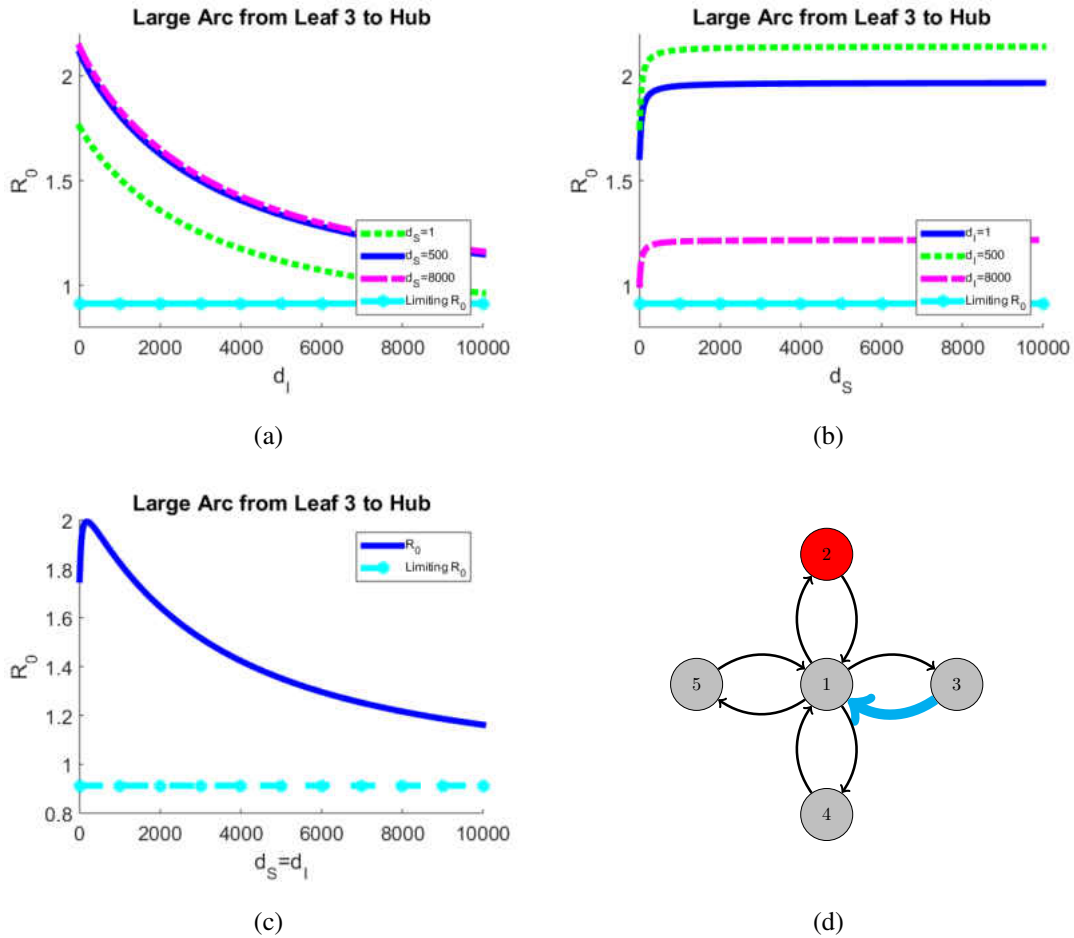
Figure 6.10: (a)-(b) The effect on $\mathcal{R}_0$ as d_I and d_S vary, respectively. (c) The effect on $\mathcal{R}_0$ as a single diffusion coefficient $d = d_S = d_I$ varies. (d) Movement network.
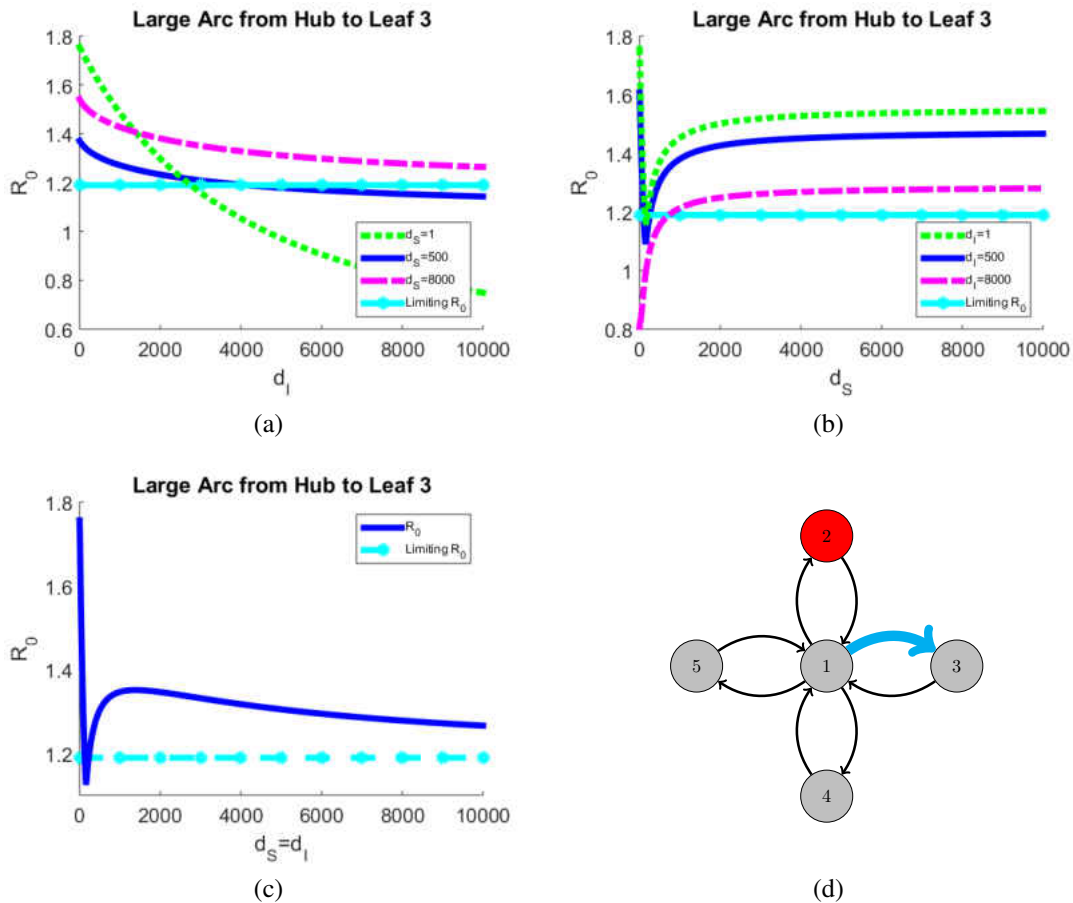
Figure 6.11: (a)-(b) The effect on $\mathcal{R}_0$ as d_I and d_S vary, respectively. (c) The effect on $\mathcal{R}_0$ as a single diffusion coefficient $d = d_S = d_I$ varies. (d) Movement network.

Finally, in Figure 6.11, we allow the most movement into one of the surrounding leafs from the hub. Again $\mathcal{R}_0$ is monotone decreasing with respect to d_I. Unlike the previous experiments, we see a drastically different graph when $d_S = 1$ and $d_S \gg 1$ in Figure 6.11(a). Slow diffusion of both susceptibles and infectives seems more problematic at first, but the overall basic reproduction number is only near

1.8 since $\mathcal{R}_0^{[2]} \approx 1.7561$. When little diffusion occurs for both compartments, it is plausible the reproduction number is that high. However, once the diffusion of infectives increases, the overall reproduction number drops below 1, which would result in extinction of the infection. For $d_S \gg 1$, the disease would persist even with fast diffusion of the infectives.

The behavior in Figure 6.11(a) can be explained via Figure 6.11(b), since $\mathcal{R}_0$ is not always monotonic with respect to d_S. Figure 6.11(a) picks an initial starting point along the green dotted line in Figure 6.11(b), since $d_I = 1$ here. With the drastic change in behavior while varying d_S, the initial conditions from the green dotted line begin $\mathcal{R}_0$ near 1.8, 1.4, and 1.6 for $d_S = 1$, $d_S = 500$, and $d_S = 8000$.

(a)

(b)
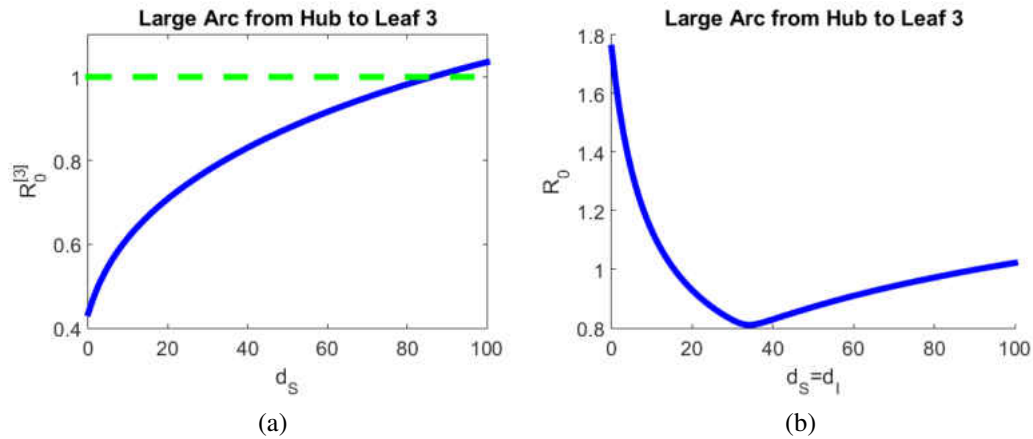
Figure 6.12: Creation of an asymmetric movement induced hot spot. (a) A zoom in of $\mathcal{R}_0^{[3]}$ as d_S varies and crosses the threshold value. (b) The corresponding graph for $\mathcal{R}_0$ as a function of d_S.

This drastic change in behavior is a result of the patch reproduction numbers. In Section 6.3, too fast of diffusion of susceptibles created this asymmetric movement

120

induced hot spot as $\mathcal{R}_0^{[3]}$ crossed the threshold value of 1. In Figure 6.12, we can see as $\mathcal{R}_0^{[3]}$ nears 1, $\mathcal{R}_0$ begins to change in behavior. As a result, this non-monotonicity is exhibited under a single diffusion coefficient, d; see Figure 6.11(c).
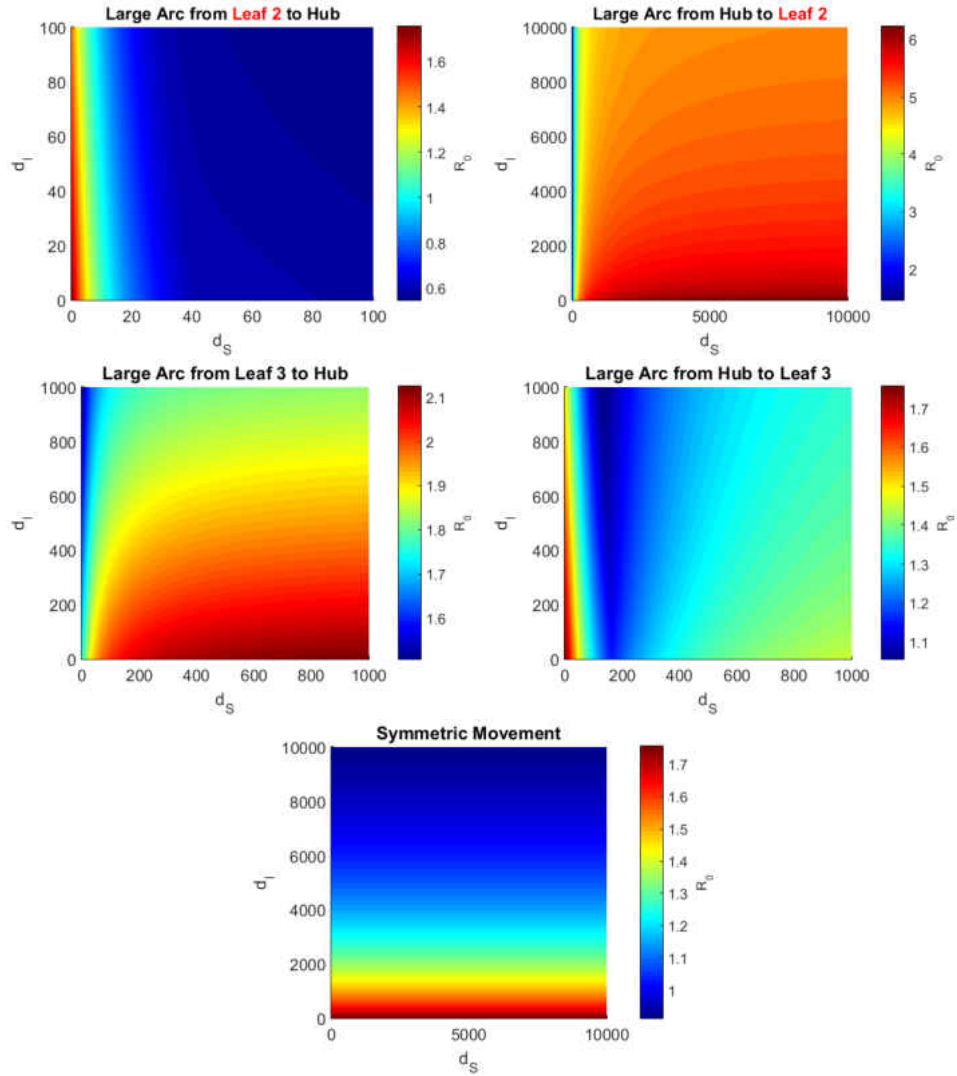
Figure 6.13: The overall effect on $\mathcal{R}_0$ for each location of the large arc as d_S and d_I vary independently.

121

Figure 6.13 gives one final visualization of the effect of d_S and d_I on $\mathcal{R}_0$. We can easily see the non-monotonicity of $\mathcal{R}_0$ as a function of d_S when the most movement is between the hub and Patch 3. Further, the diagonal of each graph represents how $\mathcal{R}_0$ is altered from a single diffusion coefficient d, allowing us to see the non-monotonic cases more readily. Finally, we can see how symmetric movement is consistent for each value of d_S, a stark contrast from the skewed asymmetric movement.

Clearly as a result of these simulations, we can see $\mathcal{R}_0$ is not monotone with respect to a single diffusion coefficient, d. We do notice this behavior when d_S and d_I do not agree in monotonicity. Table 6.2 provides a complete summary of our findings.

Table 6.2: Summary of monotonicity of $\mathcal{R}_0$ for mass action incidence with a hot spot in a leaf.

Large Arc Location	Monotonicity of $\mathcal{R}_0$ (d_I **varies**)	Monotonicity of $\mathcal{R}_0$ (d_S **varies**)	Monotonicity of $\mathcal{R}_0$ ($d_I = d_S$ **varies**)
Leaf 2 to Hub	monotone decreasing	varies	monotone decreasing
Hub to Leaf 2	monotone decreasing	monotone increasing	not monotonic
Leaf 3 to Hub	monotone decreasing	monotone increasing	not monotonic
Hub to Leaf 3	monotone decreasing	not monotonic	not monotonic

From this, we conjecture the overall monotonicity of $\mathcal{R}_0$ as a function of d depends solely on the monotonicity of $\mathcal{R}_0$ as a function of d_S.

6.5 Effect on the Endemic Equilibrium

Since $\mathcal{R}_0$ is non-monotonic for some instances, a similar effect should be present in the behavior of the endemic equilibrium. We examine the effect on the number of susceptibles individuals, the total number of infectious individuals, and the concentration of infectives, e.g. $I_i/(S_i + I_i)$, at the EE as d_S varies.

As d_S increases, $\mathcal{R}_0$ decreases below the threshold 1 when the large arc is out of the hot spot. As a result, there is no endemic state for larger movement. Thus, we begin by examining the effect on the endemic equilibrium when the large arc is from the hub into the hot spot.

In Figure 6.14, the effect on the total number of susceptibles and infectives in patch is examined, along with the concentration of infectives in each patch, for a fixed $d_I = 500$. With the susceptibles being pushed into the hot spot, the number of infectives skyrockets almost immediately as d_S increases, which is biologically feasible. Recall, from Figure 6.5, the patch reproduction number increases significantly as d_S grows larger, and consequently the number of infectives in Patch 2 increases in a similar manner.

123

Large Arc from Hub to Leaf 2

(a)

(b)

(c)

(d)

(e)

(f)

Figure 6.14: (a) The number of infectives in each patch at the endemic equilibrium for varying d_S. (b) The number of susceptibles in each patch at the endemic equilibrium for varying d_S. (c) The concentration of infectives in each patch at the endemic equilibrium for varying d_S. (d) The total number of infectives at the EE. (e) The plot of the total number of infectives, $I^*(t)$, as d_S varies. (f) The change in the basic reproduction number.

Most individuals are being pulled into the hot spot, causing a decrease in the number of susceptibles for Patches 1, 3, 4, and 5; however, the number of susceptibles in Patch 2 remains fairly constant. Initially, it seems the increase of d_S should cause an increase in S_2^*, but realistically the increase in diffusion causes the infectives to grow since the reproduction number is increasing rapidly in Patch 2. This is different than the effect of d_S on the number of susceptibles at the DFE. While d_S grows, we saw S_2^0 decreases. As the new susceptibles enter, most become infected. The influx of individuals seems to solely replenish the susceptible population. Once the reproduction number reaches a more steady state, the number of infectives plateaus, along with the number of susceptibles in the other patches, keeping the population at this endemic state.

Finally, the behavior of the concentration of infectives is determined. Since each patch now has a varying number of individuals, the concentration provides a good insight to how problematic the infection is on each patch. With a low concentration of infectives, less people are ultimately affected by the disease. Clearly, Patch 2 is very problematic to the persistence of the infection. Even with small diffusion of the susceptibles, the concentration of the infectives in Patch 2 reaches 80% rapidly. Further, even though Patch 1 loses most of their susceptible individuals, the infection spreads fairly quickly into the hub as d_S increases. More than 50% of the population becomes infected. Finally, the infection slowly dissipates into the remaining leaves. Ultimately, there are three different levels to the infection, since Patches 3-5 behavior in a similar manner.

Large Arc from Leaf 3 to Hub
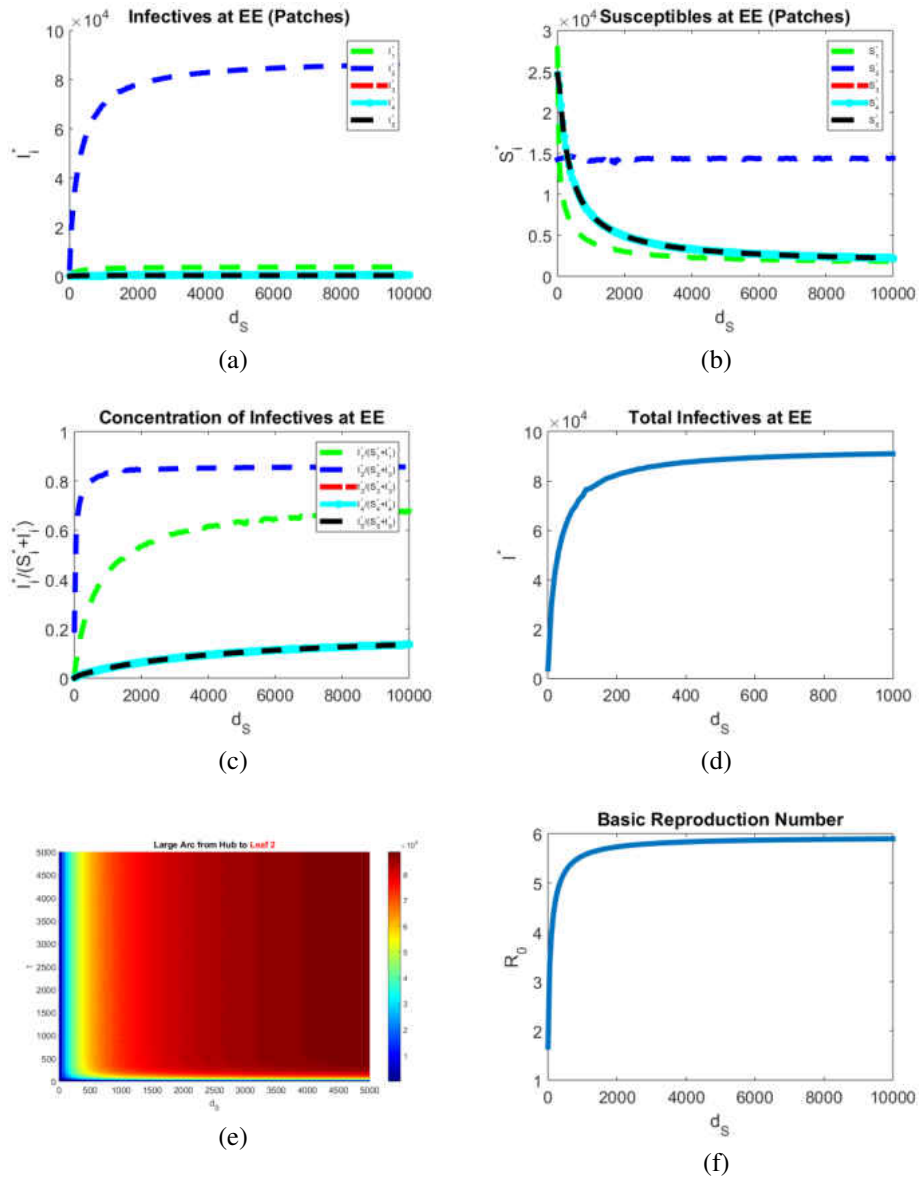

(a)

(b)

(c)

(d)

(e)

(f)
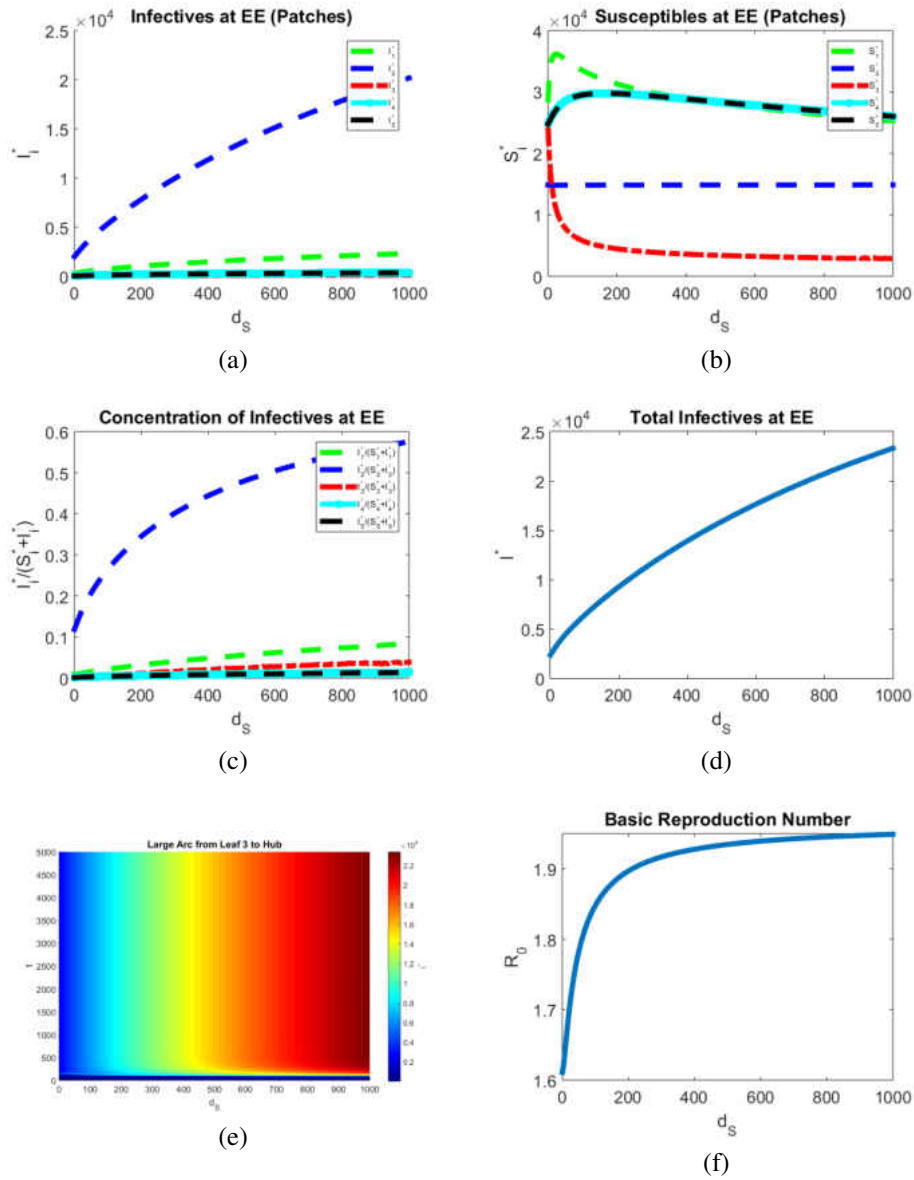
Figure 6.15: (a) The number of infectives in each patch at the endemic equilibrium for varying d_S. (b) The number of susceptibles in each patch at the endemic equilibrium for varying d_S. (c) The concentration of infectives in each patch at the endemic equilibrium for varying d_S. (d) The total number of infectives at the EE. (e) The plot of the total number of infectives, $I^*(t)$, as d_S varies. (f) The change in the basic reproduction number.

126

In Figure 6.15, we allow the most movement from Patch 3 to the hub. We have seen $\mathcal{R}_0$ is a monotone increasing function of d_S from Section 6.4 and as shown again in Figure 6.15(f). Since the susceptibles are sent to the main hub quickly as d_S increases, we can see the total number of infectives in Patch 2 increases, since more susceptibles will be pushed into Patch 2 as a result of the fast diffusion.

Once again, the number of susceptibles in Patch 2 remains consistent, but the overall concentration increases, just as in Figure 6.14. The number of infectives in Patch 3 remains at the same level as the other leafs, but the concentration of infectives increases due to the total number of susceptibles decreasing. Thus, there is a higher concentration of infectives in Patch 2 than the other leafs. Although the concentration of infectives in the hot spot increases, it caps out at roughly 60%. When the most movement is from the hub into the hot spot, the concentration reached over 80%, but here the susceptibles are sent into Patch 4 and 5 at the same rate as into Patch 2. This allows for some individuals to evade infection.

Unlike the first case, it seems the infection remains more controlled in Patch 4 and 5. The total number of infectives remains fairly small, and although the number of susceptibles is non-monotonic, the concentration of infectives remains less than 10%. With this, it may be interesting to see how re-routing individuals towards the outer patches during an outbreak could alter the total number of infectives.

In our last scenario, we let the biased movement occur the hub into one of the surrounding leafs, which provided interesting non-monotonicity of $\mathcal{R}_0$ in Section 6.4. As a result, similar dynamics occur involving the endemic equilibrium, see Figure 6.16. First, the total number of infectives drastically increases for Patch 3,

127

since a second hot spot is created when $d_S > 90$. The number of infectives in this patch slowly increases until that point, and then has a drastic increase. Even though Patch 2 always has a patch reproduction number greater than 1, the number of infectives in the hot spot is always decreasing, and eventually reaches a similar level to those in the Patch 1, 4, and 5.

Again, the number of susceptibles stays consistent for Patch 2, which causes a decrease in the overall concentration of infectives. Further, Patch 2 and 3 essentially swap roles when d_S is large enough. The concentrations switch, and Patch 3 has a higher percentage of infectives. Patch 2 even becomes similar in concentration to the remaining surrounding leafs. The hub only experiences an increase in concentration from losing more susceptibles as $d_S \gg 1$. Thus, when the movement is heavily skewed from the main hub into Patch 3, there are three main levels on infectivity. Patch 3 is the highest, the hub is second, and the remaining leafs are all similar, even though Patch 2 still has a patch reproduction number greater than 1. The concentration is less than 5% for higher values of d_S, making Patch 3 more prominent in the persistence of the infection.

Overall, this creation of a secondary hot spot leads to a less severe outbreak than what is seen when the most movement is into the hub; however, it does show biased travel away from the hot spot toward a particular location can be problematic in persistence of the disease.

Large Arc from Hub to Leaf 3

(a)

(b)

(c)

(d)

(e)

(f)
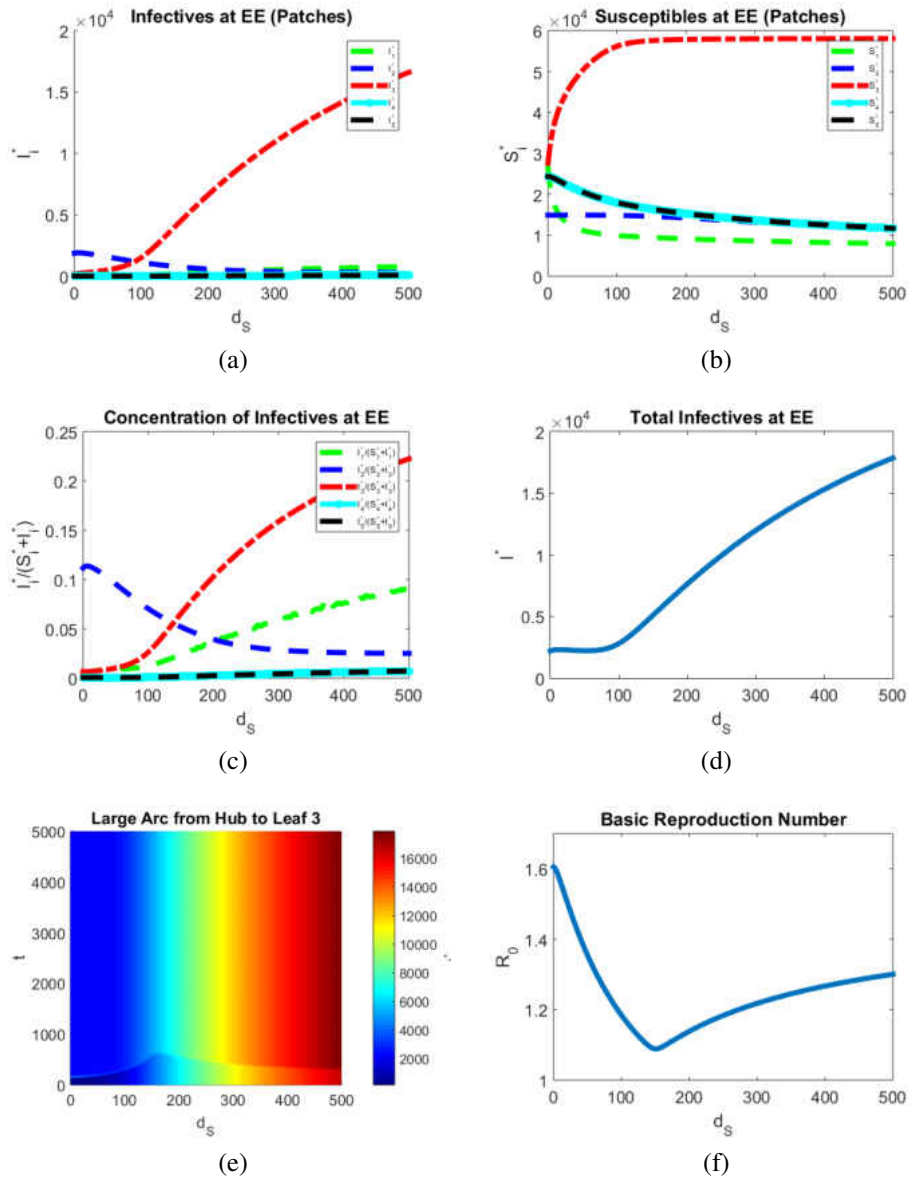
Figure 6.16: (a) The number of infectives in each patch at the endemic equilibrium for varying d_S. (b) The number of susceptibles in each patch at the endemic equilibrium for varying d_S. (c) The concentration of infectives in each patch at the endemic equilibrium for varying d_S. (d) The total number of infectives at the EE. (e) The plot of the total number of infectives, $I^*(t)$, as d_S varies. (f) The change in the basic reproduction number.

6.6   Summary of Results

It has been shown numerically that $\mathcal{R}_0$ is a monotone decreasing function of d_I, regardless of the choice of incidence function and symmetric/asymmetric movement. The theoretical establishment of this result remains open.

Interesting dynamics occurs with the mass action incidence function as a result of the biased movement. New disease hot spots can be induced due to the asymmetric movement, which further leads to a non-monotone property of $\mathcal{R}_0$ in terms of d_S.

Similar to the frequency dependent function when demographics are introduced, the infectives can persist on each population. Further, the concentration of infectives can vary as d_S increases, creating different levels of infectivity in the population.

Additionally, biased movement can be problematic in the persistence of the infection. When movement is heavily skewed away from a hot spot towards one particular location, it might create a new hot spot induced by this asymmetric movement.

CHAPTER 7: CONCLUSIONS AND FUTURE STUDIES

A general epidemiological model with spatial heterogeneity has been proposed to investigate the impact of asymmetric movement on the spatial spread of an infectious disease. The initial study for the homogeneous model provides insight into the construction of Lyapunov functions needed for global stability. Further, the comparison of Lyapunov functions in the SIS and SIR model for the homogeneous case exhibit the difficulty in global stability without additional assumptions. As a result, global stability of the endemic equilibrium when $\mathcal{R}_0 > 1$ for the SIS model cannot yet be achieved for an arbitrary nonlinear incidence function. When an infection does not increase the risk of death nor effect the rate at which an infectious individual can move, global stability can be proven for the mass action incidence function in the homogeneous environment. If these assumptions are not met, a secondary Lyapunov function can be used, which cannot be readily extended to the heterogeneous model.

For the heterogeneous model with general incidence, global asymptotic stability of the disease-free equilibrium is established under biologically reasonable assumptions for the incidence function when $\mathcal{R}_0 \leq 1$. The frequency dependent incidence function will satisfy these assumptions, while the mass action incidence function satisfies these conditions for the SIR model. Mass action incidence for the SIS model will also satisfy these assumptions, when no disease-induced death or movement inhibition for infectives occurs. When $\mathcal{R}_0 > 1$, the existence of an endemic equilibrium is determined inside our feasible region. The uniqueness and global

stability of the endemic equilibrium can be proven for the SIR model when the movement of susceptible individuals is restricted. Global stability is still open when movement of susceptibles or movement of all individuals is permitted. On the contrary, for the SIS model with mass action incidence, global asymptotic stability of the endemic equilibrium can be shown in the following cases: movement of susceptibles is restricted, movement of infectives is restricted, and movement of susceptibles is proportional to the movement of infectious individuals for a specific proportionality constant.

With these new global stability results, we focus our attention on the limiting behavior of the system. An approximation for the disease-free equilibrium and the basic reproduction number is derived when the movement of individuals is faster than the disease dynamics. The overlaying network structure determines the limiting behaviors, which is impacted by the biased movement.

Numerical explorations provide insight to the limiting behavior as the diffusion of susceptibles, d_S, tends to 0 for the frequency dependent model. It is known for the SIS patch model without demographics, the system will tend to a disease-free state as $d_S \to 0$ [2]. However, biased movement would alter this result. As the diffusion of susceptibles is halted, persistence of the infection is possible with the skewed movement is introduced between two hot spots. Further, the inclusion of demographics would also lead to persistence of the infection as $d_S \to 0$ for symmetric movement.

Our experiments exhibit $\mathcal{R}_0$ as a monotone decreasing function of d_I. Recently, Y. Wu proved this result for the SIS patch model without demographics [73]. When

132

demographics are introduced, we conjecture the same result holds for symmetric and asymmetric movement. However, the biased movement is a factor for persistence of the infection. For $d_I \gg 1$, the basic reproduction number falls below the threshold value of 1 with symmetric movement. In contrast, it is possible $\mathcal{R}_0 > 1$ even as $d_I \to \infty$ when biased movement is present.

When other incidence functions are used besides the frequency dependent function, we can see rise to interesting dynamics for $\mathcal{R}_0$ in terms of d_S. For mass action incidence, the biased movement can induce a hot spot, causing non-monotonicity of $\mathcal{R}_0$ as a function of d_S for both the SIS and SIR models. Further, when the infection does not inhibit movement as in a sexually transmitted infection, there are non-monotonic behaviors of $\mathcal{R}_0$ leading to non-monotonicty of the endemic equilibrium level. Some movement may be beneficial for reducing $\mathcal{R}_0$, but too much movement can worsen the infection. We conjecture the monotonicity of $\mathcal{R}_0$ will rely solely on the behavior of $\mathcal{R}_0$ as a function of d_S; however, most instances show fast movement of susceptibles lead to higher levels of infectivity.

We have established some global stability results for the endemic equilibrium under various assumptions on the diffusion coefficients and/or the movement network, using a graph theoretic approach and Lyapunov functions. It seems further developments of such approach or new global stability methods are required to tackle the general situation. We leave them as a possible future research direction.

We would like to further explore the dependence of $\mathcal{R}_0$ on the diffusion coefficients. For example, we hope to prove $\mathcal{R}_0$ is a monotone decreasing function of d_I for the asymmetric movement case. We will also perform a more realistic numerical in-

133

vestigation for the greater Orlando area. Orlando will be located in the center city with the frequency dependent function, while the surrounding suburbs will utilize the mass action incidence function. We will determine how tourism impacts the endemic level, and where the redirect individuals in case of an outbreak. Additionally, further studies on the limiting behavior as the diffusion of individuals is halted would be of interest. Another important and interesting area of study could be the inclusion of time-dependent parameters, representing seasonal movement patterns in metropolitan areas. An influx of individuals into a particular location either via tourism, relocation, of seasonal travel could raise biased movement, which might dramatically alter the disease dynamics. Further theoretical and numerical studies equipped with empirical data could lead to a better understanding of the spread and control of infectious diseases.

LIST OF REFERENCES

[1] *Facts about chickenpox*, Paediatrics & Child Health, **10** (2005), 413 – 414.

[2] L. J. S. Allen, B. M. Bolker, Y. Lou, and A. L. Nevai, *Asymptotic profiles of the steady states for an SIS epidemic patch model*, SIAM Journal on Applied Mathematics, **67** (2007), 1283 – 1309.

[3] L. J. S. Allen, B. M. Bolker, Y. Lou, and A. L. Nevai, *Asymptotic profiles of the steady states for an SIS epidemic reaction-diffusion model*, Discrete and Continuous Dynamical Systems, **21** (2008), 1 – 20.

[4] R. M. Anderson and R. M. May, *Infectious Diseases of Humans: Dynamics and Control*, Oxford University Press, Oxford, 1991.

[5] J. Arino, *Diseases in Metapopulations (in Z. Ma, Y. Zhou, J. Wu (eds) Modeling and Dynamics of Infectious Diseases)*, World Scientific Publishing, Singapore, 2009.

[6] J. Arino, *Spatio-temporal spread of infectious pathogens of humans*, Infectious Disease Modelling, **2** (2017), 218– 228.

[7] J. Arino, A. Ducrot, and P. Zongo, *A metapopulation model for malaria with transmission-blocking partial immunity in hosts*, Journal of Mathematical Biology, **64** (2012), 423 – 448.

[8] J. Arino and P. van den Driessche, *The Basic Reproduction Number in a Multi-city Compartmental Epidemic Model (in F. Allgöwer, M. Morari (eds) Lecture Notes in Control and Information Sciences)*, Springer, Berlin, 2003.

[9] J. Arino and P. van den Driessche, *A multi-city epidemic model*, Mathematical Population Studies, **10** (2003), 175–193.

[10] A. Berman and R. J. Plemmons, *Nonnegative Matrices in the Mathematical Sciences*, Academic Press, New York, 1979.

[11] K. T. Bernstein, J. Zenilman, G. Olthoff, V. C. Marsiglia, and E. J. Erbelding, *Gonorrhea reinfection among sexually transmitted disease clinic attendees in Baltimore, Maryland*, Sexually Transmitted Diseases, **33** (2006), 80 – 86.

[12] N. P. Bhatia and G. P. Szegö, *Dynamical Systems: Stability Theory and Applications*, Lecture Notes in Mathematics, Springer-Verlag, Berlin, 1967.

[13] F. Brauer, Z. Shuai, and P. van den Driessche, *Dynamics of an age-of-infection cholera model*, Mathematical Biosciences and Engineering, **10** (2013), 1335 – 1349.

[14] F. Brauer, P. van den Driessche, and J. Wu, *Mathematical Epidemiology*, Springer, Berlin, 2008.

[15] R. Brualdi and D. Cvetković, *A Combinatorial Approach to Matrix Theory and its Applications*, CRC Press, Boca Raton, 2009.

[16] C. E. M. Coltart, B. Lindsey, I. Ghinai, A. M. Johnson, and D. L. Heymann, *The Ebola outbreak, 2013-2016: old lessons for new epidemics*, Philosophical Transactions of the Royal Society of London. Series B, Biological Sciences, **372** (2017), 1–224.

[17] R. S. Cantrell and C. Cosner, *Spatial Ecology via Reaction-Diffusion Equations*, Wiley, Chichester, 2003.

[18] R. Cui, K. Lam, and Y. Lou, *Dynamics and asymptotic profiles of steady states of an epidemic model in advective environments*, Journal of Differential Equations, **263** (2017), 2343 – 2373.

[19] R. Cui and Y. Lou, *A spatial SIS model in advective heterogeneous environments*, Journal of Differential Equations, **261** (2016), 3305 – 3343.

[20] K. Deng and Y. Wu, *Dynamics of a susceptible-infected-susceptible epidemic reaction-diffusion model*, Proceedings of the Royal Society of Edinburg, **146A** (2016), 929 – 946.

[21] O. Diekmann, J. A. P. Heesterbeek, and J. A. J. Metz, *On the definition and the computation of the basic reproduction ratio $\mathcal{R}_0$ in models for infectious diseases in heterogeneous populations*, Journal of Mathematical Biology, **28** (1990), 365 – 382.

[22] R. Diestel, *Graph Theory*, Springer-Verlag, New York, 2000.

[23] M. C. Eisenberg, Z. Shuai, J. H. Tien, and P. van den Driessche, *A cholera model in a patchy environment with water and human movement*, Mathematical Biosciences, **246** (2013), 105 – 112.

[24] M. C. Eisenberg, Z. Shuai, J. H. Tien, and P. van den Driessche, *Disease invasion on community networks with environmental pathogen movement*, Journal of Mathematical Biology, **70** (2015), 1065 – 1092.

[25] M. Fischer, M. Hennessey, and J. E. Staples, *Zika virus spreads to new areas - region of the Americas, May 2015 - January 2016*, Centers for Disease Control and Prevention, **65** (2003), 55 – 58.

[26] H. I. Freedman, S. G. Ruan, and M. X. Tang, *Uniform persistence and flows near a closed positively invariant set*, Journal of Dynamics and Differential Equations, **6** (1994), 583–600.

[27] D. Gao, Y. Lou, D. He, T. Porco, Y. Kuang, G. Chowell, and S. Ruan, *Prevention and control of Zika as a mosquito-borne and sexually transmitted disease:*

137

a mathematical modeling analysis, Scientific Reports, **10** (2011), 400 – 432.

[28] D. Gao and S. Ruan, *An SIS patch model with variable transmission coefficients*, Mathematical Biosciences, **232** (2011), 110 – 115.

[29] D. Gao and S. Ruan, *A multipatch malaria model with logistic growth populations*, SIAM Journal on Applied Mathematics, **72** (2012), 819 – 841.

[30] W. M. Geisley, S. Y. Lensing, C. G. Press, and E. W. Hook, III, *Spontaneous resolution of genital chlamydia trachomatis infection in women and protection from reinfection*, The Journal of Infectious Diseases, **207** (2013), 1850 – 1856.

[31] D. E. Griffin and M. B. A. Oldstone, *Measles: Pathogenesis and Control*, Springer, Berlin, 2009.

[32] R. Grimshaw, *Nonlinear Ordinary Differential Equations*, Blackwell Scientific Publications, Oxford, 1990.

[33] H. W. Hethcote, *An immunization model for a heterogeneous population*, Theoretical Population Biology, **14** (1978), 338 – 349.

[34] H. W. Hethcote, *The mathematics of infectious diseases*, SIAM Review, **42** (2000), 599 – 653.

[35] H. W. Hethcote and S. A. Levin, *Periodicity in Epidemiological Models*, Springer, Berlin, 1989.

[36] H. W. Hethcote, H. W. Stech, and P. van den Driessche, *Periodicity and Stability in Epidemiological Models: A Survey (in S. N. Busenberg, K. L. Cooke (eds) Differential Equations and Applications in Ecology, Epidemics, and Population Problems)*, Academic Press, New York, 1981.

[37] H. W. Hethcote and P. van den Driessche, *Some epidemiological models with nonlinear incidence*, Journal of Mathematical Biology, **29** (1991), 271 – 287.

[38] J. Hoey, *Can you get tuberculosis twice?*, Canadian Medical Association Journal, **166** (2002), 478.

[39] R. Horn and C. R. Johnson, *Matrix Analysis*, Cambridge University Press, New York, 1985.

[40] L. S. Hung, *The SARS epidemic in Hong Kong: what lessons have we learned?*, Journal of the Royal Society of Medicine, **96** (2003), 374 – 378.

[41] Y. Jin and W. Wang, *The effect of population dispersal on the spread of a disease*, Journal of Mathematical Analysis and Applications, **308** (2005), 343 – 364.

[42] Y. Kang and C. Castillo-Chavez, *A Simple Two-Patch Epidemiological Model with Allee Effects and Disease-Modified Fitness (in A. Gumel (ed) Mathematics of Continuous and Discrete Dynamical Systems)*, American Mathematical Society, Providence, 2014.

[43] W. O. Kermack and A. G. McKendrick, *A contribution to the mathematical theory of epidemics*, Proceedings of the Royal Society of London Series A, **115** (1927), 700 – 721.

[44] W. O. Kermack and A. G. McKendrick, *Contributions to the mathematical theory of epidemics, part II- the problem of endemicity*, Proceedings of the Royal Society of London Series A, **138** (1932), 55 – 83.

[45] W. O. Kermack and A. G. McKendrick, *Contributions to the mathematical theory of epidemics, part III - further studies of the problem of endemicity*, Proceedings of the Royal Society of London Series A, **53** (1933), 89 – 118.

[46] A. Korobeinikov and G. C. Wake, *Lyapunov functions and global stability for SIR, SIRS, and SIS epidemiological models*, Applied Mathematics Letters, **15**

(2002), 955 – 960.

[47] K. Kuto, H. Matsuzawa, and R. Peng, *Concentration profile of endemic equilibrium of a reaction-diffusion-advection SIS epidemic model*, Calculus of Variations and Partial Differential Equations, **56** (2017), 1 – 28.

[48] C. E. Langenhop, *The Laurent expansion for a nearly singular matrix*, Linear Algebra and its Applications, **4** (1971), 329 – 349.

[49] J. P. LaSalle, *The Stability of Dynamical Systems*, Regional Conferences Series in Applied Math, SIAM, Philadelphia, 1976.

[50] J. Lesser, N. G. Reich, and D. A. T. Cummings, *Outbreak of 2009 pandemic influenza a (H1N1) at a New York City school*, The New England Journal of Medicine, **361** (2009), 2628 – 2636.

[51] M. Y. Li, J. R. Graef, L. Wang, and J. Karsai, *Global dynamics of a SEIR model with varying total population size*, Mathematical Biosciences, **160** (1999), 191 – 213.

[52] M. Y. Li and J. S. Muldowney, *Global stability for the SEIR model in epidemiology*, Mathematical Biosciences, **125** (1995), 155 – 164.

[53] M. Y. Li and Z. Shuai, *Global stability of an epidemic model in a patchy environment*, Canadian Applied Mathematics Quarterly, **17** (2009), 1513 – 1532.

[54] M. Y. Li and Z. Shuai, *Global-stability problem for coupled systems of differential equations on networks*, Journal of Differential Equations, **248** (2010), 1 – 20.

[55] W. Liu, H. W. Hethcote, and S. A. Levin, *Dynamical behavior of epidemiological models with nonlinear incidence rates*, Journal of Mathematical Biology,

25 (1987), 359 – 380.

[56] S. Mandal, R. R. Sarkar, and S. Sinha, *Mathematical models of malaria - a review*, Malaria Journal, **10** (2011), 175 – 188.

[57] J. W. Moon, *Counting Labelled Trees*, Canadian Mathematical Congress, Montreal, 1970.

[58] W.-M. Ni, *The Mathematics of Diffusion*, SIAM, Philadelphia, 2011.

[59] R. Peng, *Asymptotic profiles of the positive steady state for an SIS epidemic reaction-diffusion model*, Journal of Differential Equations, **247** (2009), 1096 – 1119.

[60] R. J. Plemmons, M*-matrix characterizations. I. Nonsingular* M*-matrices*, Linear Algebra and its Applications, **18** (1981), 175 – 188.

[61] S. Ruan, *Spatial-Temporal Dynamics in Nonlocal Epidemiological Models (in Y. Takeuchi, Y. Iwasa, K. Sato (eds) Mathematics for Life Science and Medicine)*, Springer, Berlin, 2007.

[62] C. Saad-Roy, J. Ma, and P. van den Driessche, *The effect of sexual transmission on Zika virus dynamics*, Journal of Mathematical Biology, **77** (2018), 1917 – 1941.

[63] Z. Shuai and P. van den Driessche, *Global dynamics of a disease model including latency with distributed delays*, Canadian Applied Mathematics Quarterly, **19** (2011), 235–253.

[64] H. L. Smith and P. E. Waltman, *The Theory of the Chemostat: Dynamics of Microbial Competition*, Cambridge University Press, Cambridge, 1995.

[65] C. Sun, W. Yang, J. Arino, and K. Khan, *Effect of media-induced social distancing on disease transmission in a two patch setting*, Mathematical Bio-

sciences, **230** (2011), 87 – 95.

[66] P. van den Driessche, *Reproduction numbers of infectious disease models*, Infectious Disease Modelling, **2** (2017), 288 – 303.

[67] P. van den Driessche and J. Watmough, *A simple SIS epidemic model with a backward bifurcation*, Journal of Mathematical Biology, **40** (2000), 525 – 540.

[68] P. van den Driessche and J. Watmough, *Reproduction numbers and subthreshold endemic equilibria for compartmental models of disease transmission*, Mathematical Biosciences, **180** (2002), 29 – 48.

[69] C. Vargas-De-León, *Constructions of Lyapunov functions for classics SIS, SIR and SIRS epidemic model with variable population size*, Revista Electrónica Foro Red Mat, **26** (2009), 1 – 12.

[70] W. Wang and G. Mulone, *Threshold of disease transmission in a patch environment*, SIAM Journal on Numerical Analysis, **285** (2003), 321 – 335.

[71] W. Wang and X. Zhao, *An epidemic model in a patchy environment*, Mathematical Biosciences, **190** (2004), 97 – 112.

[72] D. West, *Introduction to Graph Theory*, Prentice Hall, Upper Saddle River, 1996.

[73] Y. Wu, *Personal conversation*, February 2019.

[74] Y. Wu and X. Zou, *Asymptotic profiles of steady states for a diffusive SIS epidemic model with mass action infection mechanism*, Journal of Differential Equations, **261** (2016), 4424 – 4447.

[75] A. A. Yahaya, A. O. Talisuna, I. Conteh, A. Oke, and M. Stephen, et al., *Operational readiness and preparedness for Ebola virus disease outbreak in countries neighbouring the Democratic Republic of the Congo: progress, chal-*

lenges and the way forward, Weekly Epidemiological Record, **94** (1971), 39 – 43.

[76] J. Yorke, *Invariance for ordinary differential equations*, Mathematical Systems Theory, **1** (1967), 353–372.

[77] F. Zhang, *Matrix Theory: Basic Results and Techniques*, Springer, New York, 1985.